WRC RESEARCH REPORT NO. 98

STUDY OF STRATIFIED OVERFLOWS AND UNDERFLOWS

by

W. Hall C. Maxwell
Associate Professor of Civil Engineering
Edward R. Holley
Professor of Civil Engineering
Chi-Yu Lin
Research Assistant in Civil Engineering
and
Sahim Tekeli
Research Assistant in Civil Engineering

University of Illinois at Urbana-Champaign

FINAL REPORT

Project No. B-071-ILL

July 1, 1972 - December 31, 1974

The work upon which this publication is based was supported by funds provided by the U.S. Department of the Interior as authorized under the Water Resources Research Act of 1974, P.L. 88-379

Agreement No. 14-31-0001-3880

UNIVERSITY OF ILLINOIS
WATER RESOURCES CENTER
2535 C. E. Hydrosystems Lab.
Urbana, Illinois 61801

February 1975

ABSTRACT

STUDY OF STRATIFIED OVERFLOWS AND UNDERFLOWS

The study presents a general analysis of two-layered stratified flows taking into account effects of sidewall friction and variation of density with horizontal distance. The analysis is applied to the study of arrested thermal wedges and arrested cold water intrusions. Laboratory data were collected and analyzed and it was determined that bed roughness has a significant effect on the interfacial friction factor for arrested thermal wedges but not for arrested cold water intrusions. Friction factors were found to vary significantly along the wedges indicating that use of average values is perhaps undesirable. Local values of friction factor were found to increase with values of a local interfacial Reynolds number.

Maxwell, W. Hall C., Holley, Edward R., Lin, Chi-Yu, and Tekeli, Sahim
STUDY OF STRATIFIED OVERFLOWS AND UNDERFLOWS
Completion Report to Office of Water Research and Technology, Department of the Interior, Washington, D.C., February 1975, 98 pp.
KEYWORDS - fluid mechanics/ *heated water/ hydraulic engineering/ rivers/ *thermal pollution/ *thermal stratification/ *water temperature

CONTENTS

LIST OF FIGURES

NOTATION

The following symbols are used in this report:

1 = subscript referring to upper layer

2 = subscript referring to lower layer

b = subscript referring to bed

B = channel width

c = constant

c_f = resistance coefficient = f/4

f = friction factor

F = Froude number, see Eq. 37 and Eq. 40

F_Δ = densimetric Froude number, see Eq. 3, Eq. 42 and Eq. 43

g = acceleration of gravity

h = depth of layer

H = depth of channel

i = subscript referring to interface

j = subscript referring to moving layer

k = equivalent sand grain roughness diameter

L = length of arrested wedge

m = subscript referring to maximum

p = pressure

Q = discharge

r = dimensionless longitudinal distance = x/H

R = hydraulic radius

Re = Reynolds number, see Eq. 2 and Eq. 57

Ri = Richardson number, see Eq. 1

S = energy slope

t = time

T = temperature

u = component of velocity in x-direction

$\bar{u}_s$ = velocity defined by Eq. 15

$\overline{u_s^2}$ = quantity defined by Eq. 19

U = average velocity in channel

v = component of velocity in y-direction

w = component of velocity in z-direction and subscript referring to sidewall

x = co-ordinate in stream direction (see Fig. 2)

y = co-ordinate in vertical direction

z = co-ordinate in lateral direction

α = quantity defined by Eq. 14

β = quantity defined by Eq. 18

$\Delta\rho = \bar{\rho}_2 - \bar{\rho}_1$

$\Delta T = T - T_{min}$

η = dimensionless depth of lower layer = h_2/H

ν = kinematic viscosity of fluid

ρ = fluid density

σ_x^1 = deviatoric normal stress in x-direction

τ = shear stress

ϕ = function

bars denote vertical averages.

I. INTRODUCTION

In the field of water resources problems several types of situations which involves flows with density differences may exist. Such density differences may result, for example, (1) due to temperature differences associated with natural causes or with the discharge of heated cooling water from a power plant into a lake or stream; (2) due to salinity differences when river water is discharged into the ocean; or (3) when an accidental oil spill results in a layer of oil overlying a body of water. Generally the vertical density gradients are larger than those in the horizontal direction. However, this may not be true in the region where one of the fluid layers terminates.

A significant part of the problem of analyzing flows with density differences is the analysis and treatment of the vertical momentum transfer. For turbulent flows, two general types of approach may be found in the literature.

One approach is to use a two-dimensional (horizontal and vertical) analysis and an eddy viscosity. The problem then becomes one of predicting the eddy viscosity for a prescribed set of circumstances. Frequently the eddy viscosity has been correlated with the Richardson number (Ri) which may be defined as

$$Ri = \frac{g}{\rho}\frac{\partial \rho}{\partial y}/\left(\frac{\partial u}{\partial y}\right)^2 \qquad (1)$$

in which g = acceleration of gravity; ρ = density; u = component of the velocity in the horizontal (x) direction; and y is the vertical co-ordinate direction. Nelson (24)* has reviewed several literature sources which

*Numerals in parentheses refer to corresponding items in List of References.

presented empirical determinations of the eddy viscosity in flows with density differences. The data generally indicates a decrease in eddy viscosity with increasing stability (increasing Ri). However, the scatter of the data is so great that Nelson concludes that almost no direct correlation can be deduced between the stability as defined by a Richardson number and any transfer coefficient. Presuming, however, the availability of an adequate correlation, this approach permits a fully two-dimensional analysis to be made. As a result information may be obtained about the distribution of u, v (the component of velocity in the vertical direction) and ρ with both x and y. The required numerical computation and difficulty are, of course, commensurate with the two-dimensional analysis.

Another approach which may be applied in some situations is to schematize the flow as a system of distinct layers, usually two in number for simplicity. For example, the analysis of a two-layer system is presented by Schijf and Schönfield (29). There is a computational advantage in that each layer is usually treated as a one-dimensional flow. It then becomes necessary to know the interfacial shear stress (τ_i) or interfacial friction factor (f_i) in order to represent the momentum transfer between layer. Sjoberg (33), Hikkawa (12), Sherenkov et al (30), Vreugdenhil (36) (see Appendix II) and Harleman and Stolzenbach (10) have presented interfacial friction factors from several sources. Again the scatter was large and no generally consistent correlation was found. It has generally been assumed that f_i should be related to the Reynolds number (Re) and the densimetric Froude number (F_Δ) with

$$Re = u\, h/\nu \qquad (2)$$

and

$$F_\Delta = u/(\frac{\Delta\rho}{\rho} g h)^{\frac{1}{2}} \quad (3)$$

in which u = a characteristic velocity difference between layers, h = a characteristic vertical length, $\Delta\rho$ = the density difference between the fluid layers, and ν = the kinematic viscosity.

Difficulties arise in this type of analysis in defining the interface position and in defining the characteristic velocity, length, density difference, etc. in Re and F_Δ. For miscible fluids, where one layer is moving relative to the other with velocity u, experiments by Keulegan (17) and Rumer (28) indicate that a distinct interface will exist even for turbulent flow provided

$$\text{Re } F_\Delta^2 = u^3/(\frac{\Delta\rho}{\rho} g \nu) < 200 \text{ (approx.)} \quad (4)$$

Sherenkov et al (30) found that as Re F_Δ^2 increases the interface becomes more diffuse. In fact they indicate that for Re $F_\Delta^2 > 1650$ there is "waveless mixing and transition to a developed turbulent flow with neutral stratification." They present data, however, representing a relationship between the dimensionless interfacial shear velocity and Re F_Δ^2 up to Re $F_\Delta^2 \simeq 2 \times 10^5$. There is undoubtedly some limit beyond which it is unreasonable to schematize the system by two layers, but the limit has apparently not been defined. One might set the limit as Re $F_\Delta^2 \simeq 200$ i.e. a physically distinct interface. However, this is probably more restrictive than is needed for some engineering applications. Due to the associated computational advantages, it would seem reasonable to assume a layered situation for some cases where the interface is diffuse to some degree.

If a layered system is assumed, there are a number of possible definitions of the interface position. These include, for example, the position at which the density is equal to the average value for the two layers (19), the position at which the temperature gradient is a maximum (22), the middle of the diffusion zone (3), or the position which yields zero average velocity in an arrested layer (26). Since velocities involved are generally quite small, (particularly in laboratory studies), and therefore difficult to measure, definitions based on temperature (or density), which is much more readily measured, and more common in the literature.

Most analyses of experimental data have apparently assumed that the entrainment (advective transport) across the defined interface was zero. This implies that the discharge in each layer remains constant. While any entrainment velocity is no doubt small compared to the velocity of the primary flow it is conceivable that, in many situations, a small velocity integrated over a long interface could represent a change in discharge which would be a significant fraction of the primary flow. There is evidence that entrainment is also related generally to the quantity $\mathrm{Re}\ F_{\Delta}^{2}$ (35).

Attempts to combine data from several sources for either the eddy viscosity (24) or the interfacial friction factor (10)(36)(30)(12) have revealed very little consistency. The following observations may have some bearing on this scattering of results from various sources:

(1) The freedom in defining the characteristic quantities used to calculate the dimensionless parameters such as the Reynolds number etc. has resulted in a variety of definitions. The publications often contain insufficient information to permit bringing all the data to a common base for comparison.

(2) The analysis of the experimental data is very sensitive to quantities which often cannot be measured as accurately as would be desirable. For example, the calculation of interfacial friction factors is highly dependent on the determination of the interfacial slope. This slope is, however, usually quite small and hence difficult to measure accurately. It is also dependent on the definition which is used for interface position.

(3) No single investigation has yet been made in which there was a systematic variation of the major dimensionless quantities over a wide range of all the significant parameters.

(4) The attempted comparisons of data from various sources often consider only the gross flow parameters and not the internal structure of the flow. For example, considering now primarily two-layer flow and the associated friction factor some questions could be asked the answers to which might have a bearing on the comparibility of data. Is the flow fully established or not? Is the turbulence in the flow the result of a developing interfacial boundary layer downstream from a splitter plate used to create a stratified situation? How much of the total flow resistance for each layer is due to side-wall shear rather than interfacial shear? If only one layer has a mean velocity is the situation one of overflow or one of underflow? With flow over an arrested wedge or intrusion there is only interfacial shear (ignoring side-walls) so that the turbulence in the moving layer will be any residual part of the turbulence generated upstream of the wedge plus the turbulence associated with the interfacial shear. On the other hand, for flow under an arrested wedge both lower boundary and interfacial shears are active in generating turbulence in the stratified flow region. Finally, what are the hydraulic roughness characteristics of the boundaries?

Part of this report is directed toward these last two questions, namely the possible difference between overflows and underflows and the possible significance of boundary roughness taking into account longitudinal density variations. Laboratory data have been collected for arrested thermal wedges (underflows) and arrested cold water intrusions (overflows) for both rough and smooth boundaries. The arrested wedge, either in the form of thermal wedge or cold water intrusion is a stable configuration that results when the gravitational force caused by density differences between contacting layers is in equilibrium with the friction force at the interface between the two fluids (21). Fig. 1 illustrates a typical arrested thermal wedge configuration.

The authors wish to acknowledge with thanks the permission received from the Delft Hydraulics Laboratory to reproduce as an appendix to this report E. R. Holley's translation of C. B. Vreugdenhil's survey of literature on interfacial friction coefficients.

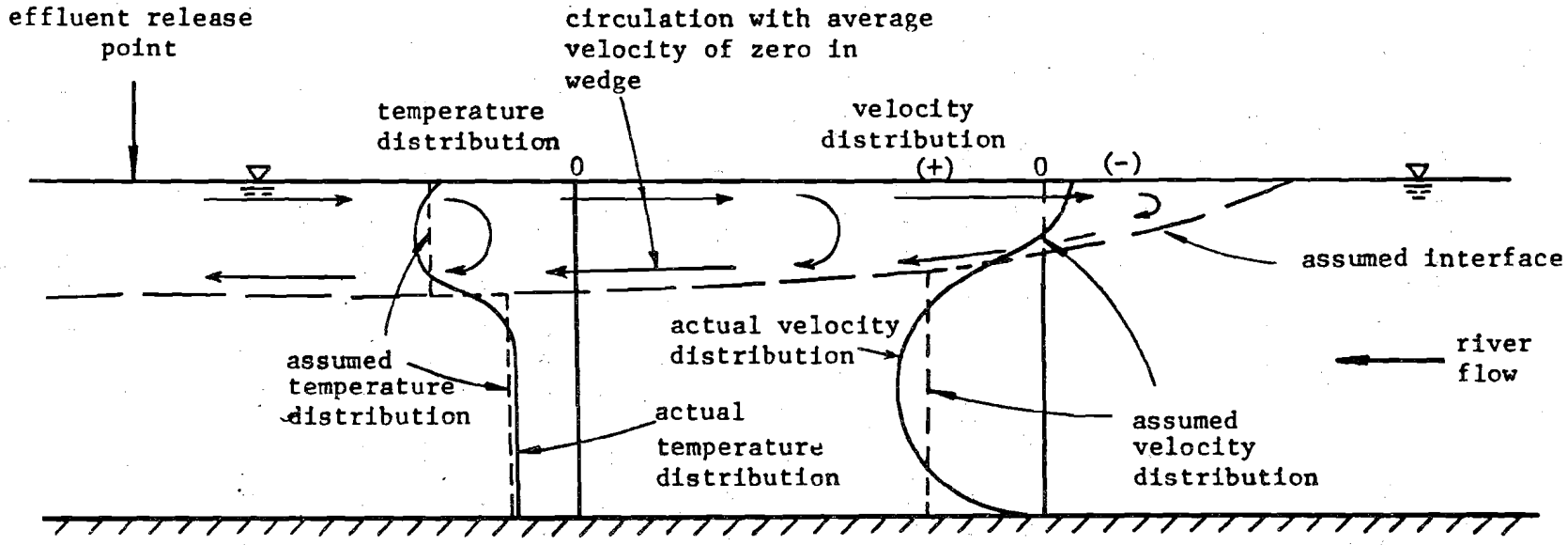

Fig. 1. Schematic Diagram of Arrested Thermal Wedge

II. REVIEW OF LITERATURE

There has been considerable attention focussed on the general problem of stratified flow during the past 30 years. This has included problems involving density difference caused by suspended sediment concentration differences, by salinity differences, by temperature differences or due to spillage of a fluid of lighter density on the surface of another (e.g. oil on water). There will be no attempt herein to deal with all of this material, rather attention will be focussed on selected items which the authors have found particularly useful in connection with the present study of arrested wedges.

Generally the Proceedings of Congresses and Symposia (13) of the International Association for Hydraulic Research contain numerous papers on various aspects of stratified flow. There are a number of "state-of-the-art" articles dealing with the mechanics of stratified flow. These include works by Harleman (8)(9), Parker and Krenkel (25), Harleman and Stolzenbach (10), and Turner (35).

Numerous studies of two-layer stratified flow relating to this investigation have been made. In 1957 Bata (3) presented an analysis of a two-layer stratified flow involving an upper, heated layer and a lower, unheated layer and derived a solution for wedge length and geometry upstream from a cooling water intake. The analysis was developed from the earlier analysis of Schijf and Schönfeld (29) and treated the two layers as distinct. In the special case of a stable thermal wedge the discharge in the upper layer is taken as zero and the upper layer is treated as "stagnant". In reality, however, there is a warm water circulation with water moving both upstream and downstream in the upper layer; mixing occurs at the interface between the warm water and the

underlying cold water so that the transition from one layer to the other is gradual and indistinct (see Fig. 1). Physically no distinct interface exists; both the velocity distribution and the temperature distribution vary continuously in the vertical direction.

Polk, et al (26), observed the circulation pattern in the warm upper layer and the gradual decrease in temperature with depth and upstream distance when they conducted field observation of density wedges at several steam power plant sites. In order to make use of Bata's wedge length formula, they calculated the average temperature in the wedge for each site using that portion of the temperature profile above the depth which will give a net discharge of zero in the upper layer when the velocity profile is integrated vertically. Their field data agreed fairly well with Bata's theoretical solution.

Majewski (21) in 1965 reported the results of laboratory experiments on the development and stabilization of overflow and underflow arrested wedges generated by density differences resulting from temperature differences between the main flow and the wedge inflow and from salinity. Some of the conclusions of his experiments were:

(i) the length of arrested wedge was a function of the densimetric Froude number.

(ii) for investigated cases it was found that variation of the wedge inflow discharge has no significant influence on the shape and the length of the arrested wedge.

(iii) for the same flow conditions and the same density differences, the underflow case has a longer arrested wedge length than the overflow case.

In order to make use of any wedge length formula to compute wedge length and geometry upstream from a critical control section, the

interfacial shear stress coefficient must be determined. When the flow is laminar it is accessible to theoretical analysis. Keulegan (16), Bata (4), Ippen and Harleman (14) have found that the interfacial shear stress coefficient is a function of Reynolds number for laminar flows. It is not subject to exact analysis when the flow at or near the interface is in any degree turbulent. Determination of the interfacial shear stress coefficient thus depends upon experiment.

The problem of determining the interfacial shear has been investigated by many authors. However, various investigators have carried out experiments in different situations and, as mentioned in the Introduction, presented their results in different ways and in different relation to different parameters. There has not therefore been established a satisfactory method for predicting suitable values of interfacial shear stress coefficient for a two-layer stratified flow.

Lofquist (19) in 1960 presented the results of extensive studies (both analytical and experimental) on the flow and stress near an interface between stratified liquids. A turbulent flow of salt water under a pool of fresh water was studied. Measurements included interface slope, the velocity and density profile, and the rate of mixing. The interfacial shear stress coefficients were computed from the observations and the equation of motion. The results showed that the interfacial shear stress coefficients depended on Reynolds number, densimetric Froude number and also on $\Delta\rho/\rho$. There was a considerable scatter in the results.

Macagno and Rouse (20), studied the problem of interfacial mixing in stratified flow in a conduit of rectangular cross-section. Experiments were performed with fresh and salt water. The interfacial

shear (which was presented in terms of the ratio of the actual stress to the viscous stress for main flow) showed a definite correlation with Reynolds number and densimetric Froude number.

The problem of interfacial shear has also drawn considerable interest in Japan. Iwasaki (15) in 1964 proposed the following formula to relate f_i with Reynolds number and densimetric Froude number

$$f_i = 31.52 \ (\mathrm{Re}\ F_\Delta^2)^{-0.8356} \tag{5}$$

Shi-igai (31) analyzed the effects of internal waves on the energy dissipation at the interface and suggested that the interfacial shear stress mainly depended upon the energy dissipation caused by internal waves. He derived theoretically the expression for f_i as a function of $\mathrm{Re}\ F_\Delta^2$

$$f_i = \frac{c}{\mathrm{Re}\ F_\Delta^2} \tag{6}$$

in which c = constant. In a later paper, Shi-igai (32) suggested a general formula

$$f_i = 31.6 \times 10^{-4} \times (6.45 \times 10^4)^n \ (\mathrm{Re}\ F_\Delta)^{-n} \tag{7}$$

By choosing suitable value of n, one can comparatively cover the forms of f_i proposed by many authors.

There have been some attempts to seek a general correlation for some of the interfacial shear stress data in the literature. Sjoberg (33) used the data given by Lofquist (19), Macagno and Rouse (20) and Michon, et al (23) and found that the ratio of the total stress to its laminar component has definite correlation with Re and $\mathrm{Re}\ F_\Delta^2$. Sherenkov et al (30) plotted data from seven sources and again found a

general correlation between f_i and Re F_Δ^2, but with relatively large scatter.

Analytical and experimental work has also been done on some special cases of a two-layered system. Keulegan (18) has done extensive experiments on an arrested salt wedge. Abraham and Eysink (1) presented an experimental relationship between f_i and Re for the case of lock exchange flow. Cross and Hoult (5), and Wilkinson (37)(38) have published data and analyses for the case of contained oil slicks.

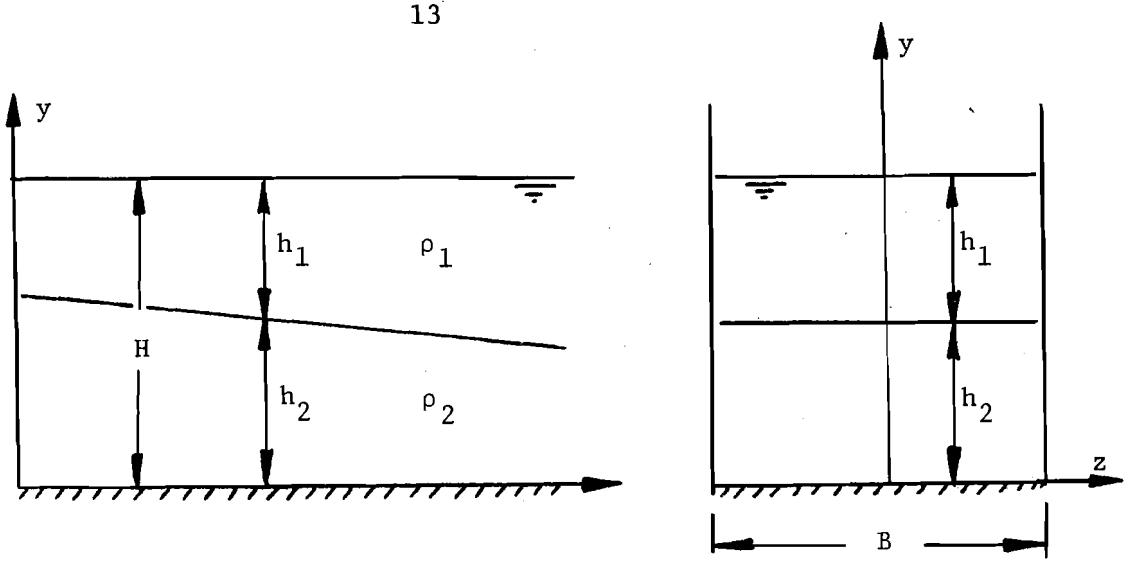

(a) General Two-Layer Stratified Flow

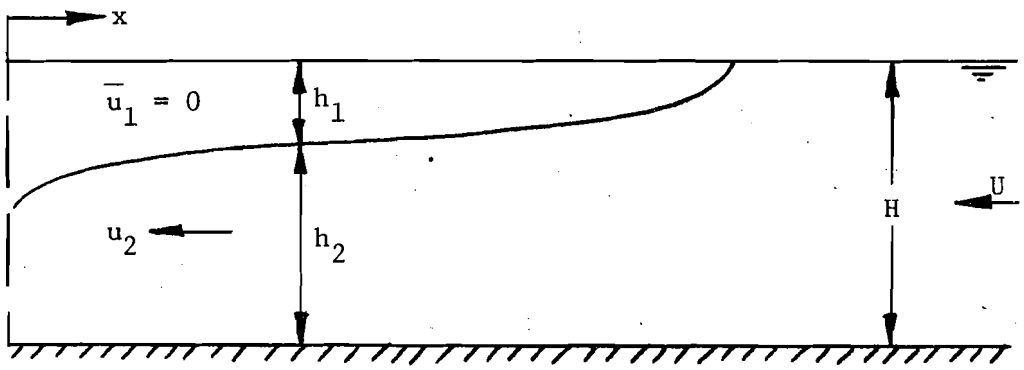

(b) Arrested Thermal Wedge (underflow)

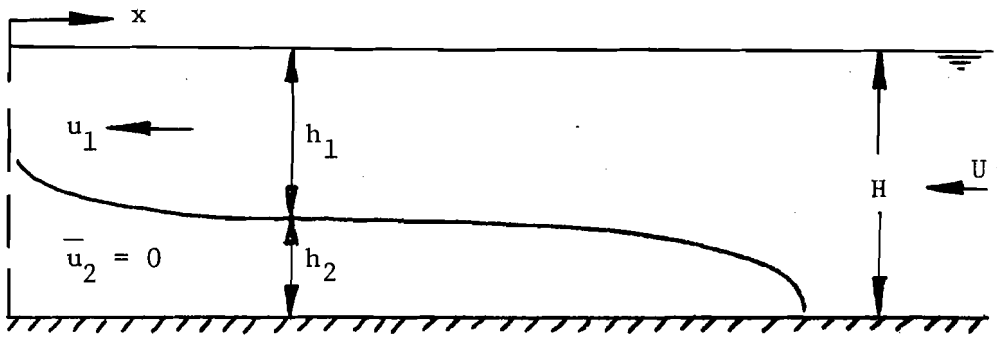

(c) Arrested Cold Water Intrusion (overflow)

Fig. 2. Definition Sketches for Stratified Flows

III. EQUATIONS FOR TWO-LAYERED FLOW

III-1. General Analysis

In the following analysis vertical and lateral components of acceleration will be ignored. With reference to the definition sketch shown in Fig. 2 the continuity equation for the upper layer of a two-layer stratified flow is given by

$$\frac{\partial \rho_1}{\partial t} + \frac{\partial}{\partial x}(\rho_1 u_1) + \frac{\partial}{\partial y}(\rho_1 v_1) + \frac{\partial}{\partial z}(\rho_1 w_1) = 0 \tag{8}$$

The x - component of the equation of motion is

$$\rho_1 \frac{\partial u_1}{\partial t} + \rho_1 u_1 \frac{\partial u_1}{\partial x} + \rho_1 v_1 \frac{\partial u_1}{\partial y} + \rho_1 w_1 \frac{\partial u_1}{\partial z}$$

$$= -\frac{\partial p_1}{\partial x} + \frac{\partial \sigma_x^1}{\partial x} + \frac{\partial \tau_{yx}}{\partial y} + \frac{\partial \tau_{zx}}{\partial z} \tag{9}$$

In these equations u_1 = local downstream velocity component in the upper layer; v_1 = local vertical velocity component in the upper layer; w_1 = local transverse velocity component in the upper layer; ρ_1 = local fluid density in the upper layer; p_1 = local pressure in the upper layer; t = time; σ_x^1 = deviatoric normal stress in x-direction; τ_{yx}, τ_{zx} = tangential stresses. The first subscript indicates the direction of the normal to the plane of action and the second the direction of action. Tangential stress is taken as positive if the outward normal and the action are both positively or both negatively directed, and negative if either one is negatively directed.

If it is assumed that the turbulent contribution to the deviatoric stress is dominant the term involving σ_x^1 may be dropped from Eq. 9. For hydrostatic variation of fluid pressure, using a bar to

denote average over the depth

$$p_1 = g \int_y^H \rho_1 \, dy \simeq \bar{\rho}_1 \, g \, (H-y) \text{ for } h_2 \leq y \leq H \tag{10}$$

Integrating Eq. 9 without the term involving σ_x^1 over the depth and across the rectangular channel of width B and using continuity to rearrange the terms on the left hand side yields:

$$\int_{-\frac{B}{2}}^{\frac{B}{2}} \int_{h_2}^{H} \{\frac{\partial(\rho_1 u_1)}{\partial t} + \frac{\partial(\rho_1 u_1^2)}{\partial x} + \frac{\partial(\rho_1 u_1 v_1)}{\partial y} + \frac{\partial(\rho_1 u_1 w_1)}{\partial z}\} \, dydz$$

$$= - \int_{-\frac{B}{2}}^{\frac{B}{2}} \int_{h_2}^{H} \frac{\partial p_1}{\partial x} \, dydz + \int_{-\frac{B}{2}}^{\frac{B}{2}} \int_{h_2}^{H} \frac{\partial \tau_{yx}}{\partial y} \, dydz + \int_{-\frac{B}{2}}^{\frac{B}{2}} \int_{h_2}^{H} \frac{\partial \tau_{zx}}{\partial z} \, dydz \tag{11}$$

Defining

$$\bar{\rho}_1 = \int_{h_2}^{H} \rho_1 \, dy \tag{12}$$

$$\bar{u}_1 = \int_{h_2}^{H} u_1 \, dy \tag{13}$$

$$\alpha_1 = \frac{1}{\bar{\rho}_1 \bar{u}_1 B h_1} \int_{h_2}^{H} \int_{-\frac{B}{2}}^{\frac{B}{2}} (\rho_1 u_1) \, dzdy \tag{14}$$

$$\bar{u}_s = \frac{1}{\bar{\rho}_1 B} \int_{-\frac{B}{2}}^{\frac{B}{2}} (\rho_1 u_1)\big|_{y=H} \, dz \tag{15}$$

$$\bar{u}_1 = \frac{1}{\bar{\rho}_1 B} \int_{-\frac{B}{2}}^{\frac{B}{2}} (\rho_1 u_1)\big|_{y=h_2} \, dz \tag{16}$$

and using Leibniz's formula the first term on the left hand side may be shown to be

$$\int_{h_2}^{H} \int_{\frac{-B}{2}}^{\frac{B}{2}} \frac{\partial}{\partial t} (\rho_1 u_1) \, dzdy = \frac{\partial}{\partial t} (\alpha_1 \bar{\rho}_1 \bar{u}_1 B h_1) - \bar{\rho}_1 \bar{u}_s B \frac{\partial H}{\partial t} + \bar{\rho}_1 \bar{u}_i B \frac{\partial h_2}{\partial t} \quad (17)$$

$$\beta_1 = \frac{1}{\bar{\rho}_1 \bar{u}_1^2 B h_1} \int_{h_2}^{H} \int_{\frac{-B}{2}}^{\frac{B}{2}} \rho_1 u_1^2 \, dzdy \quad (18)$$

$$\overline{u_s^2} = \frac{1}{\bar{\rho}_1 B} \int_{\frac{-B}{2}}^{\frac{B}{2}} (\rho_1 u_1^2)\big|_{y=H} \, dz \quad (19)$$

$$\overline{u_i^2} = \frac{1}{\bar{\rho}_1 B} \int_{\frac{-B}{2}}^{\frac{B}{2}} (\rho_1 u_1^2)\big|_{y=h_2} \, dz \quad (20)$$

The second term on the left hand side of Eq. 11 may be written

$$\int_{h_2}^{H} \int_{\frac{-B}{2}}^{\frac{B}{2}} \frac{\partial (\rho_1 u_1^2)}{\partial x} \, dzdy = \frac{\partial}{\partial x} (\beta_1 \bar{\rho}_1 \bar{u}_1^2 B h_1) - \bar{\rho}_1 \overline{u_s^2} B \frac{\partial H}{\partial x} + \bar{\rho}_1 \overline{u_i^2} B \frac{\partial h_2}{\partial x} \quad (21)$$

The free surface may be represented by

$$y - H(x,t) = 0 \quad (22)$$

The condition that the vertical fluid velocity, v_s, must match the vertical velocity of the free surface is

$$v_s = \frac{\partial H}{\partial t} + u_s \frac{\partial H}{\partial x} \quad (23)$$

in which u_s = x-component of velocity at the free surface. Similarly the interface boundary condition is

$$v_i = \frac{\partial h_2}{\partial t} + u_i \frac{\partial h_2}{\partial x} \tag{24}$$

in which u_i, v_i are the x, y components of velocity at the interface. Using the expressions for v_s and v_i given by Eq. 23 and Eq. 24 the third term on the left hand side of Eq. 11 may be written:

$$\int_{-\frac{B}{2}}^{\frac{B}{2}} \int_{h_2}^{H} \frac{\partial}{\partial y} (\rho_1 u_1 v_1) = \bar{\rho}_1 \bar{u}_s B \frac{\partial H}{\partial t} + \bar{\rho}_1 \overline{u_s^2} B \frac{\partial H}{\partial x} - \bar{\rho}_i \bar{u}_i B \frac{\partial h_2}{\partial t} - \bar{\rho}_1 \overline{u_i^2} B \frac{\partial h_2}{\partial x} \tag{25}$$

Finally, the remaining term on the left hand side of Eq. 11 may be shown to be zero since $u_1 = w_1 = 0$ at $z = \pm \frac{B}{2}$.

Approximating the pressure in the upper layer by Eq. 10 the pressure term on the right hand side of Eq. 11 may be reduced to

$$\int_{-\frac{B}{2}}^{\frac{B}{2}} \int_{h_2}^{H} \frac{\partial p_1}{\partial x} \, dydz = g \, B \left[\frac{\partial}{\partial x} \left(\bar{\rho}_1 \frac{h_1^2}{2}\right) + \bar{\rho}_1 h_1 \frac{\partial h_2}{\partial x}\right] \tag{26}$$

Assuming that shear stress is uniform on the interface and = τ_i the second term on the right hand side of Eq. 11 becomes

$$\int_{-\frac{B}{2}}^{\frac{B}{2}} \int_{h_2}^{H} \frac{\partial \tau_{yx}}{\partial y} \, dydz = - \tau_i B \tag{27}$$

Finally for uniform shear stress on each of the two sidewalls, τ_{w_1}, the remaining term of Eq. 11 may be written

$$\int_{-\frac{B}{2}}^{\frac{B}{2}} \int_{h_2}^{H} \frac{\partial \tau_{zx}}{\partial z} \, dydz = - 2 \tau_{w_1} h_1 \tag{28}$$

Substitution of Eqs. 17, 21, 25, 26, 27 and 28 in Eq. 11 finally yields

$$\frac{\partial}{\partial t} (\alpha_1 \bar{\rho}_1 \bar{u}_1 B h_1) + \frac{\partial}{\partial x} (\beta_1 \bar{\rho}_1 \bar{u}_1^2 B h_1) = - gB \frac{\partial}{\partial x} (\tfrac{1}{2} \bar{\rho}_1 h_1^2)$$

$$- gB\bar{\rho}_1 h_1 \frac{\partial h_2}{\partial x} - \tau_i B - 2\tau_{w_1} h_1 \tag{29}$$

For the lower layer, defining $\bar{\rho}_2$, $\bar{u}_2$, α_2 and β_2 analagous to $\bar{\rho}_1$, $\bar{u}_1$, α_1 and β_1, except that integrations with respect to y range from 0 to h_2, and approximating the lower layer pressure by

$$p_2 = g\bar{\rho}_1 h_1 + g \int_y^{h_2} \rho_2 \, dy \simeq g \, [\bar{\rho}_1 h_1 + \bar{\rho}_2 (h_2 - y)] \text{ for } 0 \leq y \leq h_2 \tag{30}$$

The result is

$$\frac{\partial}{\partial t} (\alpha_2 \bar{\rho}_2 \bar{u}_2 B h_2) + \frac{\partial}{\partial x} (\beta_2 \bar{\rho}_2 \bar{u}_2^2 B h_2) = - gB \frac{\partial}{\partial x} \{\tfrac{1}{2} \bar{\rho}_2 h_2^2 + \bar{\rho}_1 h_1 h_2\}$$

$$+ gB\bar{\rho}_1 h_1 \frac{\partial h_2}{\partial x} + B \, (\tau_i - \tau_b) - 2\tau_{w_2} h_2 \tag{31}$$

in which τ_b is a uniform bed shear stress and τ_{w_2} is a uniform sidewall shear stress. Now, assuming that $\alpha_1 = \alpha_2 = \beta_1 = \beta_2 = 1$, that B is a constant, and that steady state exists Eq. 29 and Eq. 31 reduce to

$$\frac{d}{dx} (\bar{\rho}_1 u_1^2 h_1 + \frac{1}{2} g\bar{\rho}_1 h_1^2) + g\bar{\rho}_1 h_1 \frac{dh_2}{dx} = - \tau_i - 2\tau_{w_1} h_1 / B \tag{32}$$

and

$$\frac{d}{dx}\left(\bar{\rho}_2\bar{u}_2^2 + \frac{1}{2}g\bar{\rho}_2h_2^2 + g\bar{\rho}_1h_1h_2\right) - g\bar{\rho}_1h_1\frac{dh_2}{dx} = \tau_i - \tau_b - 2\tau_{w_2}h_2/B \quad (33)$$

Neglecting entrainment and using B = constant, conservation of mass for the upper layer yields

$$\frac{d}{dx}\left(\bar{\rho}_1\bar{u}_1h_1\right) = 0 \quad (34)$$

and for the lower layer

$$\frac{d}{dx}\left(\bar{\rho}_2\bar{u}_2h_2\right) = 0 \quad (35)$$

Assuming H = constant, so that

$$\frac{dh_1}{dx} + \frac{dh_2}{dx} = 0 \quad (36)$$

and letting

$$F_1^2 = \bar{u}_1^2/(gh_1) \quad (37)$$

Eq. 31 may be rearranged to yield

$$F_1^2\frac{dh_2}{dx} + \left(\frac{1}{2} - F_1^2\right)\frac{h_1}{\bar{\rho}_1}\frac{d\bar{\rho}_1}{dx} + \frac{\tau_i}{\bar{\rho}_1gh_1} + \frac{2\tau_{w_1}}{\bar{\rho}_1gB} = 0 \quad (38)$$

Letting

$$\Delta\rho = \bar{\rho}_2 - \bar{\rho}_1 \quad (39)$$

and

$$F_2^2 = \bar{u}_2^2/(gh_2) \quad (40)$$

Eq. 31 may be rearranged to give

$$\left(\frac{\Delta\rho}{\bar{\rho}_2} - F_2^2\right)\frac{dh_2}{dx} + \frac{h_1}{\bar{\rho}_2}\frac{d\bar{\rho}_1}{dx} + \left(\frac{1}{2} - F_2^2\right)\frac{h_2}{\bar{\rho}_2}\frac{d\bar{\rho}_2}{dx} - \frac{\tau_i - \tau_b}{\bar{\rho}_2 g h_2} + \frac{2\tau_{w_2}}{\bar{\rho}_2 g B} = 0 \quad (41)$$

Letting

$$F_{\Delta_1}^2 = F_1^2/(\Delta\rho/\bar{\rho}_2) \quad (42)$$

and

$$F_{\Delta_2}^2 = F_2^2/(\Delta\rho/\bar{\rho}_2) \quad (43)$$

Eq. 38 and Eq. 41 may be combined to yield:

$$\left(F_{\Delta_1}^2 + F_{\Delta_2}^2 - 1\right)\frac{dh_2}{dx} = \left\{F_{\Delta_1}^2 + 1/(\Delta\rho/\bar{\rho}_1) - \frac{1}{2}/(\Delta\rho/\bar{\rho}_2)\right\}\frac{h_1}{\bar{\rho}_1}\frac{d\bar{\rho}_1}{dx}$$

$$+ \left\{\frac{1}{2}/(\Delta\rho/\bar{\rho}_2) - F_{\Delta_2}^2\right\}\frac{h_2}{\bar{\rho}_2}\frac{d\bar{\rho}_2}{dx} - \tau_i/\left(\frac{\Delta\rho}{\bar{\rho}_2}\bar{\rho}_1 g h_1\right)$$

$$- (\tau_i - \tau_b)/\left(\frac{\Delta\rho}{\bar{\rho}_2}\bar{\rho}_2 g h_2\right) - 2\tau_{w_1}/\left(\frac{\Delta\rho}{\bar{\rho}_2}\bar{\rho}_1 g B\right) + 2\tau_{w_2}/\left(\frac{\Delta\rho}{\bar{\rho}_2}\bar{\rho}_2 g B\right) \quad (44)$$

The wall, interfacial and bed shear stresses may be expressed as

$$\tau_{w_j} = \frac{1}{8} f_{w_j}\bar{\rho}_j|\bar{u}_j|\bar{u}_j;\ j = 1, 2 \quad (45)$$

$$\tau_i = \frac{1}{8} f_i \bar{\rho}_1|\bar{u}_1 - \bar{u}_2|(\bar{u}_1 - \bar{u}_2) \quad (46)$$

$$\tau_b = \frac{1}{8} f_b \bar{\rho}_2|\bar{u}_2|\bar{u}_2 \quad (47)$$

in which f_{w_j}, f_i and f_b are dimensionless friction factors.

Simplifying some terms by use of the Boussuiesq approximation ($\bar{\rho}_1/\bar{\rho}_2 \simeq 1$) and introducing the dimensionless quantities

$$r = x/H \tag{48}$$

$$\eta = h_2/H \tag{49}$$

Eq. 44 may be written

$$\frac{dr}{d\eta} = 8\,(F_{\Delta_1}^2 + F_{\Delta_2}^2 - 1)/\{8\,(F_{\Delta_1}^2 + \frac{\bar{\rho}_1-\Delta\rho}{2\Delta\rho})\,\frac{(1-\eta)}{\bar{\rho}_1}\,\frac{d\bar{\rho}_1}{dr}$$

$$+ 8\,(\frac{1}{2\Delta\rho/\bar{\rho}_2} - F_{\Delta_2}^2)\,\frac{\eta}{\bar{\rho}_2}\,\frac{d\bar{\rho}_2}{dr} - f_i H\,\frac{|\bar{u}_1-\bar{u}_2|(\bar{u}_1-\bar{u}_2)}{\frac{\Delta\rho}{\bar{\rho}_2}\,gh_1h_2}$$

$$+ f_b\,\frac{|\bar{u}_2|\bar{u}_2}{\frac{\Delta\rho}{\bar{\rho}_2}\,gh_2} - 2f_{w_1}\,\frac{|\bar{u}_1|\bar{u}_1}{\frac{\Delta\rho}{\bar{\rho}_2}\,gh_1}\,(1-\eta)\,\frac{H}{B} + 2f_{w_2}\,\frac{|\bar{u}_2|\bar{u}_2}{\frac{\Delta\rho}{\bar{\rho}_2}\,gh_2}\,\eta\,\frac{H}{B}\} \tag{50}$$

III-2. Arrested Thermal Wedge

For the special case of the arrested thermal wedge (see Fig. 2b)

$$\bar{u}_1 = F_{\Delta_1}^2 = \tau_{w_1} = 0 \text{ and } u_2 < 0$$

so that Eq. 50 simplifies to

$$\frac{dr}{d\eta} = 8\,(F_{\Delta_2}^2 - 1)/\{4\,(\frac{\bar{\rho}_1-\Delta\rho}{\Delta\rho})\,\frac{(1-\eta)}{\bar{\rho}_1}\,\frac{d\bar{\rho}_1}{dr} + 8\,(1/(2\Delta\rho/\bar{\rho}_2) - F_{\Delta_2}^2)\,\frac{1}{\bar{\rho}_2}\,\frac{d\bar{\rho}_2}{dr}\,\eta$$

$$- F_{\Delta_2}^2\,(f_i/(1-\eta) + f_b + 2\frac{H}{B}\eta f_{w_2})\} \tag{51}$$

III-3. Arrested Cold Water Intrusion

For the special case of the arrested cold water intrusion (see Fig. 2c)

$$\bar{u}_2 = F_{\Delta_2}^2 = \tau_{w_2} = 0 \text{ and } u_1 < 0$$

so that Eq. 50 simplifies to

$$\frac{dr}{d\eta} = 8\,(F_{\Delta_1}^2 - 1)/\{F_{\Delta_1}^2\,(f_i/\eta + 2\frac{H}{B}f_{w_1}\,(1-\eta)) + 8\,(F_{\Delta_1}^2 + \frac{\bar{\rho}_1-\Delta\rho}{\Delta\rho})\,\frac{(1-\eta)}{\bar{\rho}_1}\,\frac{d\bar{\rho}_1}{dr} + \frac{4}{\Delta\rho}\,\frac{d\bar{\rho}_2}{dr}\,\eta\} \qquad (52)$$

III-4. Evaluation of Sidewall Friction and Bed Friction

When the longitudinal variation in density and the sidewall friction for each of the two layers is neglected the above equations reduce to those obtained by others (3)(9).

In order to evaluate the sidewall, bed and interfacial friction factors in the above equations a means must be utilized for associating a Reynold's number with each. In this study the method proposed by Einstein and Barbarossa (7)(2) was adopted. Parts of the total flow are considered to be associated with the bed, the sidewalls and the interface. The energy slope, S, is taken common to all parts and the mean velocity in each part is assumed equal to the overall mean velocity. For the arrested thermal wedge, equating areas

$$Bh_2 = R_b B + 2R_{w_2} h_2 + R_i B \qquad (53)$$

in which R_b, R_{w_2} and R_i are the hydraulic radii and B, h_2 and B are the wetted perimeters associated with the bed, sidewalls and interface respectively.

For the arrested cold water intrusion the corresponding result is

$$Bh_1 = 2R_{w_1} h_1 + R_i B \tag{54}$$

For the arrested thermal wedge the Darcy-Weisbach equation then yields

$$\frac{f_i}{R_i} = \frac{f_b}{R_b} = \frac{f_{w_2}}{R_{w_2}} = \frac{8S_2 g}{\bar{u}_2^2} \tag{55}$$

in which S_2 is the energy slope for the lower layer. The corresponding result for the arrested cold water intrusion is

$$\frac{f_i}{R_i} = \frac{f_{w_1}}{R_{w_1}} = \frac{8S_1 g}{\bar{u}_1^2} \tag{56}$$

Defining

$$Re = \frac{\bar{U}H}{\nu} \tag{57}$$

and assuming $\nu_1 \simeq \nu_2 \simeq \nu$, the kinematic viscosity of the fluid, Eqs. 53, 55 and 57 yield

$$R_b = \eta H/(1 + f_i/f_b + 2 \frac{f_{w_2}}{f_b} \frac{H}{B} \eta) \tag{58}$$

and

$$Re_b = 4\bar{u}_2 R_b/\nu = 4Re/(1 + f_i/f_b + 2 \frac{f_{w_2}}{f_b} \frac{H}{B} \eta) \tag{59}$$

Moreover

$$R_{w_2} = R_b f_{w_2}/f_b \tag{60}$$

so that

$$Re_{w_2} = 4\bar{u}_2 R_{w_2}/\nu = Re_b f_{w_2}/f_b \tag{61}$$

For the arrested cold water intrusion

$$R_{w_1} = (1-\eta)\ H/(f_i/f_{w_2} + 2\ (1-\eta)\ H/B) \tag{62}$$

and

$$Re_{w_1} = 4\bar{u}_1 R_{w_1}/\nu = 4Re/(f_i/f_{w_2} + 2\ (1-\eta)\ H/B) \tag{63}$$

Friction factors were calculated using a modified Colebrook relation (11) for open channels

$$\frac{1}{\sqrt{f_j}} = -\ 2\ \log_{10}\ \left(\frac{k_j}{12R_j} + \frac{2.5}{Re_j\sqrt{f_j}}\right) \tag{64}$$

in which k_j = equivalent sand grain roughness diameter. For smooth walls k_j may be set equal zero, or, for values of $Re_j < 10^5$ Eq. 64 may be replaced by the simpler Blasius relationship:

$$f_j = 0.316/(Re_j)^{1/4} \tag{65}$$

III-5. Laminar Overflow Versus Laminar Underflow

In the Introduction it was pointed out that there may be differences in the internal mechanics, and therefore in the interfacial momentum transfer, between overflows and underflows. Without knowing the details of the turbulence structure it is not possible to calculate the momentum transfer from basic principles for turbulent flow. However, it is possible for laminar flow under certain simplifying assumptions. As

shown below such computations indicate a different f_i for underflows and overflows for laminar flow. Thus, it may be reasonable to expect a difference for turbulent flows also.

Ippen and Harleman (14) considered the case of a steady, uniform, laminar underflow for which the depth was small in comparison to the upper fluid. Their work indicated a constant ratio between the fluid velocity at the interface, u_i, and the maximum fluid velocity, u_m, such that

$$u_i/u_m = 0.59 \tag{66}$$

This yielded the result

$$\frac{1}{c_f} = 0.114 Re_2 \tag{67}$$

in which c_f is a resistance coefficient = f/4. This includes both the resistance of the interface and the bottom. The Reynolds number is based on $\bar{u}_2$ and h_2. The analysis also indicated that $\tau_i = 0.64\tau_b$, where τ is the shear stress.

$$\tau = \tau_b + \tau_i = c_f \frac{\rho_2 \bar{u}^2}{2} = \frac{f}{8} \rho_2 \bar{u}^2 \tag{68}$$

With

$$\tau_b = \frac{f_b}{8} \rho_2 \bar{u}_2^2 \tag{69}$$

and

$$\tau_i = \frac{f_i}{8} \rho_2 \bar{u}_2^2 \tag{70}$$

it follows that $f_i = 0.64 f_b$ and Eq. 68 yields

$$f = f_b + f_i = 2.56 f_i \tag{71}$$

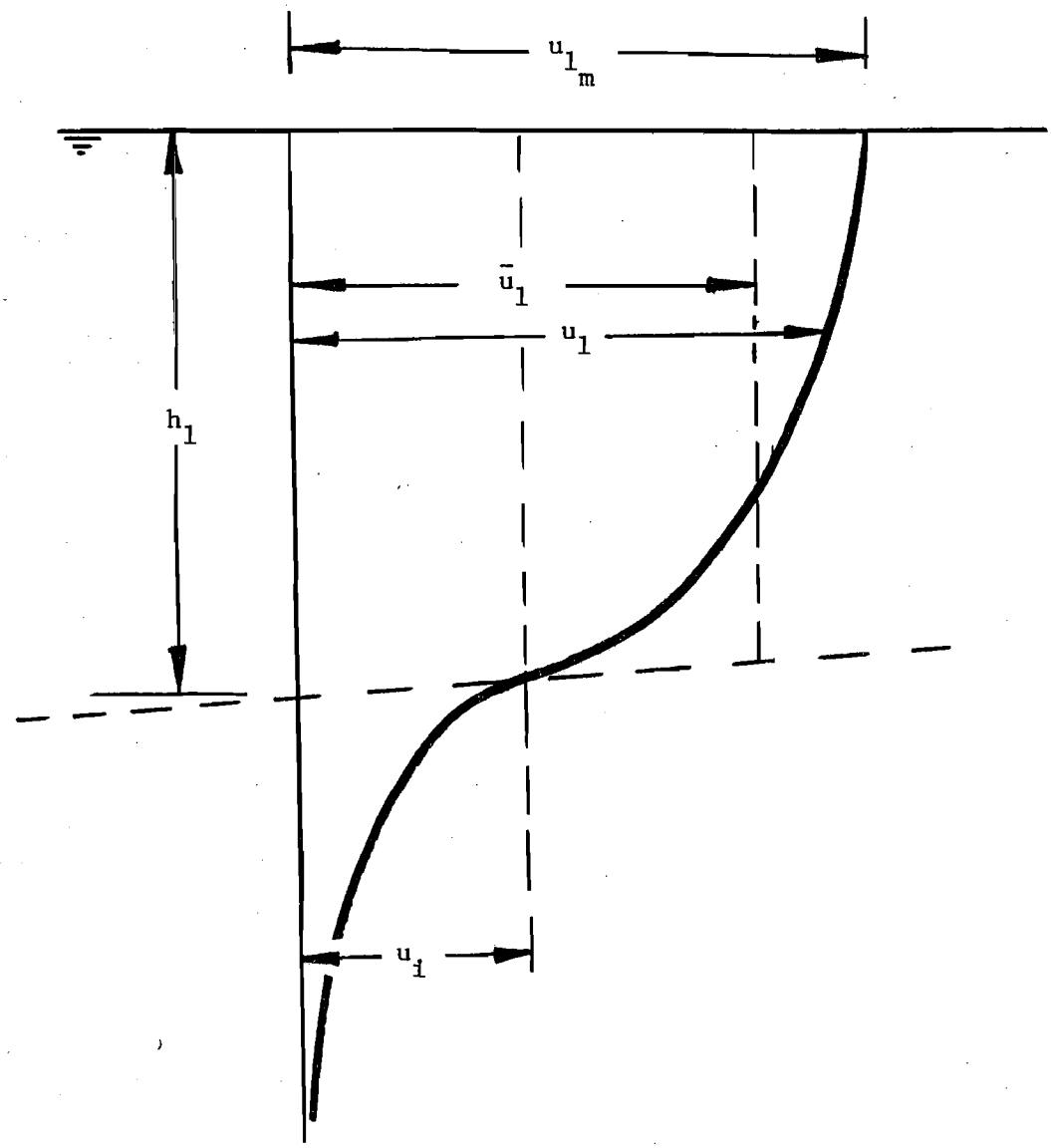

Fig. 3 - Laminar Overflow

Then, from Eq. 67

$$\frac{4}{f} = \frac{4}{2.56f_i} = 0.114Re_2 \tag{72}$$

Hence

$$f_i = \frac{13.7}{Re_2} \tag{73}$$

An analysis similar to the above can be carried out for the case of a laminar overflow as depicted in Fig. 3. For flow over an infinitely deep, now flowing layer, it is not possible to have uniform flow in the upper, moving layer. In addition to the assumptions used by Ippen and Harleman (14) it will be assumed that the flow is gradually varied and that the velocity distribution at each section is the same as it would be for fully developed laminar free surface flow over a boundary moving with the local value of the velocity, u_i. The velocity distribution would then be a combination of a uniform flow with velocity u_i, plus a parabolic distribution varying from u_i at the interface to u_{l_m} at the free surface. This is, no doubt, not exactly correct but would appear to be a reasonable first estimate by virture of the fact that the velocity distribution for other gradually varied, laminar flows is nearly parabolic e.g. a laminar boundary layer on a stationary plate with no pressure gradient (27). Since the velocity distribution is assumed to be the sum of a uniform distribution and a parabolic distribution, the velocity gradient at the interface, and therefore τ_i, will be the same as for a laminar open-channel flow whose velocity distribution is just the parabolic part, or $(u_l - u_i)$. For laminar open-channel flow, the bed friction factor is (14)

$$f_b = \frac{24}{Re} \tag{74}$$

Applying this to the parabolic part of the velocity distribution in Fig. 3, for which the average velocity is given by

$$\bar{u}_1 = \frac{2}{3} (u_{1_m} - u_i) \tag{75}$$

the interfacial friction factor is

$$f_i = \frac{24}{\frac{2}{3} (u_{1_m} - u_i) h_1 / \nu} \tag{76}$$

Again, assuming $u_i = 0.59\ u_{1_m}$ as in Eq. 66 then

$$\bar{u}_1 = u_i + \frac{2}{3} (u_{1_m} - u_i) = 0.863 u_{1_m} \tag{77}$$

Eq. 76 then gives.

$$f_i = \frac{75.8}{Re_1} \tag{78}$$

in which Re_1 is based on $\bar{u}_1$ and h_1.

Whereas Ippen and Harleman performed experiments and verified their analysis which led to Eq. 73, there is no direct experimental verification of Eq. 78. Nevertheless, due to the similarity of assumptions in their analysis of the underflow and the present analysis of the overflow, it seems reasonable to expect Eq. 78 to give a reasonable first estimate of f_i for overflows. Comparison of Eq. 73 and Eq. 78 indicates that, for the same value of Reynolds number based on layer depth and mean velocity, the overflow friction factor will be approximately 5.5 times that for the underflow. Note that for the special cases of two-dimensional arrested thermal wedges and arrested cold water intrusions $Re_1 = Re_2 = Re = UH/\nu$. The increased interfacial momentum transfer is due to differences in the details of the flow, specifically

the velocity gradient at the interface for this laminar case, rather than to differences in the gross characteristics of the flows. It may be possible for similar differences to exist for two-dimensional turbulent underflows and overflows. The data presented in Chapter V of this report are used to compare the friction factors for arrested thermal wedges and arrested cold water intrusions in a long 0.98 ft wide channel for which the boundary layer of the main flow could be expected to be fully developed before encountering the wedge. Thus, sidewall effects on the velocity distribution and on the relation between the interface velocity and the maximum velocity would be quite marked. The data, in this circumstance indicate the opposite behavior from that predicted in the two-dimensional laminar analysis. It is interesting to note the sensitivity of the results given by Eq. 73 and Eq. 78 to the assumption of a value for u_i/u_m. If both computations are repeated assuming $u_i/u_m = 0.20$ rather than 0.59 the end result indicates that the overflow friction factor will be 0.76 rather than 5.5 times that for the underflow One might expect a decrease in u_i/u_m as a consequence of boundary layer growth from the sidewalls requiring an increase in maximum velocity to satisfy continuity.

III-6. Dimensional Considerations

Consider a steady one-dimensional, two-layer stratified flow in a wide horizontal channel as shown in the left portion of Fig. 2a. The interfacial friction factor is given functionally as:

$$f_i = \phi\ (f_b, u_1, u_2, h_1, h_2, \mu_1, \mu_2, \rho_1, \rho_2, g) \tag{79}$$

Using the Buckingham π-theorem this relationship can be expressed as

$$f_i = \phi_1\ (f_b, Re_1, Re_2, F_{\Delta_1}, F_{\Delta_1}, F_1, u_1/u_2) \tag{80}$$

If only one layer is moving Eq. 80 may be reduced to

$$f_i = \phi_1 \left(f_b, Re_j, F_{\Delta_j}, F_j\right) \tag{81}$$

in which the dimensionaless parameters are evaluated for the moving layer, j. If the upper layer is the one moving, then f_b could be dropped from Eq. 81. Further, if the free surface slope is negligibly small, then it would be expected that F_j would be small and not significant in Eq. 81 so that

$$f_i = \phi_1 \left(Re_1, F_{\Delta_1}\right) \text{ for overflows} \tag{82}$$

and

$$f_i = \phi_1 \left(f_b, Re_2, F_{\Delta_2}\right) \text{ for underflows} \tag{83}$$

Since f_b is a function of the relative roughness k/h_2 and the Reynolds number Eq. 83,is equivalent to

$$f_i = \phi_1 \left(k/h_2, Re_2, F_{\Delta_2}\right) \text{ for underflows} \tag{84}$$

In developing Eq. 81 several terms were eliminated on the basis of a layer velocity being zero. This is consistent with the original assumption of one-dimensional flow in each layer since a zero velocity would then imply no notion. However, since the non-flowing layer is of course a fluid rather than a solid, there will be some circulation whose average velocity is zero. Thus, one might expect that Eqs. 82 and 84 should also include terms such as h_1/h_2 and μ_1/μ_2. Also, as mentioned in the Introduction, the detailed mechanics of the flow may be different between overflows and underflows and between various other situations so that the actual two-dimensional nature of the flow should lead to other

considerations in defining the functional dependence of f_i.

Even omitting these possible additional considerations from Eqs. 82 through 84, most of the correlations which have been attempted in the literature between f_i and flow parameters have assumed simplifications of these equations. For example, Harleman and Stolzenbach (10) used

$$f_i = \phi\ (Re) \tag{85}$$

on the assumption that F_Δ would be so large for many thermal discharge problems that F_Δ would not be a significant parameter. Sherenkov et al (30) assumed

$$f_i = \phi\ (F_\Delta^2 Re) \tag{86}$$

on the basis of the fact that $F_\Delta^2 Re$ appears as a parameter in defining the stability conditions at the interface. Comparison of Eq. 86 with Eqs. 73 and 78 indicates that Eq. 86 is inconsistent with the analytical results for laminar flows. However, that observation does not speak against the possible usefulness of Eq. 86 for turbulent flows. Abraham and Eysink (1) qualitatively considered the dependence of f_i on both F_Δ and Re. They argued that for constant F_Δ there is probably some value of Re above which f_i would be constant just as for single layer flow over a rough boundary. They also postulated that for constant Re, f_i should increase as F_Δ increased. In short, the reasoning was that f_i is representative of momentum transport across the interface and more momentum should be transfered (larger f_i) for given velocities and layer thickness when there was less density stabilization (smaller $\Delta\rho/\rho_2$ and therefore larger F_Δ). This reasoning appears to be sound except for the fact that there is considerable data indicating an

opposite trend. (See Appendix II and Chapter V.) The mechanics responsible for this observed trend have not been fully explained, as far as the writers know. There is a significant diversity between the results of various investigators so that even fairly extensive studies of one investigator into the functional dependence of f_i on flow parameters are in general not confirmed by another investigator. Again, this points to the need to consider more details of the flow in addition to just the average velocity and layer depths in comparing results of various investigators and in examining the behavior of f_i.

IV. APPARATUS AND EXPERIMENTAL PROCEDURE

IV-1. Apparatus & Measurements

The experimental data are summarized in Appendix I of this report. The series of runs numbered 18 to 30 were made in a 6-ft wide, 4-ft deep and 161-ft long tilting channel. The channel has plexiglass sidewalls and a painted steel bed. The channel bottom was kept horizontal during all the tests. The ambient flow was supplied from the laboratory's constant head tank and introduced to the channel at the head box. Flow depth was controlled by a tail gate.

Water for arrested warm water wedges established in this channel was heated using two A. O. Smith Corp. 40.5 KW, 480 volt electric heaters which could supply about 28 gpm at a temperature of 20F° above ambient. Heated water was fed to 2 ITT Lawler PX-9700 thermostatic mixing valves, together with a separate cold water supply. In order to provide additional head to overcome head losses in the water heaters and in the mixing valves a Gorman-Rupp self-priming centrifugal pump (1 1/2 HP, 3450 RPM) was placed in the head tank supply line common to both the hot and cold water lines. The mixing valves were capable of controlling outlet temperature to ±0.5F° of the setting, regardless of pressure fluctuations in the supply lines. The warm outflow was then distributed evenly across the channel by a diffuser located 8-ft upstream from the tail gate (see Fig. 4).

Observations and measurements were taken from an instrument carriage and a personnel carriage mounted on the channel top rails. Temperature surveys at the water surface and in the air immediately above indicated excessive heat dissipation from the thermal wedges. Since the laboratory was closed the accumulation of heat in the air above the water resulted in the development of unsteady, non-uniform

temperature distributions in the arrested thermal wedges. This was further enhanced by the continuous increase of the ambient temperature during the course of an experiment due to recirculation of the mixed flow and the presence of supply pumps in the system. Moreover, there was a tendency for three-dimensional flow patterns to develop in the vicinity of the upstream end of the arrested wedge. To avoid some of these problems further experiments were conducted in a 0.98-ft wide, 1-ft deep, by 140-ft long channel.

This second, narrower channel, which was levelled horizontally, fed into an 8-ft long, 4-ft wide by 4-ft deep tail box. The water depth in both the tail box and channel was controlled by a skimming box clamped to one side of the tail box. The overflow into the skimming box was pumped into a floor sump, with the discharge rate being set to provide fairly constant cover of the pump suction. The upstream end of the channel was fitted with wire mesh screens to minimize disturbance of the flow, downstream from the point at which flow was introduced. The sidewalls of the channel were of smooth painted fiberglass. The bottom was of the same material with a wire mesh glued to the surface for the entire width and length of the channel. To minimize heat loss from the water surface the entire channel top was draped with clear plastic sheets. These permitted ease of access for taking measurements.

The tests conducted in the 0.98-ft channel are summarized at the beginning of Appendix I. Tests 35 to 59 studied arrested cold water intrusions. For these tests the mixing valve arrangement used for tests 18-30 in the 6-ft channel was now used to deliver a warm water supply through a diffuser placed behind the screens at the upstream end of the 0.98-ft channel. The cold water intrusion was formed by supplying city

water near the bed at the tail box end of the channel. The details of the method of introducing this flow are illustrated in Fig. 4. The diffuser was constructed of 1/4-in. plexiglass with the flow introduced through a hose in the center of the downstream wall. The volume between the plate and the bed was packed with rubberized hair. City water was used in preference to sump water since it was 5 C° cooler.

For the study of arrested thermal wedges the city water supply was inadequate to supply the ambient flow. Head tank water was introduced to the upstream end of the channel behind the screens mentioned previously. At the tail box end of the channel warm water, obtained by mixing hot water from a nearby faucet with cold city water using a single ITT Lawler PX-9700 mixing valve, was supplied. The method of introduction is again illustrated in Fig. 4. Discharge was backwards to the vertical wall of the diffuser box through a layer of rubberized hair.

To investigate the effect of changes of bottom roughness a number of tests were conducted in both the 6-ft and 0.98-ft channels with the bed covered with pea gravel (see Summary Table in Appendix I). A sieve analysis of gravel samples yielded a mean grain size, D_{50} = 0.315-ins. The average thickness of the gravel layers in both channels was about 0.8-ins. The gravel was spread as uniformly as possible. For the analysis of experimental data the effective local flow depth was taken to be the depth from the top of the gravel layer to the water surface plus half of the median grain size diameter. The top of the gravel layer was established by placing a 4-in. diameter circular plate of known thickness on top of the gravel.

Due to the very low magnitude of the velocities encountered, particularly within the wedges, it was not found practical to measure

Tests 18-30
6-ft wide channel
arrested thermal wedges
smooth and rough bed

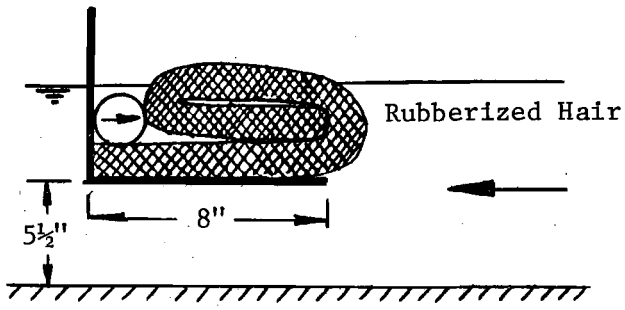

Tests 35-38
0.98-ft wide channel
arrested cold water
intrusions, mesh bed

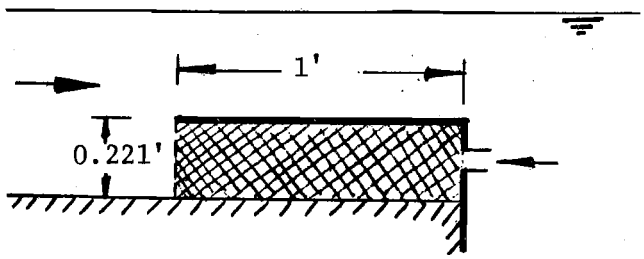

Tests 39-46
0.98-ft wide channel
arrested cold water
intrusions, mesh bed

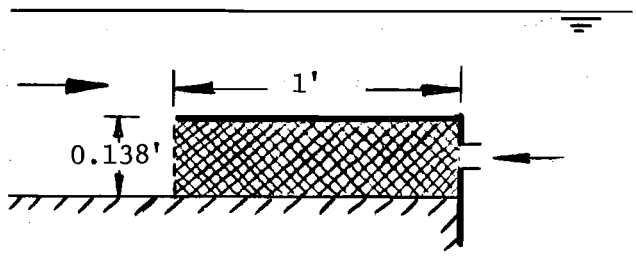

Tests 47-59
0.98-ft wide channel
arrested cold water
intrusions, rough bed

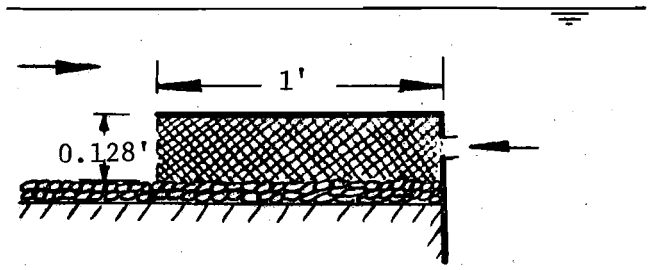

Tests 60-79
0.98-ft wide channel
arrested thermal wedges
mesh and rough bed

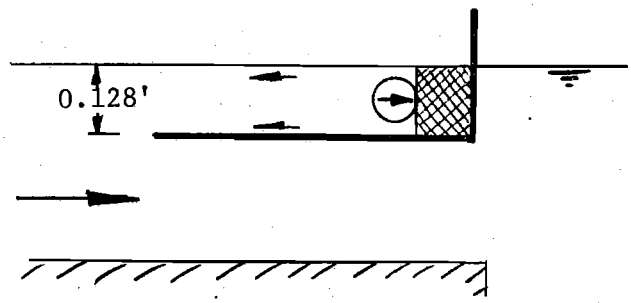

Fig. 4 - Entrance Geometries for Introduction of Wedge Flows

velocities. Consequently the data collection consisted of measurements of temperatures, discharges, flow depths, location of null velocity points, and observations of flow patterns by dye injection.

Vertical temperature profiles along the wedges were measured using YSI 401 thermistor probes. These probes have a time constant of 7 secs and an interchangeability tolerance of ±1C° within a 0 to 80°C range. The probes were monitored using a YSI model 46 tele-thermometer which had an accuracy and readability of ±0.5C° and ±0.05C° respectively.

For arrested thermal wedge measurements in the 6-ft wide channel 9 thermistors were fitted through 7mm. O.D. glass tubes. The tubes were bent at 90° so that the tip faced into the ambient flow. The tip openings were sealed with epoxy. The probes were rigidly clamped to a horizontal plate at 8-in. intervals symmetrically about the channel centerline. The clamping plate was aligned normal to the ambient flow direction and supported by two point gages attached to the instrument carriage. The probes were levelled and aligned with respect to a stagnant water surface. Their submergence was measured to 0.001-ft. Preliminary measurements indicated that not all probes were required to represent lateral variations of temperature. Consequently the number of probes was reduced to five, spaced sixteen inches apart and again set symmetrically about the channel centerline. The probe readings were used to establish an average value for the section.

In the 0.98-ft channel a single vertical profile was obtained at the centerline of the channel for each longitudinal station. The thermistor probe was passed down through a copper tube which replaced the point on a standard Lory Point Gage. The lead then passed through the interior of the main body of the point and out the top. The probe tip

was not bent in the direction of the ambient flow but protruded vertically below the end of the copper tube, with which it was not in contact. The end of the tube was again sealed with epoxy.

Ambient and wedge flow discharges were measured using elbow meters and orifice meters which had been calibrated in situ.

Points of null velocity and wedge tips were located by observing flow reversals. For location of null velocity points a solution of potassium permanganate was oozed through a hypodermic needle under the action of gravity. The injector was fixed to a point gage to monitor submergences. It was generally quite difficult to find the null point at sections close to the injection point for the wedge fluid due to vigorous mixing between the two layers in that vicinity. The wedge tips could be located accurately by dropping potassium permanganate crystals in the flow.

Flow depths were obtained using point gages which could be read to 0.001 ft. Initially gravel layer thicknesses were measured at various stations using the plate mentioned previously to determine the top of the layer. During actual tests the standard point was replaced by a much finer one which could be forced through the gravel layer to locate the channel bed. The distance from the water surface to the bed was thus measured directly and the effective depth of flow, as defined earlier, found by subtraction of the gravel layer thickness.

In order to calibrate the roughness of the pea gravel in situ in both channels, to establish that the 6-ft channel indeed behaved as though the walls and bed were smooth in the absence of gravel, and to calibrate the roughness of the wire mesh on the bed of the 0.98-ft wide channel a number of tests were conducted for unstratified flows, using

discharges well above those encountered in the wedge studies. Water surface profiles, referred to stagnant horizontal water surfaces, were measured, together with flow depths. In the 6-ft channel a vertical turbine pump delivering about 9 cfs provided the discharge which was measured in a calibrated volumetric basin below the tail gate. This had a capacity of 1323 cubic feet. In the 0.98-ft wide channel a closed recycling line with a 15 HP Crane Co. Deming pump, discharging through a calibrated orifice meter provided the necessary discharge.

In the 6-ft channel an average surface slope was established and used to compute the friction factor. In the 0.98-ft channel there were sufficient longitudinal variations that the channel was subdivided into a number of longitudinal segments and the friction factor computed for each. An average value was then used for the entire channel. The calculations took into account and corrected for wall shear as outlined in Eqs. 53 through 65. In this case the absence of stratification somewhat simplified the procedure. Equating areas, as in the development of Eq. 53 now yields

$$BH = R_b B + 2HR_w \tag{87}$$

The Darcy-Weisbach equation yields

$$\frac{8Sg}{U^2} = \frac{f_b}{R_b} = \frac{f_w}{R_w} = \frac{f}{R} \tag{88}$$

in which f and R are overall section values. Thus

$$R = BH/(B+2H) \tag{89}$$

Combining the above equations it may be shown that

$$f_b = (1+2\frac{H}{B})\ f - 2\frac{H}{B} f_w \qquad (90)$$

For smooth walls f_w may be calculated using Eq. 64, with $k_w = 0$, or for $Re_w < 10^5$, using Eq. 65. Since f and R are known from the measurements, R_b may now be found from Eq. 88. Finally with $Re_b = 4UR_b/\nu$, Eq. 64 may be used to solve for k_b. The results for the various channels are listed on the first page of Appendix I.

The apparent difference between k_b for pea gravel in the 6-ft and the 0.98-ft wide may reflect differences in linearity of the bed. The apparent difference is substantially modified by the logarithmic relationship in Eq. 64, yielding closer values of f for the same R and Re than one might at first glance expect.

IV-2. Typical Experimental Procedure

(i) The ambient flow depth was set by adjusting either the tail gate for the 6-ft channel, or the skimming box for the 0.98-ft channel, while at the same time adjusting the discharge to obtain a desired Reynolds number. In the 6-ft channel the flow depth was generally kept constant and the flow varied. The ambient temperature was checked.

(ii) The wedge flow was turned on and its temperature set to obtain a desired temperature difference (In the case of arrested cold water wedges the ambient temperature was adjusted). Since Majewski's (21) tests indicated little dependence on wedge flow discharge no attempt was made to vary wedge flow discharges systematically.

(iii) The flow was permitted to develop for 30 to 60 minutes, depending upon the expected wedge length. The wedge tip location was then checked frequently to determine if the flow was stabilized.

(iv) Once the flow became steady, vertical temperature traverses were taken, proceeding towards the wedge tip. Determination of null veloc- and flow depth was made at each cross section immediately upon completion of the vertical temperature traverse. Depending on wedge length, two to seven cross sectional traverses were made.

(v) Mixing valve temperatures, discharge meter manometers and wedge tip location were monitored at fifteen to thirty minute intervals for the duration of the test. Overall averages were used for data analysis.

The entire test procedure generally lasted for about four hours.

V. ANALYSIS AND RESULTS

V-1. Analysis of Experimental Data

A consistent method for defining wedge thickness was sought which would never result in local values of densimetric Froude number at the downstream station in excess of unity. The method finally selected for the final analysis of the data was to prepare plots of $\Delta T/\Delta T_{max}$ versus $(H-y)/H$. Here T = temperature, $\Delta T = T - T_{min}$, and $\Delta T_{max} = T_{max} - T_{min}$, with T_{max} = maximum temperature and T_{min} = minimum temperature. A straight line was fitted to the data for a particular profile with particular emphasis on the data points in the range $0.20 < \Delta T/\Delta T_{max} < 0.80$. For the definition of the arrested thermal wedge this straight line was projected to the right axis ($\Delta T/\Delta T_{max} = 1$) and the intercept defined to be the interface. For an arrested cold water intrusion the analogous procedure was to project the line to the left axis ($\Delta T/\Delta T_{max} = 0$) and define this intercept to be the interface.

Following such definitions of the interface the dimensionaless plots shown in Fig. 5 and Fig. 6 were prepared for arrested thermal wedges and arrested cold water intrusions respectively. It will be noted from Fig. 5 that the temperature profiles taken in the 6-ft channel virtually collapse into a single curve when plotted in this manner, whereas the data for the narrower 0.98-ft wide vary with aspect ratio of the flow cross section. For a particular wedge there is a consistent trend with B/h_2. However there is no apparent consistency with B/h_2 when several different wedges are compared. The data for arrested cold water intrusions shown in Fig. 6 also exhibit variations with flow cross section aspect ratio.

A comparison was made between the vertical position of null velocity points and interface position as defined above. For the

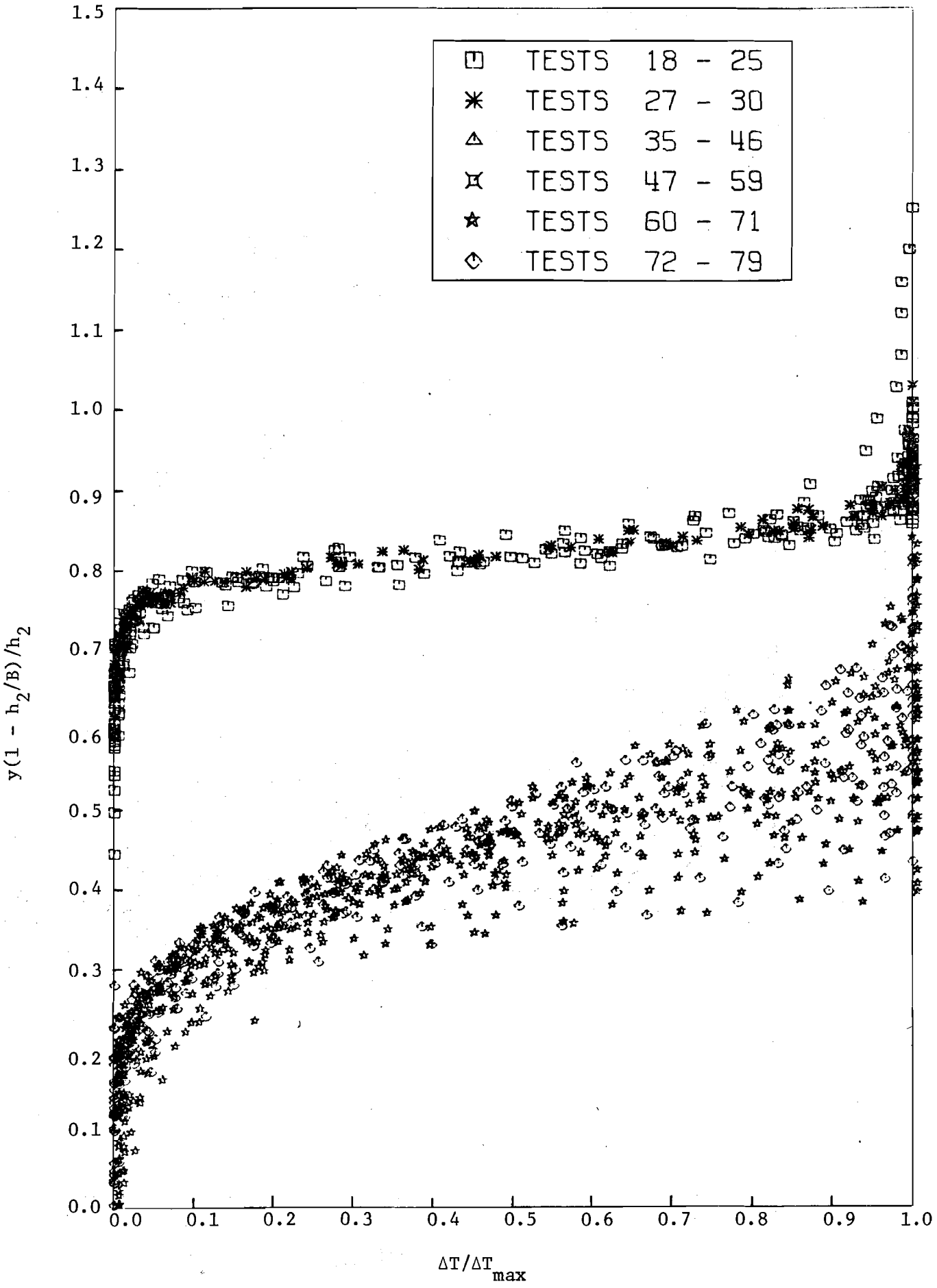

Fig. 5 - Dimensionless Temperature Profiles for Arrested Thermal Wedges

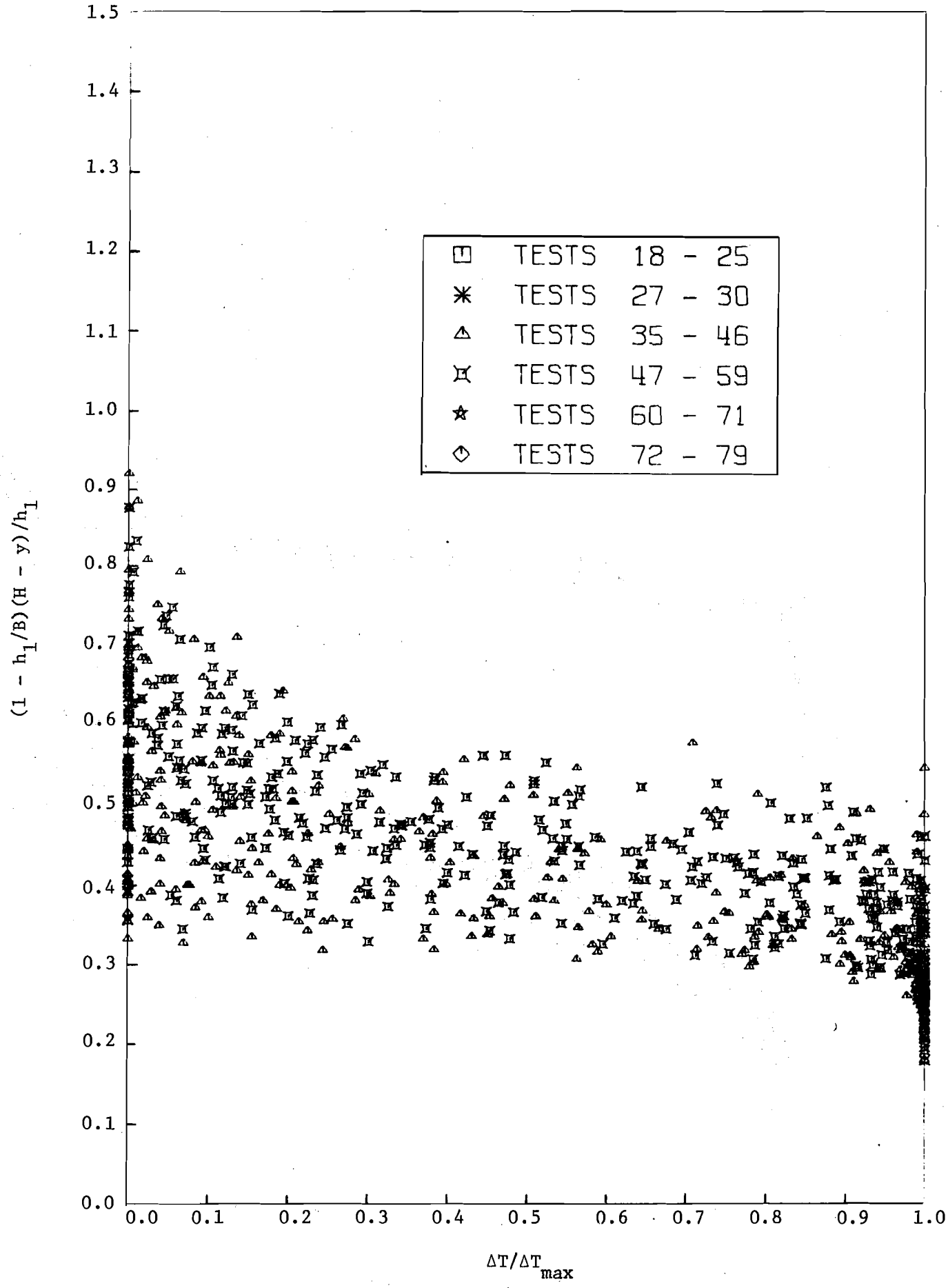

Fig. 6 - Dimensionless Temperature Profiles for Arrested Cold Water Intrusions

arrested thermal wedge the measured null points were generally found to fall slightly below the defined interface in the 0.98-ft wide flume and to be generally coincident with it in the 6-ft wide flume. For arrested cold water intrusions the measured null points were found to lie above the defined interface. In all cases therefore the wedge definition will not result in zero vertically averaged horizontal velocity in the wedge. However, since the velocities in the wedges are generally small it is to be expected that assumption of zero average velocity in the mathematical analysis is a reasonable approximation.

During preliminary analysis average wedge temperatures were found by planimetering the temperatures above and below the defined interface. This procedure proved to be lengthy and tedious and was abandoned for later analyses. In the analysis presented herein the vertically averaged arrested thermal wedge temperature was approximated using T_{max} and the vertically averaged underflow temperature using T_{min}. For the arrested cold water intrusion the vertically averaged wedge temperature was approximated by T_{min}, and the vertically averaged overflow temperature by T_{max}. Values of density for water were computed from Ref. 34 using 1 gm/cc = 0.999967 gm/ml. Values of kinematic viscosity were taken from Ref. 6.

For the benefit of readers who might wish to define the interface and evaluate representative temperatures differently the temperature traverse data are presented in Appendix I.

The details of the analysis of the data will be described for the arrested thermal wedge. The analysis for arrested cold water intrusions was carried out in similar fashion using the appropriate equations presented in Chapter III.

Two general methods of evaluation were followed, one averaging over the entire wedge length, and the other analyzing specific longitudinal sections of a wedge to evaluate local values of the parameters.

For both methods of evaluation for the arrested thermal wedge Eq. 51 was used. The more involved procedure was to evaluate variations along the wedge. Proceeding in the positive x direction toward the wedge tip the data were used to determine the location of the interface location at two longitudinal stations. The region between these stations will be referred to as the reach. The end values of temperature were used to define an average value of $\bar{\rho}_1$, $\bar{\rho}_2$ and hence $\Delta\rho$ for the reach. A constant average value of H was used over the entire wedge. The densimetric Froude number may be written

$$F_{\Delta_2}^2 = Q^2/(\frac{\Delta\rho}{\bar{\rho}_2} gB^2H^3\eta^3) \tag{91}$$

Thus the local value of η is used and all other values are constants or averages for the reach. The quantities $d\bar{\rho}_1/dr$ and $d\bar{\rho}_2/dr$ were evaluated by assuming linear variation between the end values for the reach. To begin the computation a value of f_i for the reach was guessed, η was changed by a small increment (for which dr was to be calculated), f_{w_2} and f_b were guessed, R_b, Re_b, R_{w_2} and Re_{w_2} then computed using Eqs. 58, 59, 60 and 61. By substitution in Eq. 64 new guesses for f_{w_2} and f_b were obtained. This procedure was repeated until two successive evaluations of f_{w_2} or f_b varied by less than 0.0005, η was then incremented and this process repeated. The procedure was continued until the sum of the increments in η totalled the difference in η between the two ends of the reach. The computed value of dr for the reach was then compared with the measured value. If the difference was less than

one-half per cent the guess of f_i was accepted as correct. Otherwise, if the calculated length was too long, the guess for f_i was increased, if too short it was reduced and the calculation repeated until the test was met. The final result was then taken as yielding values of f_i, f_{w_2}, f_b, R_i, Re_{w_2} and Re_b for the reach.

For the evaluation of average values of f_i for the wedge over the region from the furthermost downstream measurement station and the wedge tip ($\eta = 1$), Eq. 51 was simplified by setting $d\bar{\rho}_1/dr = d\bar{\rho}_2/dr = 0$. A simple average of the values of $\bar{\rho}_1$ and $\bar{\rho}_2$ at the longitudinal measurement stations was used. The computation proceedure was otherwise similar to that described above.

V-2. Results and Discussion

Fig. 7 shows a comparison between local values of f_i and average values of f_i for the wedges, computed by the two different techniques described in the previous section. It is evident from the figure that, particularly for arrested cold water intrusions, the local variation of f_i is so great that use of an average value to describe the wedge behavior is questionable. The terms including $d\bar{\rho}_1/dr$ and $d\bar{\rho}_2/dr$ in the denominator of Eq. 50 are quite significant in determining the value of the local shear stress coefficient. These were compared to the portion of the denominator which remains when they are dropped. For the 0.98-ft wide channel they generally ranged in magnitude up to at most 20% of the remaining term. For the 6-ft wide channel they were generally 10 to 20% of the remaining term but were frequently as high as 45%, and in one case 71%. The data for the 6-ft channel, however, reflect the rather long time required to collect data at a section before moving on to the next section. During this period the ambient temperature of the sump system was increasing. Consequently the data reflect the effects of

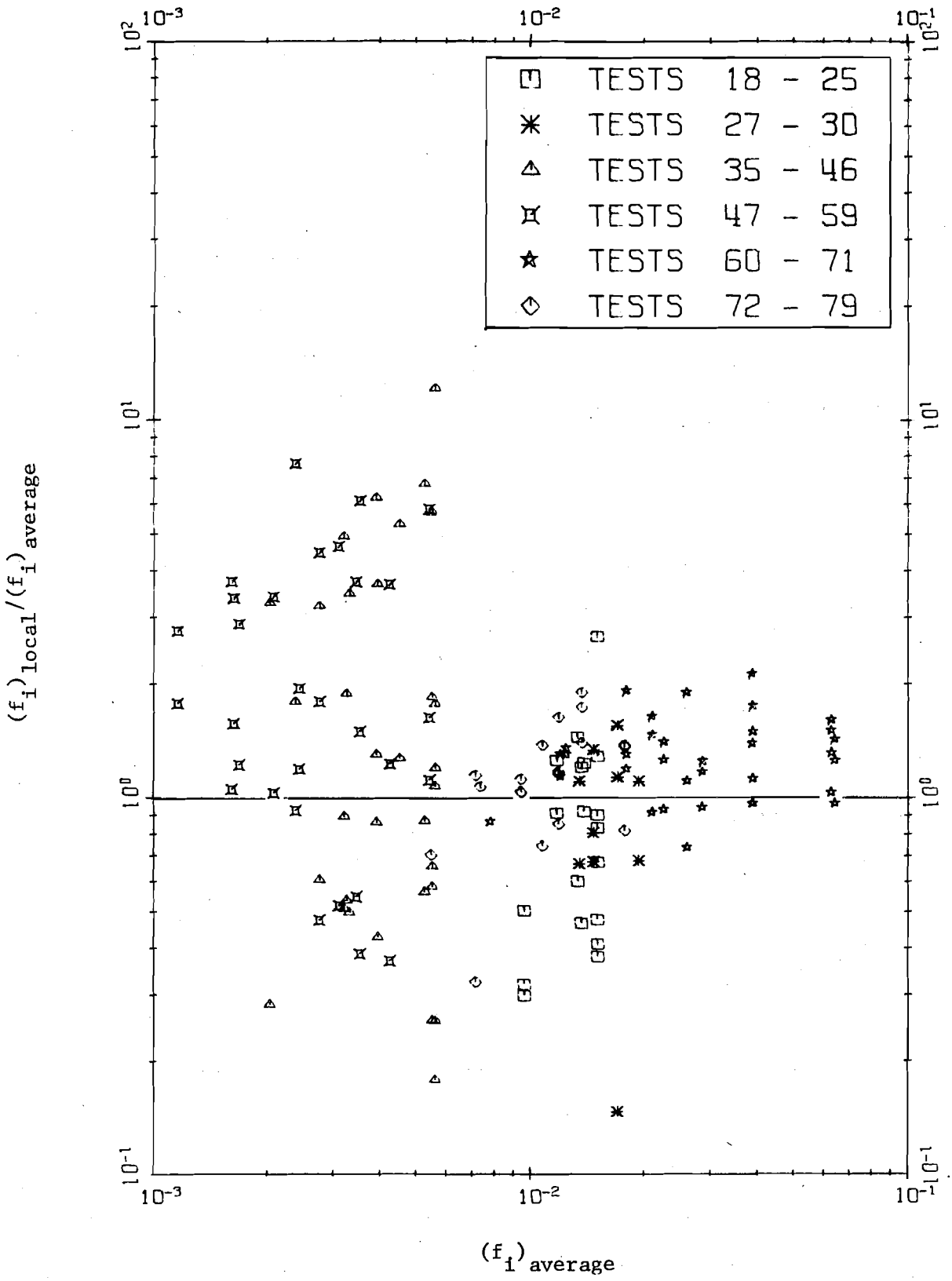

Fig. 7 - Comparison of Local Interfacial Friction Factors with Average Wedge Values

unsteadiness as well as non-uniformity. No effective method was found for separating the two effects and thus all variations of $\bar{\rho}$ with distance along the wedge have been incorporated in the terms involving $d\bar{\rho}_1/dr$ and $d\bar{\rho}_2/dr$. Consequently correlations have been sought between local values of f_i and local values of other parameters.

Fig. 8 shows a plot of local values of f_i versus local values of interfacial Reynolds number = $4\bar{u}_j R_i/\nu$, with j referring to the moving layer. For arrested thermal wedges the trend for F_Δ, based on U and H and an average value of $\Delta\rho/\bar{\rho}_2$ over the length of the wedge, is indicated. The data, when presented in this way, show trends quite different from those expected (1). The friction factor for any data set with the same F_Δ, bed roughness, channel width and wedge type appears to increase with Reynolds number (as is the case for corrugated conduit).

The interfacial friction factors obtained in the 0.98-ft wide channel for arrested thermal wedges are higher than those for the 6-ft wide channel. This may, however, be dependent on the validity of the technique used to separate sidewall effects, or to the incorporation of density changes with time in the terms involving $d\bar{\rho}_1/dr$ and $d\bar{\rho}_2/dr$. Both sets of data indicate that for the arrested thermal wedge the local interfacial friction factor was significantly higher when the lower boundary was roughened with pea gravel. In the case of cold water intrusions in the 0.98-ft channel there is no apparent difference in behavior depending on the roughness of the channel bed. The local friction factors for arrested cold water intrusions are considerably lower than those for arrested thermal wedges at corresponding values of the local Reynolds numbers.

Fig. 9 shows the correlation between local values of f_i and a local Reynolds number-densimetric Froude number combination to eliminate

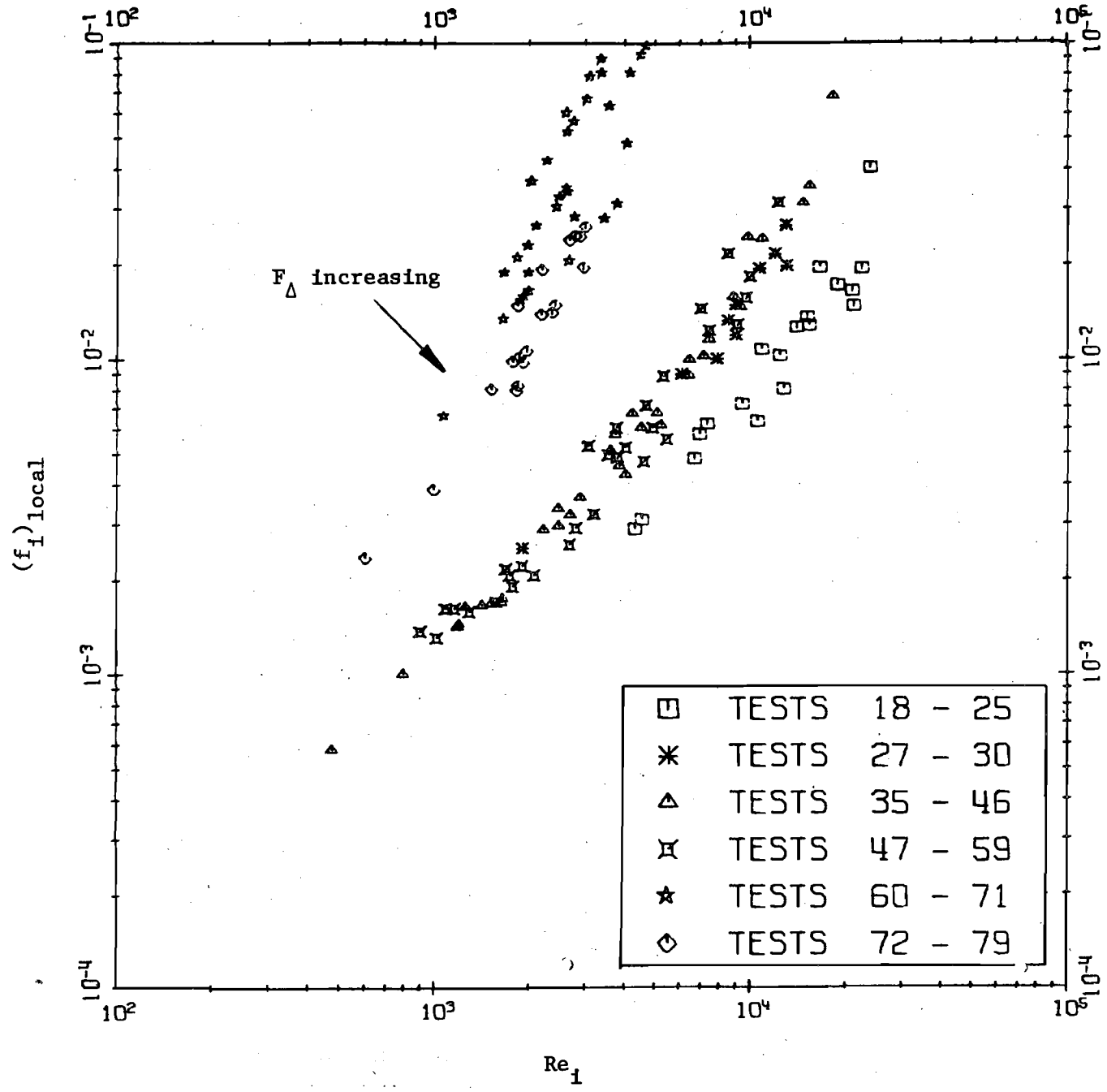

Fig. 8 - Variation of Local Interfacial Friction Factors with Local Interfacial Reynolds Number

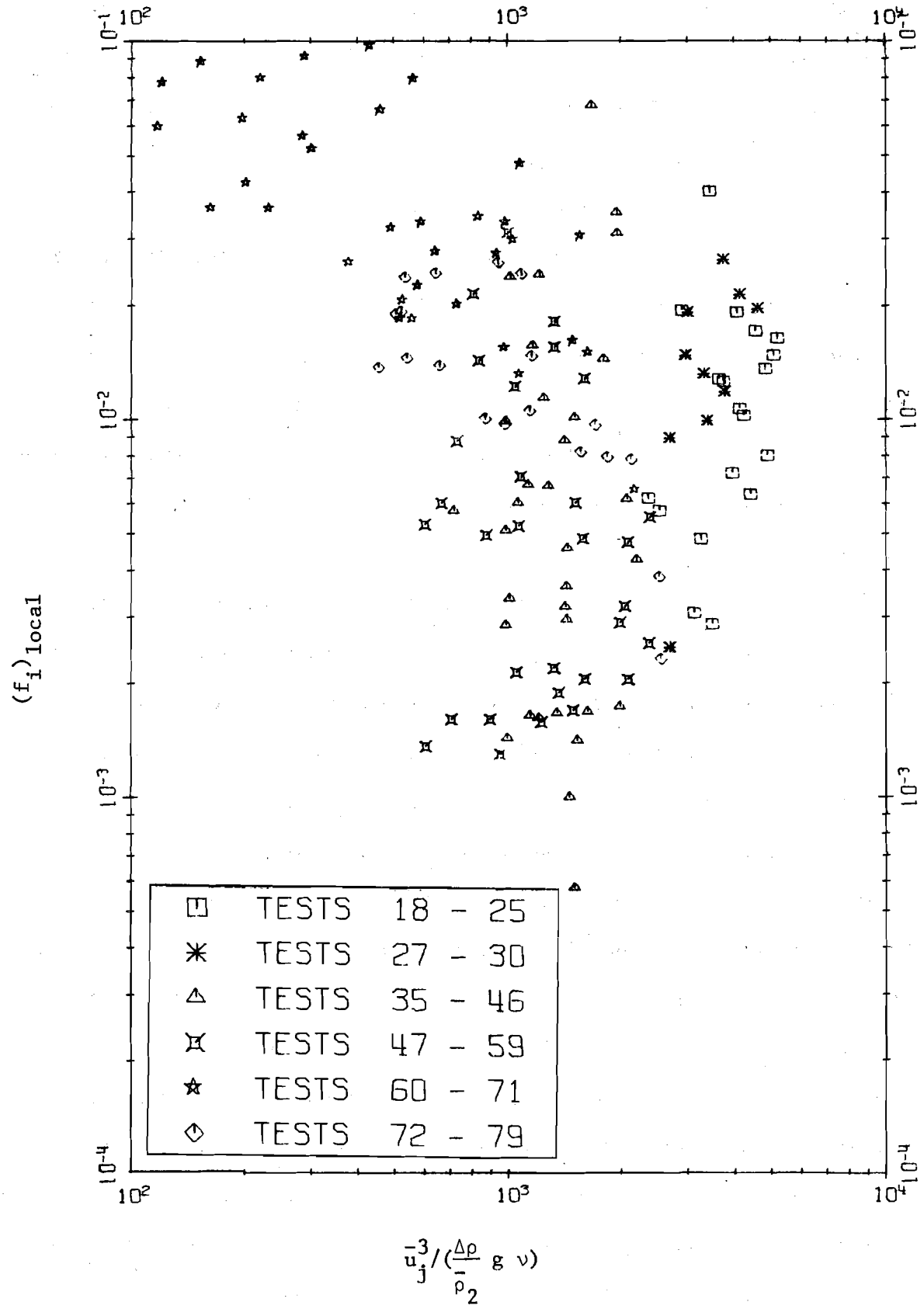

Fig. 9 - Variation of Local Interfacial Friction Factors with Local Interface Stability Parameter

length scale akin to the $F_\Delta^2 Re$ combination discussed earlier. Here the combination = $\bar{u}_j^3/(\frac{\Delta\rho}{\bar{\rho}_2} g \nu)$, in which j refers to the moving layer. Another combination which was examined based the densimetric Froude number on the depth of the moving layer, and the Reynolds number on the hydraulic radius associated with the interface, thereby introducing a "shape" factor R_i/h_j. This, however, yielded a deterioration in correlation, compared to that shown in Fig. 9. The data in Fig. 9 exhibit the same distinctions between 6-ft wide flume, 0.98-ft wide flume, rough bed, mesh bed or smooth bed, and arrested thermal wedges or arrested cold water intrusions as in Fig. 8. There is a general declining trend in f_i with increasing values of the abscissa. The correlation obtained is, however, markedly deteriorated from that obtained in Fig. 8.

Since local correlations for friction factor would be difficult to use for design purposes the relationship between average values of f_i for the wedges and readily evaluated overall flow parameters will be presented. As pointed out earlier, however, the wide variation of f_i over the wedge renders the use of average values questionable.

Fig. 10 presents variation of average values of f_i with a Reynolds number based on hydraulic radius for the channel UR/ν or Re R/H. For two dimensional flows R/H equals 1 and the Reynolds number is based on overall flow depth. Eq. 73 and Eq. 78 for two-dimensional laminar wedge flows are plotted on Fig. 10. The range of overall Reynolds numbers in the narrow channel and the wide channel is sufficiently small that no clear trend with Reynolds number may be distinguished. The friction factors for arrested thermal wedges over rough beds are again higher than for those above smooth beds in both the narrow and wide channels. There is no clear difference in behavior depending on bed roughness for arrested cold water intrusions.

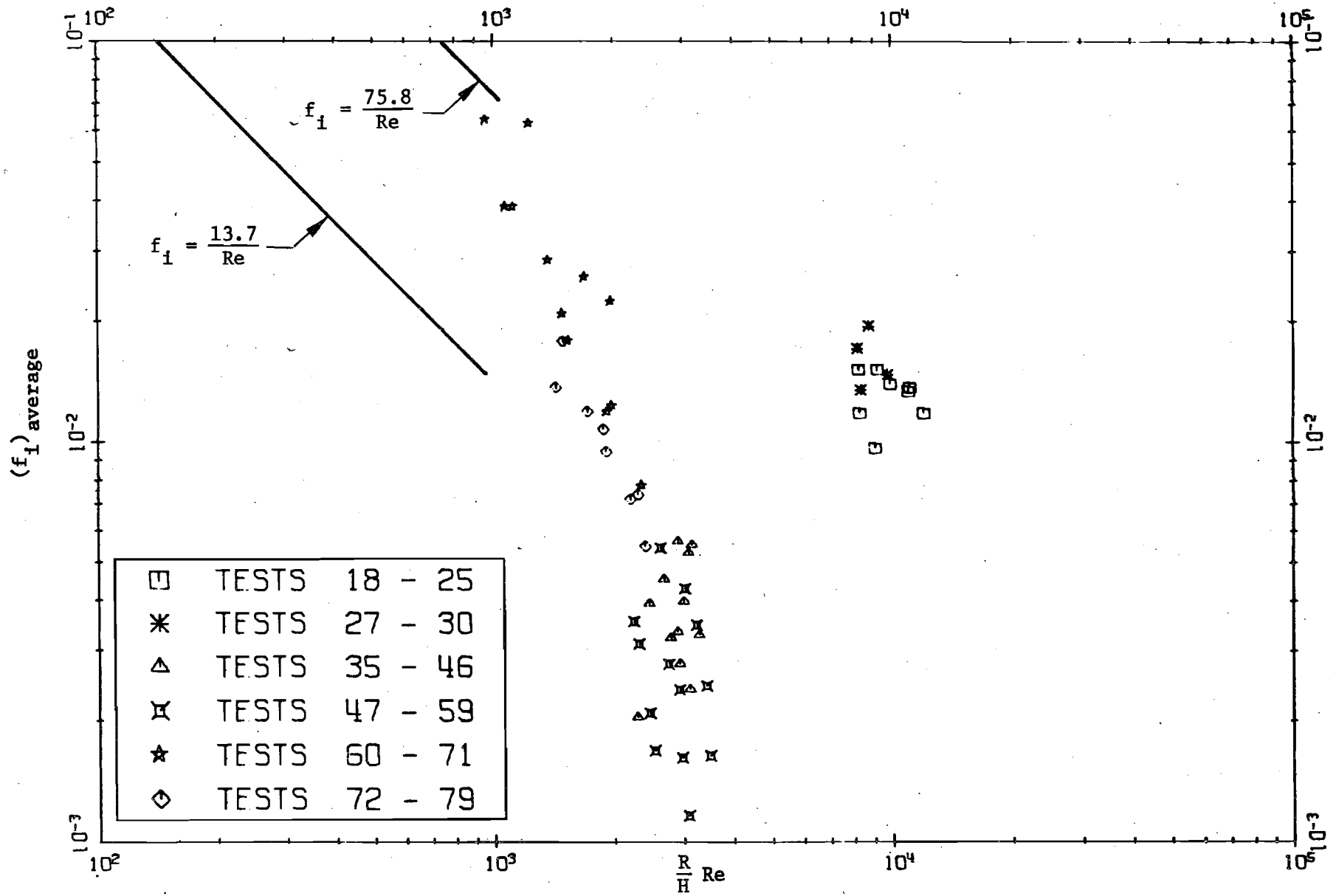

Fig. 10 - Variation of Average Interfacial Friction Factor with Overall Reynolds Number

Fig. 11 shows the variation of average interfacial friction factors for the wedges with the Reynolds number-densimetric Froude number combination = $U^3/(\frac{\Delta\rho}{\bar{\rho}_2} g \nu)$. The friction factors generally decline with increasing magnitude of the abscissa for data in a given channel. Again, in both channels friction factors for arrested thermal wedges above rough beds are seen to be generally higher than for those above smooth beds. No corresponding distinct difference in behavior is evident for arrested cold water intrusions.

Fig. 12 shows the variation of wedge length, L, measured from the vertical wall of the wedge flow inlet (see Fig. 4) to the wedge tip with an overall densimetric Froude number, $F_\Delta^2 = U^2/(\frac{\Delta\rho}{\bar{\rho}_2} g H)$. $\Delta\rho/\bar{\rho}_2$ is a simple average of the values at the various measuring stations along the wedge. This figure again illustrates that there is no distinguishable difference in behavior of arrested cold water intrusions with differences in bed roughness. The data for arrested cold water intrusions plot about a line which has a slope very close to that observed by Keulegan (18) for arrested salt wedges (exponent -5/2). A line with the slope observed by Keulegan is plotted on the figure for comparative purposes. The data for arrested thermal wedges, however tend to fall around lines of different slope. The lines for rough and smooth bed are close to being parallel, with the shorter wedges occurring for the rough bed case in both the 0.98-ft wide and 6-ft wide channels. It is noteworthy that there is substantial variation in slope with variation in channel width. Keulegan (18) obtained the same slope for a number of different aspect ratios in his study of arrested salt water intrusions. His analysis for very wide channels, however, proceeded from an experimental evaluation of stresses and a theoretical generalization of them.

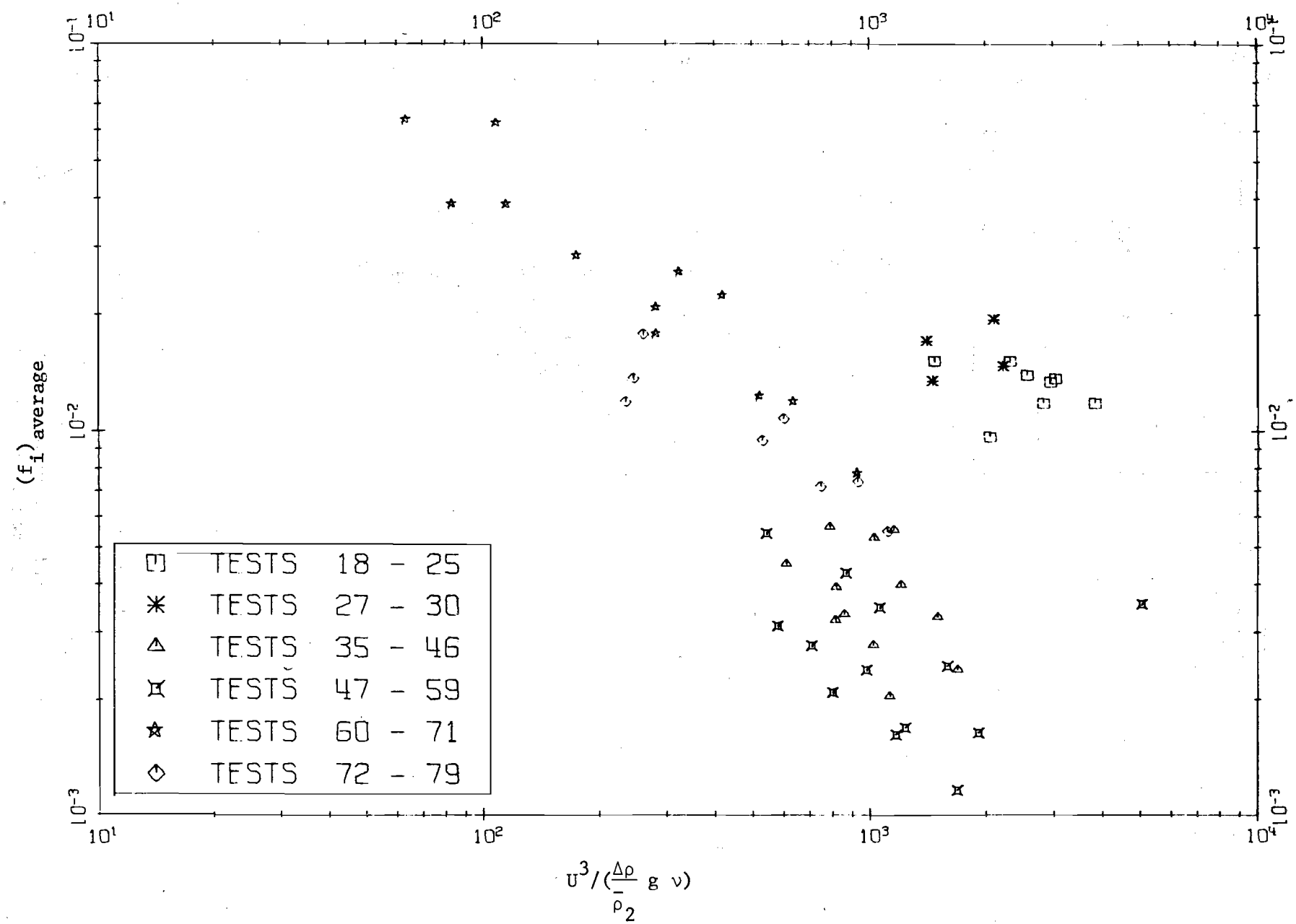

Fig. 11 - Variation of Average Interfacial Friction Factor with Overall Interface Stability Parameter

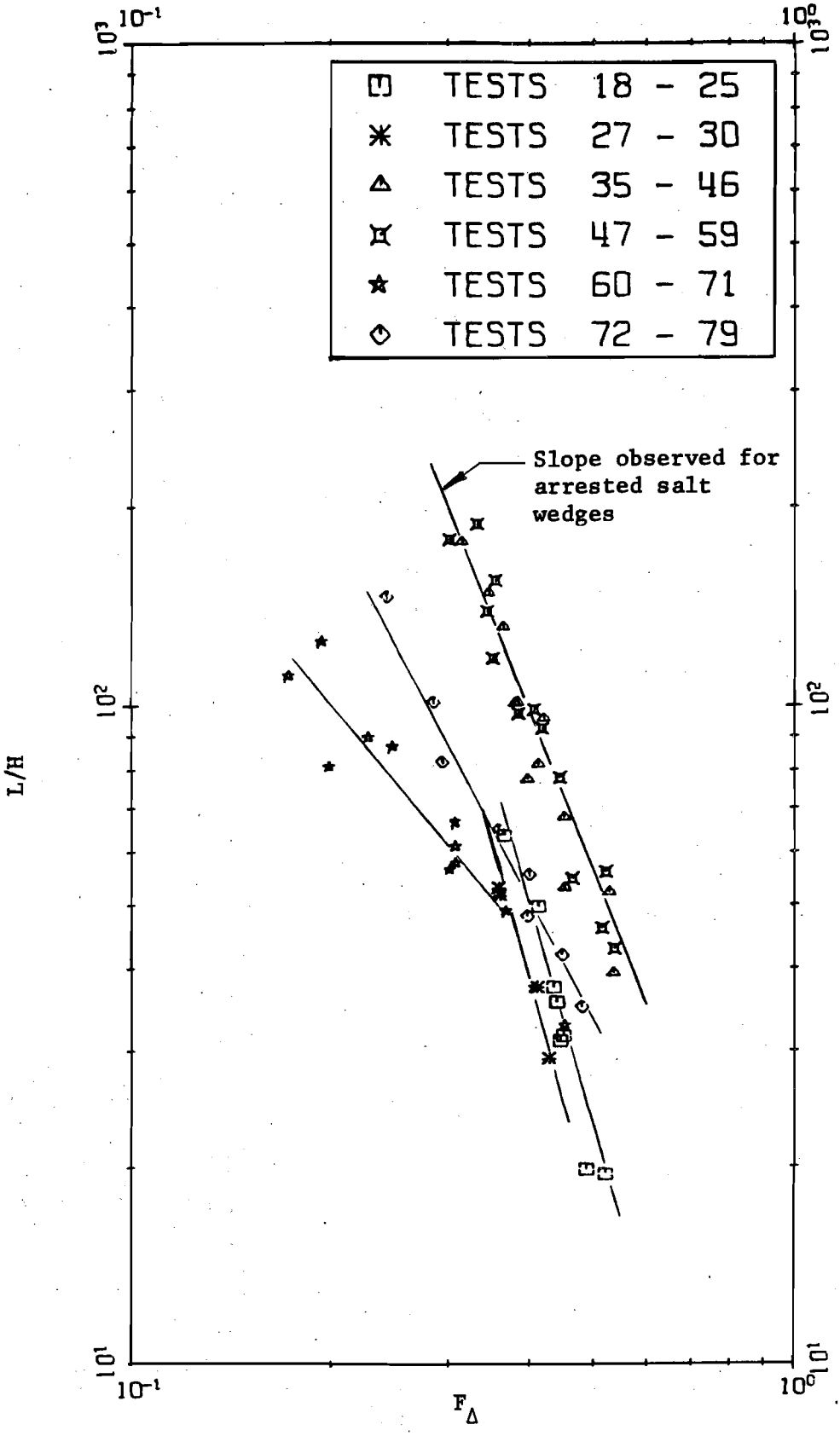

Fig. 12 - Variation of Wedge Length with Overall Densimetric Froude Number

Fig. 13 shows dimensionless plots of the wedge shapes. Least squares cubic curves have been fitted to the data for illustrative purposes. There is little or no distinction in wedge shape depending on bed roughness for either form of wedge. The shapes do exhibit some variation with channel width. The dashed line represents the average shape of arrested thermal wedges for both channel widths.

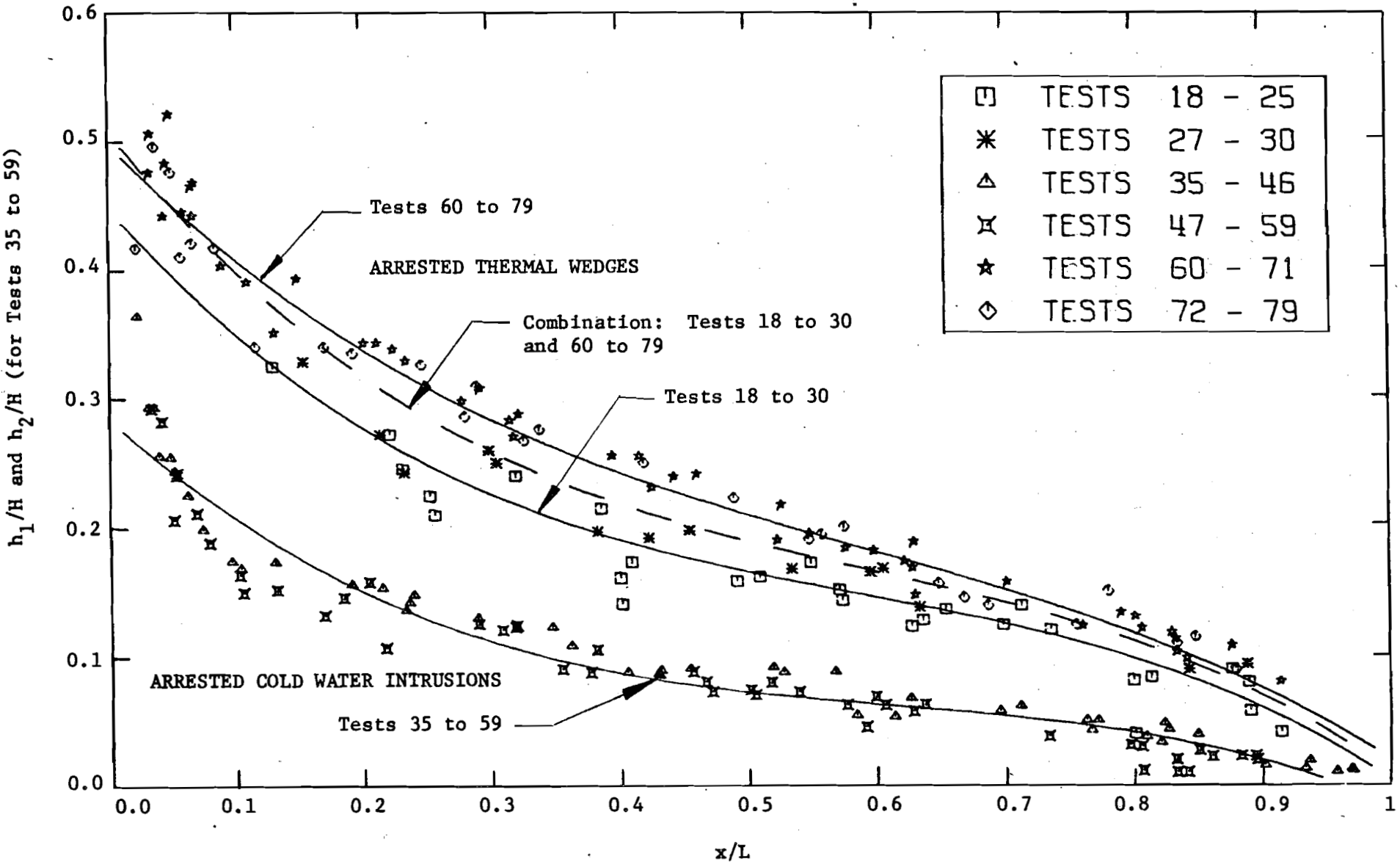

Fig. 13 - Dimensionless Arrested Wedge Profiles

VI. CONCLUSIONS

1. There is considerable variation of interfacial friction factor along an arrested wedge, making use of average values questionable.

2. Values of friction factor along an arrested wedge may be very dependent on the wedge definition and the validity of the method used for separation of sidewall effects.

3. Variations in density along the wedge have a significant effect in the evaluation of the interfacial friction factor.

4. Good correlation was obtained between local values of interfacial friction factor and local Reynolds number based on the velocity of the moving layer and the hydraulic radius associated with the interface. The data indicate that local interfacial friction factors increase with increasing local Reynolds number.

5. An increase in bed roughness results in an increase in interfacial friction factor for arrested thermal wedges but has no significant effect for arrested cold water intrusions.

6. For the same Reynolds number, densimetric Froude number, and bed condition the interfacial friction factor for an arrested thermal wedge exceeds that for an arrested cold water intrusion in a narrow channel of the same width when flow is turbulent.

7. Local friction factors correlate better with a local Reynolds number than with a local densimetric Froude number, Reynolds number combination which eliminates length, $(F_{\Delta}^{2}Re)$.

8. Dimensionless plots of wedge length versus an overall densimetric Froude number plot as straight lines on log-log paper. The slope for arrested cold water intrusions is very close to that found by Keulegan (18) for arrested salt water intrusions. The lines for arrested

thermal wedges shift with bed roughness and their slope changes with channel width.

9. Dimensionless or affine wedge shapes show little effect of bed roughness. The arrested thermal wedge shapes are dependent on channel width.

LIST OF REFERENCES

1. Abraham, G., and Eysink, W. D., "Magnitude of Interfacial Shear in Exchange Flow," Jr. Hyd. Res., Vol. 9, No. 2, 1971.

2. Anderson, A. G., "Sedimentation," Ch. 18 of Handbook of Fluid Dynamics, McGraw-Hill, 1961.

3. Bata, G. L., "Recirculation of Cooling Water in Rivers and Canals," Proc. ASCE, Vol. 83, No. HY3, June 1957, pp. 1265-1 to 27.

4. Bata, G. L., "Frictional Resistance at the Interface of Density Currents," Proc. VIIIth Congress, IAHR, No. 12C, Montreal, 1959, 15 pp.

5. Cross, R. H., and Hoult, D. P., "Collection of Oil Slicks," Proc. ASCE, Vol. 97, No. WW2, May 1971, pp. 313-322.

6. Daugherty, R. L., "Fluid Properties," Ch. 1 in Handbook of Fluid Dynamics, V. L. Streeter, ed., McGraw-Hill Book Co., N.Y., 1961.

7. Einstein, H. A., and Barbarossa, N., "River Channel Roughness," Trans. ASCE, Vol. 117, 1952, pp. 1121-1146.

8. Harleman, D.R.F., "Stratified Flow," Ch. 26, Handbook of Fluid Dynamics, V. L. Streeter, ed., McGraw-Hill, 1961.

9. Harleman, D.R.F., "Mechanics of Condenser-Water Discharge from Thermal-Power Plants," Ch. 5, Engineering Aspects of Thermal Pollution, F. L. Parker and P. A. Krenkel, eds., Vanderbilt University Press, 1969.

10. Harleman, D.R.F., and Stolzenbach, K. D., "Fluid Mechanics of Heat Disposal from Power Generation," Annual Review of Fluid Mechanics, van Dyke, M. et al (eds.), Vol. 4, 1972, pp. 7-32.

11. Henderson, F. M., "Open Channel Flow," The Macmillan Co., N.Y., 1966.

12. Hikkawa, H., ed., "Handbook of Hydraulics", Japanese Society of Civil Engineers, 1971.

13. International Association for Hydraulic Research, Proceedings of the International Symposium on Stratified Flows, Novosibirsk, U.S.S.R., 1972, 749 pp.

14. Ippen, A. T., and Harleman, D.R.F., "Steady-State Characteristics of Subsurface Flow," Gravity Waves, Ch. 12, National Bureau of Standards Circular 521, Washington, D.C., 1952.

(List of References - cont'd)

15. Iwasaki, T., "On the Shear Stress at the Interface and its Effects in the Stratified Flow," Proc. 9th Conf. on Coastal Eng., Pt. 4, Ch. 51, Lisbon, June 1964, pp. 879-892.

16. Keulegan, G. H., "Laminar Flow at the Interface of Two Liquids," Jl. of Res., National Bureau of Standards, Vol. 32, p. 303, 1944, RP 1591.

17. Keulegan, G. H., "Interfacial Instability and Mixing in Stratified Flows," Journal of Research, National Bureau of Standards, Vol. 43, p. 487, 1949, RP 2040.

18. Keulegan, G. H., "The Mechanism of an Arrested Saline Wedge," Estuary and Coastal Hydrodynamics, Ch. 11, A. T. Ippen, ed., McGraw-Hill, 1966.

19. Lofquist, K., "Flow and Stress near an Interface between Stratified Liquids," The Physics of Fluids, Vol. 3, No. 2, March/April 1960, pp. 158-175.

20. Macagno, E. O., and Rouse, H., "Interfacial Mixing in Stratified Flow," Proc. ASCE, Vol. 87, No. EM5, Oct. 1961, pp. 55-81.

21. Majewski, W., "The Outfall of Waste Waters, including the Effect of Density Differences: Laboratory Investigations on the Arrested Wedge," Proc. 11th Congress, IAHR, Vol. II, Paper No. 28, Leningrad, 1965, 9 pp.

22. Majewski, W., "Laboratory Investigation on Heat Transfer in Thermally Stratified Flow," Paper A-25, Proc. XIVth Congress, IAHR, Paris, 1971, pp. 207-216.

23. Michon, X., Goddet, J., and Bonnefille, R., "Etude Théorique et Expérimentale des Courants de Densité," Tome II, Laboratoire National d'Hydraulique, Chatou, 1955.

24. Nelson, J. E., "Vertical Mixing in Stratified Flow - A Comparison of Previous Experiments," Univ. of Cal., Berkeley, Rpt. No. WHM-3, December, 1972, 33 pp.

25. Parker, F. L., and Krenkel, P. A., "Physical and Engineering Aspects of Thermal Pollution," CRC Press, Cleveland, 1970.

26. Polk, E. M., Benedict, B. A., and Parker, F. L., "Cooling Water Density Wedges in Streams," Proc. ASCE, Vol. 97, No. HY10, Oct. 1971, pp. 1639-1652.

27. Rouse, H., "Elementary Mechanics of Fluids," John Wiley & Sons, Inc., N.Y., 1946, p. 185.

(List of References - cont'd)

28. Rumer, R. R., Jr., "Interfacial Wave Breaking in Stratified Liquids," Proc. ASCE, Vol. 99, No. HY3, March 1973, pp. 509-524.

29. Schijf, J. B., and Schönfeld, J. C., "Theoretical Considerations on the Motion of Salt and Fresh Water," Minnesota International Hydraulics Convention, Minneapolis, Minn., Sept. 1953, pp. 321-334.

30. Sherenkov, I. A., Netjukhailo, A. P., and Telezhkin, E. D., "Research Investigation of Transfer Process in Two-Dimensional Stratified Flow" Proc. XIVth Congress, IAHR, Paper A-26, Paris, 1971, 9 pp.

31. Shi-igai, H., "On the Resistance Coefficient at the Interface between Salt and Fresh Water," Trans. of JSCE, No. 123, Nov. 1965, pp. 27-31.

32. Shi-igai, H., "Experimental and Theoretical Modeling of Saline Wedges," Proc. XIIIth Congress IAHR, No. C-4, Vol. 3, Kyoto, 1969, pp. 29-36.

33. Sjöberg, A., "Diffusive Properties of Interfacial Layers," Proc. XIIth Congress, IAHR, No. D8, Fort Collins, Col., 1967, pp. 71-78.

34. Smithsonian Physical Tables, 9th Revised Ed., Table 287, Washington, D.C., 1954.

35. Turner, J. S., "Buoyancy Effects in Fluids", Cambridge University Press, 1973.

36. Vreugdenhil, C. B., "Friction Coefficients on the Interface of a Two-Layer System," Delft Hydraulics Laboratory, Internal Information Report No. V204, Nov. 1971. (Translation appended to this report - see Appendix)

37. Wilkinson, D. L., "Dynamics of Contained Oil Slicks," Proc. ASCE, Vol. 98, No. HY6, June 1972, pp. 1013-1030.

38. Wilkinson, D. L., "Limitations to Length of Contained Oil Slicks," Proc. ASCE, Vol. 99, No. HY5, May 1973, pp. 701-712.

APPENDIX I

EXPERIMENTAL DATA

SUMMARY OF TEST CONDITIONS

Tests	Channel Width, ft.	Bed Condition	k_b, ft.	Wedge Type
18-25	6	Smooth	-	Thermal
27-30	6	Pea gravel	0.039	Thermal
35-46	0.98	Wire mesh	0.010	Cold water
47-59	0.98	Pea gravel	0.051	Cold water
60-71	0.98	Pea gravel	0.051	Thermal
72-79	0.98	Wire mesh	0.010	Thermal

Sidewalls were smooth for all tests

TEST-18: H = 0.990 ft, L = 35.0 ft, Q_a = 0.775 cfs, Q_w = 26 gpm

x(ft)	E-y(ft)	T(°C)	x(ft)	H-y(ft)	T(°C)	x(ft)	H-y(ft)	T(°C)
8.	0.00	33.30	20.	0.00	32.60	32.	0.00	31.60
	.02	34.05		.02	33.45		.02	32.50
	.04	34.30		.04	33.75		.05	31.70
	.07	34.25		.07	33.75		.08	29.10
	.10	34.30		.12	33.70		.11	27.25
	.13	34.35		.15	32.75		.14	25.50
	.16	34.25		.18	29.40		.17	24.75
	.19	34.15		.21	26.05		.22	24.45
	.22	33.90		.24	24.55		.29	24.40
	.25	33.10		.29	24.20		.49	24.35
	.28	29.75		.39	24.15	null =	.074	
	.31	25.05	null =	.147				
	.34	24.10						
	.39	23.90						
	.44	23.85						
null =	.215							

TEST-19: H = 1.020 ft, L = 31.5 ft, Q_a = 0.850 cfs, Q_w = 26 gpm

x(ft)	H-y(ft)	T(°C)	x(ft)	H-y(ft)	T(°C)	x(ft)	H-y(ft)	T(°C)
8.	0.00	34.50	20.	0.00	34.55	28.	0.00	33.50
	.02	35.20		.02	35.15		.02	34.25
	.05	35.25		.05	35.25		.05	33.60
	.08	35.30		.08	35.20		.07	32.85
	.11	35.30		.11	35.10		.09	31.95
	.14	35.30		.14	34.30		.11	28.70
	.17	35.15		.17	31.40		.14	27.10
	.20	34.75		.20	28.00		.17	25.80
	.23	33.35		.23	26.25		.21	25.40
	.26	30.05		.26	25.75		.26	25.25
	.29	26.70		.31	25.50		.36	25.20
	.32	25.50		.41	25.40	null =	.081	
	.35	25.10	null =	.146				
	.38	24.95						
	.43	24.90						
null =	.206							

TEST-20: H = 0.995 ft, L = 63.0 ft, Q_a = 0.690 cfs, Q_w = 27 gpm

x(ft)	H-y(ft)	T(°C)	x(ft)	H-y(ft)	T(°C)	x(ft)	H-y(ft)	T(°C)
8.	0.00	34.50	20.	0.00	32.30	32.	0.00	31.80
	.02	34.90		.02	32.65		.02	32.15
	.05	35.00		.05	32.70		.05	32.20
	.09	34.95		.09	32.70		.09	32.30
	.12	34.80		.14	32.70		.14	32.05
	.15	34.80		.19	32.60		.17	30.85
	.19	34.80		.22	32.10		.19	28.90
	.22	34.70		.25	30.60		.21	26.40
	.25	34.35		.27	27.80		.23	23.60
	.28	34.15		.29	24.40		.26	21.90
	.31	33.15		.32	21.75		.29	21.55
	.34	31.10		.39	21.00		.34	21.40
	.37	24.70		.49	20.95		.39	21.35
	.40	21.90	null =	.215		null =	.156	
	.43	21.00						
	.49	20.75						
	.54	20.70						
null =	.262							

TEST-20 (Continued)

x(ft)	H-y(ft)	T(°C)	x(ft)	H-y(ft)	T(°C)
44.	0.00	31.15	56.	0.00	30.55
	.02	31.65		.02	31.10
	.05	31.80		.05	31.35
	.09	31.80		.09	29.70
	.12	30.95		.12	24.50
	.15	28.60		.15	22.25
	.17	26.10		.19	21.85
	.19	23.60		.29	21.80
	.24	21.80	null =	.079	
	.29	21.65			
	.39	21.60			
null =	.119				

TEST-21: H = 1.020 ft, L = 32.0 ft, Q_a = 0.900 cfs, Q_w = 26.5 gpm

x(ft)	H-y(ft)	T(°C)
8.	0.00	34.30
	.02	34.60
	.05	34.80
	.08	34.80
	.12	34.80
	.15	34.75
	.18	34.65
	.22	34.10
	.25	31.65
	.27	27.90
	.29	24.90
	.32	23.00
	.37	22.75
	.42	22.70
	.52	22.65
null =	.205	

x(ft)	H-y(ft)	T(°C)
20.	0.00	33.20
	.02	33.70
	.07	33.85
	.12	33.30
	.15	30.70
	.17	27.85
	.19	24.80
	.22	23.40
	.27	23.05
	.37	23.00
	.47	22.95
null =	.130	

x(ft)	H-y(ft)	T(°C)
26.	0.00	32.90
	.02	33.55
	.05	33.70
	.08	33.05
	.10	31.35
	.12	28.55
	.14	25.60
	.17	23.90
	.22	23.40
	.32	23.25
	.42	23.20
null =	.094	

TEST-22: H = 1.016 ft, L = 20.0 ft, Q_a = 0.955 cfs, Q_w = 26.5 gpm

x(ft)	H-y(ft)	T(°C)
8.	0.00	34.10
	.02	34.80
	.06	34.75
	.09	34.75
	.12	34.30
	.16	32.45
	.19	29.55
	.22	26.25
	.25	24.80
	.28	24.20
	.33	24.00
	.41	23.85
	.51	23.80
null =	.146	

x(ft)	H-y(ft)	T(°C)
16.	0.00	33.90
	.02	34.40
	.05	33.90
	.08	30.45
	.11	27.00
	.14	25.05
	.17	24.50
	.21	24.05
	.26	24.00
null =	.071	

TEST-23: H = 0.992 ft, L = 49.0 ft, Q_a = 0.680 cfs, Q_w = 25.7 gpm

x(ft)	H-y(ft)	T(°C)
20.	0.00	33.70
	.02	33.80
	.05	33.80
	.09	33.80
	.14	33.75
	.17	33.30
	.19	32.20
	.21	30.50
	.23	28.45
	.25	26.90
	.27	26.10
	.29	25.90
	.32	25.80
null =	.171	

x(ft)	H-y(ft)	T(°C)
24.	0.00	33.20
	.02	33.80
	.05	33.90
	.09	33.95
	.14	33.85
	.17	32.80
	.19	31.55
	.21	29.55
	.23	27.45
	.25	26.50
	.27	26.10
	.30	25.95
	.35	25.85
null =	.159	

x(ft)	H-y(ft)	T(°C)
28.	0.00	33.00
	.02	33.70
	.05	33.85
	.09	33.95
	.14	33.70
	.17	32.50
	.19	30.80
	.21	29.40
	.23	27.50
	.25	26.45
	.27	26.20
	.30	26.00
null =	.152	

TEST-23 (Continued)

x(ft)	H-y(ft)	T(°C)
32.	0.00	33.20
	.02	33.75
	.05	33.95
	.09	33.95
	.12	33.75
	.15	32.65
	.17	30.95
	.19	28.65
	.21	27.40
	.23	26.40
	.25	26.25
	.29	26.20
	.35	26.10
	.40	26.05
null =	.139	

x(ft)	H-y(ft)	T(°C)
36.	0.00	33.05
	.02	33.75
	.05	33.95
	.09	33.90
	.12	33.45
	.15	31.10
	.17	28.90
	.19	27.35
	.21	26.60
	.25	26.25
	.30	26.20
	.40	26.15
null =	.126	

TEST-24: H = 0.979 ft, L = 36.5 ft, Q_a = 0.685 cfs, Q_w = 22.5 gpm

x(ft)	H-y(ft)	T(°C)	x(ft)	H-y(ft)	T(°C)	x(ft)	H-y(ft)	T(°C)
8.	0.00	33.60	14.	0.00	33.60	20.	0.00	33.30
	.02	34.25		.02	34.15		.02	33.90
	.05	34.35		.05	34.15		.05	33.95
	.08	34.35		.09	34.20		.10	33.95
	.11	34.40		.13	34.20		.13	33.95
	.17	34.40		.17	34.10		.16	33.60
	.20	34.35		.20	33.75		.18	32.85
	.22	34.35		.22	33.00		.20	31.20
	.24	34.25		.24	31.60		.22	29.65
	.26	34.00		.26	29.55		.24	27.55
	.28	32.95		.28	27.65		.26	26.90
	.30	31.60		.30	26.70		.28	26.60
	.32	29.10		.32	26.40		.30	26.45
	.34	27.15		.35	26.30		.35	26.40
	.36	26.35		.40	26.25	null =	.168	
	.40	26.00		.45	26.20			
	.45	25.90	null =	.203				
null =	.244							

TEST-24 (Continued)

x(ft)	H-y(ft)	T(°C)	x(ft)	H-y(ft)	T(°C)
26.	0.00	33.00	32.	0.00	32.45
	.02	33.55		.02	33.05
	.05	33.55		.05	33.05
	.08	33.60		.08	32.95
	.11	33.50		.10	32.00
	.13	33.10		.12	30.25
	.15	32.30		.14	28.45
	.17	30.35		.16	27.50
	.19	28.25		.18	27.05
	.21	27.25		.21	26.80
	.23	26.80		.25	26.70
	.25	26.65		.30	26.65
	.30	26.60	null =	.101	
	.35	26.55			
null =	.138				

TEST-25: H = 0.775 ft, L = 15.0 ft, Q_a = 0.610 cfs, Q_w = 21.8 gpm

x(ft)	H-y(ft)	T(°C)	x(ft)	H-y(ft)	T(°C)
6.	0.00	32.85	12.	0.00	32.40
	.01	33.15		.02	32.85
	.03	33.55		.04	32.95
	.06	33.55		.06	32.40
	.08	33.50		.08	30.65
	.10	33.45		.09	29.30
	.12	33.30		.10	28.00
	.13	32.30		.11	26.90
	.14	31.45		.13	25.40
	.15	30.30		.15	24.90
	.16	28.90		.17	24.75
	.18	26.60		.20	24.65
	.20	24.95		.25	24.60
	.22	24.65	null =	.080	
	.26	24.50			
	.30	24.45			
null =	.131				

TEST-27: H = 0.927 ft, L = 27.0 ft, Q_a = 0.685 cfs, Q_w = 28 gpm

x(ft)	H-y(ft)	T(°C)	x(ft)	H-y(ft)	T(°C)	x(ft)	H-y(ft)	T(°C)
8.	0.00	32.40	16.	0.00	32.00	24.	0.00	31.10
	.02	33.10		.02	32.85		.02	32.25
	.05	33.65		.05	33.15		.05	32.60
	.08	33.75		.08	33.30		.08	32.15
	.11	33.75		.11	33.30		.10	31.05
	.14	33.80		.15	32.80		.12	28.80
	.19	33.80		.17	31.20		.14	26.45
	.22	33.80		.19	28.90		.16	24.85
	.25	32.45		.21	26.30		.18	24.20
	.27	30.20		.23	24.55		.20	23.95
	.29	26.95		.25	23.90		.25	23.80
	.31	24.65		.28	23.75		.30	23.75
	.33	23.90		.33	23.65	null =	.090	
	.35	23.70		.38	23.60			
	.38	23.55	null =	.145				
	.40	23.50						
null =	.216							

TEST-28: H = 1.004 ft, L = 53.0 ft, Q_a = 0.650 cfs, Q_w = 28.5 gpm

x(ft)	H-y(ft)	T(°C)
8.	0.00	32.40
	.02	33.20
	.05	33.70
	.10	33.80
	.15	33.90
	.24	33.90
	.27	33.85
	.30	33.75
	.32	33.50
	.34	32.40
	.36	30.20
	.38	27.30
	.40	25.25
	.42	24.00
	.45	23.70
	.50	23.60
	.55	23.55
null =	.280	
16.	0.00	31.95
	.02	33.00
	.05	33.45
	.10	33.55
	.15	33.60
	.20	33.60
	.23	33.50
	.26	32.35
	.28	30.75
	.30	28.20
	.32	25.80
	.34	24.50
	.37	24.00
	.40	23.80
	.45	23.70
null =	.213	
24.	0.00	32.00
	.02	32.85
	.05	33.15
	.10	33.25
	.15	33.25
	.18	33.10
	.20	32.55
	.22	31.30
	.24	29.65
	.26	27.40
	.28	25.35
	.30	24.40
	.35	23.95
	.40	23.85
	.45	23.80
null =	.179	

TEST-29 (Continued): Q_a = 0.780 cfs, Q_w = 26.5 gpm

x(ft)	H-y(ft)	T(°C)
24.	0.00	32.60
	.02	33.60
	.05	33.80
	.10	33.75
	.13	33.40
	.16	31.10
	.18	28.60
	.20	26.05
	.22	24.70
	.24	24.25
	.28	23.90
	.33	23.85
null =	.135	
32.	0.00	32.05
	.02	32.90
	.05	33.15
	.10	31.95
	.12	29.70
	.14	26.20
	.16	25.25
	.18	24.45
	.21	24.10
	.25	24.00
null =	.095	

TEST-28 (Continued)

x(ft)	H-y(ft)	T(°C)
32.	0.00	31.80
	.02	32.60
	.05	33.00
	.08	33.05
	.12	33.05
	.15	32.80
	.18	31.70
	.20	30.25
	.22	28.10
	.24	26.00
	.27	24.55
	.30	24.10
	.35	24.00
null =	.154	

TEST-29: H = 1.018 ft, L = 38.0 ft

x(ft)	H-y(ft)	T(°C)
8.	0.00	33.05
	.02	34.10
	.05	34.40
	.10	34.45
	.15	34.45
	.20	34.40
	.23	34.40
	.26	34.20
	.29	32.40
	.31	30.15
	.33	26.50
	.35	24.60
	.38	23.85
	.43	23.60
	.48	23.55
null =	.248	
16.	0.00	33.10
	.02	33.95
	.05	34.10
	.10	34.15
	.15	34.10
	.18	33.85
	.21	32.40
	.23	29.40
	.25	26.70
	.27	24.90
	.29	24.10
	.31	23.90
	.35	23.80
	.40	23.75
null =	.177	

TEST-30: H = 1.020 ft, L = 52.5 ft, Q_a = 0.725 cfs, Q_w = 22 gpm

x(ft)	H-y(ft)	T(°C)
12.	0.00	31.70
	.03	32.40
	.08	32.60
	.13	32.70
	.18	32.70
	.21	32.60
	.24	31.70
	.26	30.80
	.28	28.20
	.30	24.90
	.32	22.25
	.35	20.40
	.40	20.05
	.45	20.00
20.	0.00	31.80
	.03	32.45
	.08	32.55
	.13	32.55
	.18	32.40
	.21	31.15
	.23	28.70
	.25	25.65
	.27	22.80
	.30	21.00
	.35	20.20
	.40	20.15
28.	0.00	31.10
	.03	32.00
	.06	32.00
	.09	32.00
	.12	32.00
	.15	32.00
	.18	30.50
	.20	28.45
	.22	25.55
	.24	22.45
	.26	21.05
	.30	20.40
	.35	20.25

TEST-35: H = 0.621 ft, L = 32.8 ft, Q_a = .065 cfs, Q_w = .0146 cfs

x(ft)	H-y(ft)	T(°C)	x(ft)	H-y(ft)	T(°C)	x(ft)	H-y(ft)	T(°C)
7.	0.00	25.20	17.	0.00	26.15	27.	0.00	26.40
	.03	27.20		.03	27.45		.03	27.40
	.08	28.00		.08	28.20		.08	28.00
	.13	28.35		.13	28.35		.13	28.20
	.18	28.45		.18	28.40		.18	28.25
	.23	28.45		.23	28.40		.23	28.25
	.28	28.50		.28	28.40		.28	28.25
	.33	28.45		.33	28.40		.33	28.25
	.38	27.35		.38	28.40		.38	28.25
	.43	22.80		.43	28.00		.43	28.25
	.46	19.90		.46	26.35		.48	28.15
	.49	17.60		.49	23.10		.51	27.20
	.52	16.25		.52	19.95		.54	23.35
	.55	15.25		.55	17.70		.57	19.90
	.57	14.80		.57	16.85		.59	18.80
	.59	14.35		.59	16.05		.603	18.20
	.60	14.20		.60	15.80			

TEST-36: H = 0.631 ft, L = 63.6 ft, Q_a = 0.060 cfs, Q_w = .0146 cfs

x(ft)	H-y(ft)	T(°C)	x(ft)	H-y(ft)	T(°C)	x(ft)	H-y(ft)	T(°C)
2.	0.00	25.55	12.	0.00	23.30	36.	0.00	24.00
	.05	29.00		.05	28.40		.05	28.40
	.10	29.60		.10	29.40		.10	29.60
	.15	29.75		.15	29.80		.15	29.80
	.20	29.80		.20	29.80		.20	29.95
	.25	29.60		.25	29.85		.30	29.95
	.30	25.70		.30	29.85		.40	29.95
	.35	20.00		.35	29.55		.45	29.60
	.40	17.50		.40	26.60		.50	27.60
	.45	15.10		.45	21.35		.55	20.60
	.50	14.00		.50	17.50		.59	18.25
	.55	13.45		.55	15.70		.62	16.80
	.60	13.35		.60	14.55			
				.62	14.20			

TEST-36 (Continued)

x(ft)	H-y(ft)	T(°C)
54.	0.00	25.20
	.05	28.90
	.10	29.60
	.15	29.65
	.20	30.00
	.25	30.05
	.30	30.10
	.40	30.10
	.45	30.05
	.50	29.95
	.55	27.05
	.59	22.65
	.62	20.95

TEST-37: H = 0.630 ft, L = 92.8 ft, Q_w = .0146 cfs

x(ft)	H-y(ft)	T(°C)	x(ft)	H-y(ft)	T(°C)
2.	0.00	24.55	12.	0.00	23.00
	.05	29.60		.05	29.00
	.10	30.45		.10	30.40
	.15	30.80		.15	30.80
	.20	30.95		.20	30.95
	.25	30.20		.25	30.95
	.30	23.40		.30	30.80
	.35	18.60		.35	29.40
	.40	16.40		.40	25.00
	.45	14.90		.45	19.80
	.50	14.00		.50	16.80
	.55	13.65		.55	15.35
	.60	13.45		.60	14.40
	.623	13.25		.628	14.20

TEST-37 (Continued): Q_a = 0.055 cfs

x(ft)	H-y(ft)	T(°C)	x(ft)	H-y(ft)	T(°C)	x(ft)	H-y(ft)	T(°C)
22.	0.00	26.20	32.	0.000	24.20	42.	0.00	25.55
	.05	29.40		.045	29.00		.05	29.40
	.10	30.65		.095	30.40		.10	30.75
	.15	30.85		.145	31.00		.15	31.05
	.20	31.00		.195	31.00		.20	31.15
	.25	31.00		.245	31.00		.25	31.20
	.30	31.00		.295	31.05		.35	31.15
	.35	30.50		.345	31.00		.40	30.80
	.40	27.50		.395	30.45		.45	28.35
	.45	22.30		.445	26.60		.50	23.00
	.50	18.35		.495	21.40		.55	19.25
	.55	16.25		.545	18.00		.60	16.80
	.60	14.90		.595	16.10		.62	16.20
	.62	14.60		.615	15.45			

TEST-37 (Continued)

x(ft)	H-y(ft)	T(°C)	x(ft)	H-y(ft)	T(°C)
66.	0.00	25.20	90.	0.00	24.80
	.05	29.40		.15	31.05
	.15	31.05		.25	31.30
	.20	31.20		.35	31.30
	.25	31.25		.45	31.30
	.30	31.25		.50	31.25
	.35	31.25		.55	31.20
	.40	31.20		.60	29.80
	.45	31.05		.62	28.20
	.50	29.40		.63	27.85
	.55	24.40			
	.60	21.00			
	.62	20.15			

TEST-38 (Continued)

x(ft)	H-y(ft)	T(°C)	x(ft)	H-y(ft)	T(°C)	x(ft)	H-y(ft)	T(°C)
32.	0.00	24.00	42.	0.00	25.25	49.	0.00	23.50
	.05	27.60		.05	28.15		.09	28.60
	.10	28.70		.10	29.00		.19	29.35
	.15	29.05		.15	29.20		.29	29.40
	.20	29.20		.20	29.25		.39	29.45
	.25	29.20		.255	29.30		.49	29.45
	.30	29.20		.305	29.35		.54	29.40
	.35	29.20		.355	29.35		.59	29.00
	.40	29.20		.405	29.35		.62	25.95
	.45	29.20		.455	29.35		.64	23.40
	.50	28.95		.505	29.25		.66	22.00
	.54	26.50		.54	29.10		.665	21.45
	.57	22.40		.57	27.15			
	.60	19.80		.60	23.00			
	.63	18.25		.63	20.65			
	.65	17.45		.655	19.45			
	.655	17.25		.665	19.05			

TEST-38: H = 0.665 ft, L = 51.2 ft, Q_a = 0.064 cfs, Q_w = .0146 cfs

x(ft)	H-y(ft)	T(°C)	x(ft)	H-y(ft)	T(°C)	x(ft)	H-y(ft)	T(°C)
2.	0.00	23.80	12.	0.00	24.60	22.	0.00	26.50
	.05	27.80		.05	27.70		.05	28.25
	.10	28.40		.10	28.60		.10	28.80
	.15	28.80		.15	28.95		.15	29.00
	.20	28.85		.20	29.00		.20	29.10
	.25	28.85		.25	29.05		.25	29.10
	.30	28.60		.30	29.05		.30	29.10
	.34	27.05		.35	29.00		.35	29.10
	.37	23.40		.40	28.80		.40	29.05
	.40	20.60		.43	27.60		.44	28.95
	.45	17.55		.46	25.10		.48	27.65
	.50	15.45		.50	20.60		.51	25.20
	.55	14.40		.55	17.30		.54	21.60
	.60	13.80		.59	15.90		.57	18.95
	.64	13.45		.63	14.90		.60	17.55
	.66	13.45		.65	14.55		.64	16.00
							.66	15.45

TEST-39: H = 0.378 ft, L = 19.6 ft, Q_a = 0.034 cfs, Q_w = .0146 cfs

x(ft)	H-y(ft)	T(°C)	x(ft)	H-y(ft)	T(°C)	x(ft)	H-y(ft)	T(°C)
2.	0.00	24.20	12.	0.00	26.80	19.	0.00	27.30
	.05	29.00		.05	29.00		.05	29.25
	.10	30.00		.10	29.85		.10	30.00
	.13	30.35		.15	30.25		.15	30.20
	.16	30.40		.20	30.35		.20	30.25
	.20	29.80		.25	30.25		.25	30.25
	.23	26.55		.28	29.60		.30	30.25
	.26	22.30		.31	25.50		.33	30.25
	.30	19.10		.33	22.40		.35	28.95
	.33	17.55		.35	20.60		.37	26.40
	.35	16.90		.37	19.50		.375	25.80
	.37	16.40		.376	19.25	null =	.361	
null =	.279		null =	.310				

TEST-40: H = 0.439 ft, L = 42.8 ft, Q_a = 0.038 cfs, Q_w = .0146 cfs

x(ft)	H-y(ft)	T(°C)	x(ft)	H-y(ft)	T(°C)	x(ft)	H-y(ft)	T(°C)
2.	0.00	25.50	12.	0.00	28.60	22.	0.00	28.00
	.05	30.60		.05	31.00		.05	31.25
	.10	31.40		.10	31.55		.10	31.75
	.15	31.65		.15	31.80		.15	31.95
	.20	30.30		.20	31.95		.20	31.95
	.25	22.15		.25	31.70		.25	32.00
	.30	18.50		.29	29.85		.30	31.20
	.35	16.10		.33	23.80		.33	28.40
	.39	14.80		.36	20.60		.36	23.85
	.43	13.65		.40	18.15		.40	20.40
null =	.242			.43	16.70		.43	18.75
				.438	16.35		.435	18.55
			null =	.319		null =	.350	

TEST-41: H = 0.485 ft, L = 32.7 ft, Q_a = 0.049 cfs, Q_w = .0146 cfs

x(ft)	H-y(ft)	T(°C)	x(ft)	H-y(ft)	T(°C)	x(ft)	H-y(ft)	T(°C)
2.0	0.00	24.25	14.	0.00	27.90	27.	0.00	28.70
	.05	29.75		.05	30.60		.05	30.50
	.10	31.00		.10	31.00		.10	31.00
	.15	31.15		.15	31.20		.15	31.20
	.20	31.05		.20	31.25		.20	31.30
	.25	28.50		.25	31.25		.30	31.35
	.28	24.00		.30	31.20		.35	31.30
	.31	20.35		.34	30.20		.40	30.40
	.35	18.25		.37	26.80		.43	25.95
	.40	15.80		.40	21.85		.45	23.40
	.44	14.50		.43	19.60		.47	22.00
	.47	13.60		.45	18.60		.48	21.60
null =	.255			.47	17.60			
				.475	17.50			
			null =	.386				

TEST-40 (Continued)

x(ft)	H-y(ft)	T(°C)	x(ft)	H-y(ft)	T(°C)
32.	0.00	29.20	39.	0.00	28.30
	.05	31.10		.05	31.00
	.10	31.65		.10	31.45
	.15	31.95		.20	31.85
	.20	32.00		.30	31.85
	.25	32.05		.35	31.85
	.30	32.00		.38	31.85
	.35	31.00		.40	30.80
	.38	27.20		.42	28.40
	.41	23.50		.43	27.30
	.43	22.20		.435	26.85
null =	.377				

TEST-42: H = 0.442 ft, L = 17.3 ft, Q_a = 0.049 cfs, Q_w = .0146 cfs

x(ft)	H-y(ft)	T(°C)	x(ft)	H-y(ft)	T(°C)
4.	0.00	27.85	14.	0.00	29.00
	.05	30.20		.05	30.40
	.10	30.75		.10	30.85
	.15	31.00		.15	31.00
	.20	31.00		.20	31.05
	.25	30.95		.25	31.10
	.28	30.25		.30	31.10
	.31	27.25		.35	31.00
	.34	22.35		.37	30.20
	.37	19.40		.39	26.40
	.40	18.15		.41	22.75
	.43	16.95		.43	20.90
	.435	16.70		.435	20.60
null =	.328		null =	.389	

TEST-43: H = 0.593 ft, L = 77.7 ft, Q_a = 0.051 cfs, Q_w = .0146 cfs

x(ft)	H-y(ft)	T(°C)
4.	0.00	28.60
	.05	30.40
	.10	30.70
	.15	30.80
	.20	30.80
	.25	30.45
	.30	27.40
	.34	22.90
	.38	19.20
	.42	17.00
	.46	15.65
	.50	14.50
	.54	14.00
	.58	13.65
	.583	13.45
null =	.380	

x(ft)	H-y(ft)	T(°C)
28.	0.00	24.30
	.05	29.40
	.10	30.40
	.15	30.75
	.20	30.80
	.25	30.80
	.30	30.80
	.35	30.45
	.38	29.20
	.41	26.70
	.44	23.60
	.47	20.40
	.50	18.55
	.54	16.75
	.58	15.45
	.585	15.35
null =	.457	

x(ft)	H-y(ft)	T(°C)
54.	0.00	27.10
	.05	30.00
	.10	30.60
	.15	30.80
	.25	30.85
	.35	30.85
	.40	30.75
	.44	30.30
	.47	28.70
	.50	25.50
	.54	21.90
	.58	19.95
null =	.505	

TEST-44 (Continued): Q_a = 0.051 cfs, Q_w = .0146 cfs

x(ft)	H-y(ft)	T(°C)
66.	0.00	27.85
	.05	30.05
	.10	30.65
	.15	31.00
	.25	31.00
	.35	31.00
	.40	30.95
	.45	29.80
	.48	28.00
	.51	25.40
	.54	22.40
	.57	20.70
	.61	18.60
	.63	17.75
	.64	17.35
null =	.523	

x(ft)	H-y(ft)	T(°C)
106.	0.00	25.20
	.05	29.20
	.10	30.50
	.15	30.95
	.20	31.00
	.30	31.05
	.40	31.05
	.45	31.05
	.50	31.00
	.55	30.50
	.58	28.55
	.61	26.40
	.64	25.20
	.648	25.05
null =	.577	

TEST-43 (Continued)

x(ft)	H-y(ft)	T(°C)
70.	0.00	27.40
	.05	30.15
	.09	30.55
	.15	30.85
	.25	30.95
	.35	30.95
	.45	30.90
	.50	30.75
	.53	29.45
	.56	26.70
	.58	25.30
	.59	24.85
null =	.546	

TEST-44: H = 0.643 ft, L = 113.3 ft,

x(ft)	H-y(ft)	T(°C)
4.	0.00	28.00
	.05	30.00
	.10	30.60
	.15	30.80
	.20	30.80
	.25	30.65
	.28	29.80
	.31	27.45
	.35	22.55
	.39	19.35
	.43	17.00
	.48	15.40
	.53	14.45
	.58	13.80
	.61	13.60
	.635	13.40
null =	.378	

x(ft)	H-y(ft)	T(°C)
36.	0.00	28.40
	.05	30.15
	.10	30.70
	.15	30.95
	.20	30.95
	.30	30.95
	.35	30.60
	.39	29.50
	.42	27.25
	.45	24.60
	.48	21.80
	.51	19.40
	.56	17.00
	.61	15.30
	.63	14.85
	.635	14.80
null =	.468	

TEST-45: H = 0.544 ft, L = 54.5 ft, Q_a = 0.05 cfs, Q_w = .0146 cfs

x(ft)	H-y(ft)	T(°C)
4.	0.00	28.60
	.05	30.25
	.10	30.80
	.15	30.95
	.20	30.95
	.25	30.60
	.28	29.30
	.31	26.35
	.34	22.70
	.37	19.80
	.41	17.00
	.45	15.40
	.49	14.20
	.53	13.50
	.535	13.40
null =	.356	

x(ft)	H-y(ft)	T(°C)
22.	0.00	28.20
	.05	30.25
	.10	30.70
	.15	30.90
	.20	30.95
	.25	30.95
	.30	30.95
	.35	30.40
	.38	28.60
	.41	25.35
	.44	21.30
	.47	18.90
	.51	16.70
	.54	15.40
null =	.428	

x(ft)	H-y(ft)	T(°C)
42.	0.00	27.00
	.05	30.20
	.10	30.80
	.15	31.00
	.20	31.05
	.30	31.05
	.40	30.95
	.45	28.95
	.48	24.90
	.51	22.10
	.535	20.70
	.545	20.20
null =	.470	

TEST-46: H = 0.518 ft, L = 42.0 ft, Q_a = 0.05 cfs, Q_w = .0146 cfs

x(ft)	H-y(ft)	T(°C)	x(ft)	H-y(ft)	T(°C)	x(ft)	H-y(ft)	T(°C)
4.	0.00	27.25	18.	0.00	25.00	32.	0.00	26.95
	.05	30.05		.05	29.65		.05	29.65
	.10	30.50		.10	30.50		.10	30.60
	.15	30.80		.15	30.80		.15	30.85
	.20	30.80		.20	30.85		.20	30.90
	.25	30.65		.30	30.85		.30	30.90
	.28	29.85		.35	30.35		.40	30.65
	.31	27.20		.38	28.15		.43	29.10
	.34	23.35		.41	24.00		.46	24.20
	.37	20.05		.44	20.05		.49	21.20
	.40	17.80		.47	18.05		.51	20.05
	.43	16.30		.50	16.55	null =	.437	
	.47	14.90		.513	15.95			
	.51	13.75	null =	.412				
null =	.361							

TEST-47: H = 0.569 ft, L = 31.0 ft, Q_a = 0.062 cfs

x(ft)	H-y(ft)	T(°C)	x(ft)	H-y(ft)	T(°C)	x(ft)	H-y(ft)	T(°C)
4.	0.00	28.20	16.	0.00	28.20	25.	0.00	23.40
	.05	29.70		.05	29.40		.05	28.40
	.10	30.10		.10	29.85		.10	29.45
	.15	30.25		.15	30.05		.15	29.85
	.20	30.30		.20	30.10		.20	30.00
	.25	30.30		.25	30.10		.25	30.00
	.30	30.25		.35	30.05		.30	30.00
	.33	29.95		.40	29.95		.35	30.00
	.36	27.80		.43	29.10		.40	30.00
	.39	24.65		.46	26.20		.45	30.00
	.42	21.20		.49	21.10		.50	29.40
	.45	18.60		.52	18.85		.53	24.80
	.50	16.30		.55	17.60		.56	21.25
	.55	14.80		.575	16.80		.58	20.04
	.58	14.20	null =	.479		null =	.528	
null =	.418							

TEST-48: H = 0.606 ft, L = 58.7 ft, Q_a = 0.060 cfs

x(ft)	H-y(ft)	T(°C)	x(ft)	H-y(ft)	T(°C)	x(ft)	H-y(ft)	T(°C)
4.	0.00	27.95	22.	0.00	25.00	43.	0.00	23.00
	.05	30.00		.05	29.20		.05	28.85
	.10	30.50		.10	30.25		.10	30.15
	.15	30.80		.15	30.55		.15	30.55
	.20	30.80		.20	30.65		.20	30.70
	.25	30.70		.25	30.70		.30	30.75
	.30	30.00		.30	30.70		.40	30.70
	.33	28.10		.40	29.85		.45	30.50
	.36	25.35		.43	27.70		.50	28.15
	.39	21.60		.46	24.50		.53	24.60
	.42	19.00		.49	20.80		.56	21.60
	.45	17.15		.52	18.45		.59	20.20
	.50	15.20		.57	16.25		.62	18.85
	.55	14.00		.60	15.15	null =	.526	
	.59	13.40		.62	14.75			
	.62	13.35	null =	.48				
null =	.430							

TEST-49: H = 0.655 ft, L = 77.0 ft, Q_a = 0.059 cfs

x(ft)	H-y(ft)	T(°C)	x(ft)	H-y(ft)	T(°C)	x(ft)	H-y(ft)	T(°C)
4.	0.00	27.30	24.5	0.00	26.15	49.	0.00	27.00
	.05	29.60		.05	29.40		.05	29.45
	.10	30.20		.10	30.20		.10	30.25
	.15	30.40		.15	30.40		.15	30.50
	.25	30.40		.20	30.55		.20	30.60
	.30	30.20		.25	30.55		.30	30.60
	.33	29.30		.35	30.50		.40	30.60
	.36	26.90		.40	30.05		.45	30.45
	.39	23.50		.43	28.55		.49	29.50
	.42	20.65		.46	26.25		.52	27.35
	.45	18.70		.49	23.20		.55	23.70
	.49	16.60		.52	19.70		.58	21.00
	.53	15.40		.56	17.60		.61	19.40
	.57	14.35		.60	16.00		.64	18.05
	.60	14.00		.64	14.95		.655	17.35
	.64	13.60		.655	14.45	null =	.556	
	.655	13.50	null =	.528				
null =	.455							

TEST-49 (Continued)

x(ft)	H-y(ft)	T(°C)
68.	0.00	25.65
	.05	29.20
	.10	30.20
	.15	30.50
	.20	30.60
	.30	30.60
	.40	30.60
	.50	30.60
	.55	30.20
	.58	28.50
	.61	25.50
	.64	23.80
	.655	23.30
null =	.604	

TEST-50: H = 0.523 ft, L = 24.0 ft, Q_a = 0.060 cfs

x(ft)	H-y(ft)	T(°C)
4.	0.00	27.80
	.05	29.85
	.10	30.35
	.15	30.55
	.20	30.60
	.25	30.60
	.30	30.55
	.33	30.00
	.35	28.75
	.37	26.50
	.39	23.40
	.41	21.00
	.44	18.80
	.47	17.40
	.51	15.85
	.54	15.20
null	.394	

x(ft)	H-y(ft)	T(°C)
12.	0.00	27.00
	.05	29.40
	.10	30.20
	.15	30.60
	.20	30.65
	.25	30.70
	.30	30.70
	.35	30.65
	.40	29.95
	.42	28.40
	.44	24.90
	.46	21.90
	.49	19.50
	.51	18.70
	.53	17.85
null =	.445	

TEST-51: Q_w = .0146 cfs (Cont'd)

x(ft)	H-y(ft)	T(°C)
30.5	0.00	29.80
	.05	31.05
	.10	31.45
	.15	31.60
	.20	31.65
	.30	31.65
	.35	31.55
	.39	30.20
	.41	28.60
	.43	25.75
	.45	23.05
	.49	20.25
	.52	18.75
null =	.431	

x(ft)	H-y(ft)	T(°C)
42.5	0.00	28.80
	.05	31.00
	.10	31.40
	.15	31.65
	.20	31.70
	.25	31.70
	.30	31.70
	.40	31.60
	.43	31.05
	.45	29.65
	.47	27.20
	.49	24.90
	.51	23.65
	.53	22.95
null =	.467	

TEST-52: H = 0.578 ft

x(ft)	H-y(ft)	T(°C)
4.	0.00	29.45
	.05	30.90
	.10	31.05
	.15	31.25
	.20	31.25
	.25	31.00
	.30	28.20
	.33	24.70
	.36	22.20
	.39	19.80
	.42	17.70
	.45	16.55
	.50	15.05
	.55	14.30
	.58	14.00
null =	.371	

TEST-50: Q_w = .0146 cfs (Cont'd)

x(ft)	H-y(ft)	T(°C)
20.	0.00	27.20
	.05	29.65
	.10	30.40
	.15	30.65
	.20	30.70
	.30	30.80
	.40	30.80
	.45	30.70
	.48	28.65
	.49	26.70
	.50	25.20
	.51	23.60
	.53	21.80
null =	.491	

TEST-51: H = 0.519 ft, L = 51.0 ft, Q_a = 0.049 cfs

x(ft)	H-y(ft)	T(°C)
4.	0.00	28.90
	.05	30.90
	.10	31.25
	.15	31.45
	.20	31.50
	.25	31.30
	.29	30.25
	.31	27.80
	.32	26.60
	.33	25.30
	.35	23.25
	.37	21.00
	.40	18.40
	.43	17.15
	.46	16.00
	.49	15.20
	.53	14.35
null =	.360	

x(ft)	H-y(ft)	T(°C)
18.	0.00	23.20
	.05	30.20
	.10	31.20
	.15	31.55
	.20	31.65
	.25	31.65
	.30	31.55
	.34	30.70
	.37	28.45
	.39	26.15
	.41	23.45
	.44	20.20
	.47	18.50
	.50	17.10
	.53	16.15
null =	.401	

TEST-52 (Continued): L = 80.0 ft, Q_a = 0.049 cfs, Q_w = .0146 cfs

x(ft)	H-y(ft)	T(°C)
24.5	0.00	28.60
	.05	30.70
	.10	31.10
	.15	31.30
	.20	31.35
	.25	31.40
	.30	31.30
	.35	30.30
	.38	28.55
	.41	25.60
	.44	21.80
	.47	19.65
	.52	17.25
	.56	15.85
	.578	15.40
null =	.429	

x(ft)	H-y(ft)	T(°C)
46.	0.00	26.85
	.05	30.40
	.10	31.05
	.15	31.40
	.20	31.45
	.30	31.45
	.35	31.45
	.40	30.80
	.43	29.30
	.46	26.40
	.49	23.10
	.52	20.90
	.56	18.80
	.578	17.65
null =	.466	

x(ft)	H-y(ft)	T(°C)
68.	0.00	27.80
	.05	30.90
	.10	31.25
	.15	31.40
	.20	31.45
	.30	31.55
	.35	31.55
	.40	31.50
	.45	31.25
	.48	30.10
	.51	27.60
	.54	25.20
	.56	24.35
	.578	23.35
null =	.508	

TEST-53: H = 0.630 ft, L = 112.1 ft, Q_a = 0.049 cfs, Q_w = .0146 cfs

x(ft)	H-y(ft)	T(°C)	x(ft)	H-y(ft)	T(°C)	x(ft)	H-y(ft)	T(°C)
4.	0.00	28.05	24.5	0.00	27.40	46.	0.00	27.80
	.05	30.60		.06	30.50		.05	30.40
	.10	31.00		.10	30.95		.10	31.00
	.15	31.20		.15	31.20		.15	31.25
	.20	31.20		.20	31.30		.20	31.35
	.25	31.00		.25	31.30		.25	31.35
	.30	28.60		.30	31.20		.30	31.35
	.33	25.55		.35	30.20		.35	31.25
	.36	22.00		.38	28.20		.40	30.00
	.39	19.80		.41	25.55		.43	28.40
	.44	16.95		.44	22.25		.46	26.25
	.49	15.45		.47	19.45		.49	22.70
	.54	14.55		.52	17.30		.52	20.35
	.59	14.05		.57	15.60		.57	17.85
	.63	13.85		.61	14.80		.61	16.35
null =	.385			.64	14.40		.64	15.65
			null =	.445		null =	.480	

TEST-53 (Continued)

x(ft)	H-y(ft)	T(°C)	x(ft)	H-y(ft)	T(°C)
71.5	0.00	28.20	97.5	0.00	29.05
	.05	30.45		.05	30.60
	.10	31.05		.10	31.20
	.15	31.35		.15	31.40
	.20	31.45		.20	31.45
	.30	31.45		.30	31.50
	.40	31.35		.40	31.50
	.45	30.60		.45	31.45
	.48	28.70		.50	31.00
	.51	26.30		.53	29.90
	.54	23.45		.56	27.40
	.57	21.60		.59	25.50
	.60	20.20		.62	24.45
	.63	18.70		.64	24.00
null =	.509		null =	.545	

TEST-54: H = 0.494 ft, L = 38.3 ft, Q_a = 0.049 cfs, Q_w = .0146 cfs

x(ft)	H-y(ft)	T(°C)	x(ft)	H-y(ft)	T(°C)	x(ft)	H-y(ft)	T(°C)
4.	0.00	28.30	18.	0.00	26.50	30.5	0.00	28.45
	.05	30.45		.05	29.90		.05	30.60
	.10	31.00		.10	30.80		.10	31.00
	.15	31.05		.15	31.15		.15	31.25
	.20	31.05		.20	31.20		.20	31.35
	.25	31.00		.25	31.25		.25	31.35
	.28	30.50		.30	31.20		.30	31.35
	.30	29.20		.33	31.00		.35	31.35
	.32	27.00		.35	30.30		.38	31.30
	.34	24.35		.37	29.00		.41	30.45
	.36	22.20		.39	26.95		.43	28.00
	.38	19.60		.41	23.80		.45	25.05
	.41	18.05		.43	21.40		.47	23.05
	.44	16.80		.45	20.15		.50	21.60
	.47	15.85		.48	18.55	null =	.435	
	.50	14.85		.50	17.70			
null =	.352		null =	.400				

TEST-55: H = 0.437 ft, L = 18.6 ft, Q_a = 0.048 cfs, Q_w = .0146 cfs

x(ft)	H-y(ft)	T(°C)	x(ft)	H-y(ft)	T(°C)	x(ft)	H-y(ft)	T(°C)
4.	0.00	28.45	10.	0.00	29.20	16.	0.00	29.30
	.05	30.40		.05	30.60		.05	30.60
	.10	30.95		.10	30.95		.10	31.00
	.15	31.05		.15	31.15		.15	31.20
	.20	31.05		.20	31.20		.20	31.20
	.25	31.00		.25	31.20		.25	31.25
	.30	29.80		.30	31.20		.30	31.25
	.32	27.40		.35	28.80		.35	31.20
	.34	24.55		.37	25.10		.38	30.10
	.36	21.20		.39	21.85		.40	26.60
	.38	19.60		.41	20.25		.42	23.20
	.40	18.65		.43	19.35		.44	21.80
	.43	17.40		.45	18.80	null =	.399	
	.45	16.60	null =	.362				
null =	.329							

TEST-56: H = 0.433 ft, L = 39.8 ft, Q_a = 0.038 cfs, Q_w = .0146 cfs

x(ft)	H-y(ft)	T(°C)	x(ft)	H-y(ft)	T(°C)	x(ft)	H-y(ft)	T(°C)
4.	0.00	28.00	18.5	0.00	27.85	30.5	0.00	29.20
	.05	30.60		.05	30.30		.05	30.80
	.10	31.00		.10	31.05		.10	31.25
	.15	31.15		.15	31.30		.15	31.40
	.20	31.00		.20	31.35		.20	31.45
	.23	30.25		.25	31.25		.25	31.50
	.25	28.65		.28	30.80		.30	31.30
	.27	26.35		.30	29.75		.33	30.70
	.29	24.00		.32	27.80		.35	29.80
	.31	21.20		.34	25.00		.37	27.15
	.33	19.10		.36	22.30		.39	24.40
	.35	18.20		.38	20.75		.41	22.80
	.37	17.40		.40	19.50		.433	21.50
	.39	16.70		.42	18.55	null =	.370	
	.42	15.70		.433	17.55			
	.433	15.00	null =	.339				
null =	.296							

TEST-57: H = 0.493 ft, L = 76.0 ft, Q_a = 0.038 cfs, Q_w = .0146 cfs

x(ft)	H-y(ft)	T(°C)	x(ft)	H-y(ft)	T(°C)	x(ft)	H-y(ft)	T(°C)
4.	0.00	29.45	24.5	0.00	29.00	46.	0.00	28.60
	.05	31.05		.05	31.00		.05	30.55
	.10	31.55		.10	31.50		.10	30.80
	.15	31.75		.15	31.60		.15	31.00
	.20	31.40		.20	31.60		.20	31.00
	.225	30.55		.25	31.15		.25	31.00
	.25	28.60		.28	30.55		.30	30.95
	.27	26.50		.31	29.00		.33	30.60
	.29	24.00		.33	27.00		.36	29.25
	.31	21.85		.35	24.75		.39	26.65
	.33	19.80		.37	22.15		.42	23.35
	.35	18.45		.39	20.45		.45	21.40
	.38	17.25		.42	18.80		.48	20.20
	.43	15.70		.46	17.20		.493	19.40
	.48	14.70		.493	15.85	null =	.395	
	.493	14.60	null =	.361				
null =	.306							

TEST-57 (Continued)

x(ft)	H-y(ft)	T(°C)
68.	0.00	24.40
	.05	29.20
	.10	30.70
	.15	31.15
	.20	31.30
	.25	31.25
	.30	31.25
	.33	31.15
	.36	31.05
	.39	30.95
	.42	30.15
	.45	28.05
	.48	26.65
	.493	26.15
null =	.425	

TEST-58: H = 0.518 ft, L = 97.3 ft

x(ft)	H-y(ft)	T(°C)	x(ft)	H-y(ft)	T(°C)
4.	0.00	29.00	28.	0.00	26.00
	.05	30.60		.05	30.10
	.10	31.00		.10	30.80
	.15	31.10		.15	31.05
	.20	30.65		.20	31.15
	.23	29.80		.25	31.00
	.25	27.40		.30	29.50
	.27	25.35		.32	28.15
	.29	23.00		.34	26.85
	.32	20.80		.36	24.50
	.35	18.25		.38	22.15
	.40	16.55		.41	20.00
	.45	15.30		.44	18.50
	.50	14.55		.47	17.20
	.518	14.40		.51	16.05
null =	.311			.518	15.80
			null =	.365	

TEST-58 (Continued): Q_a = 0.038 cfs, Q_w = .0146 cfs

x(ft)	H-y(ft)	T(°C)	x(ft)	H-y(ft)	T(°C)	x(ft)	H-y(ft)	T(°C)
49.	0.00	27.50	61.	0.00	28.70	87.	0.00	28.80
	.05	30.40		.05	30.60		.05	30.80
	.10	30.80		.10	30.95		.10	30.95
	.15	31.05		.15	31.10		.15	31.05
	.20	31.15		.20	31.15		.20	31.15
	.25	31.10		.25	31.20		.30	31.15
	.30	30.90		.30	31.10		.35	31.10
	.33	30.35		.35	30.50		.40	30.95
	.35	29.55		.38	29.40		.43	30.40
	.37	28.15		.40	28.15		.45	29.40
	.39	26.30		.42	26.00		.47	28.10
	.41	24.20		.44	24.20		.49	27.20
	.44	21.65		.46	22.80		.51	26.60
	.47	20.20		.49	21.40		.518	26.25
	.50	18.80		.518	20.05	null =	.466	
	.518	17.85	null =	.417				
null =	.396							

TEST-59: H = 0.394 ft, L = 22.0 ft, Q_a = 0.038 cfs, Q_w = .0146 cfs

x(ft)	H-y(ft)	T(°C)	x(ft)	H-y(ft)	T(°C)	x(ft)	H-y(ft)	T(°C)
4.	0.00	28.40	10.	0.00	27.85	18.5	0.00	28.25
	.05	30.10		.05	29.80		.05	30.00
	.10	30.60		.10	30.40		.10	30.40
	.15	30.75		.15	30.65		.15	30.60
	.20	30.65		.20	30.65		.20	30.65
	.23	30.05		.25	30.55		.25	30.65
	.25	28.70		.28	29.60		.30	30.65
	.27	25.80		.30	27.60		.34	29.70
	.29	23.00		.32	24.50		.36	27.00
	.31	20.60		.34	21.80		.38	24.40
	.33	19.50		.37	20.20		.40	23.00
	.36	18.30		.40	19.00			
	.38	17.55						
	.40	16.90						

TEST-60: H = 0.580 ft, L = 32.1 ft, Q_a = 0.034 cfs, Q_w = .0073 cfs

x(ft)	H-y(ft)	T(°C)	x(ft)	H-y(ft)	T(°C)	x(ft)	H-y(ft)	T(°C)
2.	0.00	30.65	10.	0.00	30.40	20.	0.00	30.25
	.05	32.40		.025	31.45		.025	31.25
	.10	32.95		.05	32.00		.05	31.95
	.15	33.05		.075	32.40		.075	32.35
	.20	33.10		.10	32.65		.10	31.95
	.25	32.80		.125	32.80		.125	30.80
	.275	32.20		.15	32.55		.15	29.35
	.30	30.90		.175	31.75		.175	28.15
	.325	29.60		.20	30.60		.20	27.15
	.35	28.45		.225	29.20		.225	26.15
	.375	27.70		.25	27.95		.25	25.80
	.40	26.85		.275	26.90		.275	25.40
	.425	26.20		.30	26.20		.325	24.95
	.45	25.80		.325	25.65		.375	24.75
	.475	25.35		.35	25.25		.425	24.70
	.50	24.95		.425	24.80		.475	24.65
	.58	24.65		.525	24.65	null =	.126	
null =	.263		null =	.172				

TEST-60 (Continued)

x(ft)	H-y(ft)	T(°C)
28.	0.00	30.10
	.025	30.65
	.05	30.80
	.075	30.10
	.10	28.70
	.125	27.65
	.15	27.00
	.175	26.35
	.20	25.80
	.225	25.40
	.25	25.15
	.30	24.85
	.35	24.75
	.40	24.70
null =	.091	

TEST-61: H = 0.650 ft, L = 36.8 ft

x(ft)	H-y(ft)	T(°C)	x(ft)	H-y(ft)	T(°C)
2.	0.00	30.50	10.	0.00	29.25
	.05	32.15		.025	30.80
	.10	32.95		.05	31.85
	.15	33.15		.075	32.65
	.20	33.35		.10	33.00
	.275	33.35		.125	33.20
	.30	32.90		.15	33.20
	.325	31.85		.175	33.15
	.35	30.90		.20	32.60
	.375	29.40		.225	31.45
	.40	28.30		.25	30.10
	.425	27.65		.275	28.80
	.45	26.90		.30	27.75
	.475	26.40		.325	26.80
	.525	25.55		.35	26.25
	.575	25.20		.45	25.20
	.65	25.05		.55	25.00
null =	.246		null =	.158	

TEST-61 (Continued): Q_a = 0.042 cfs, Q_w = .0080 cfs

x(ft)	H-y(ft)	T(°C)	x(ft)	H-y(ft)	T(°C)
20.	0.00	29.70	30.5	0.00	28.80
	.02	31.25		.02	30.80
	.04	32.10		.04	31.50
	.06	32.60		.06	31.80
	.08	32.80		.08	31.30
	.10	32.85		.10	30.30
	.12	32.65		.12	29.20
	.14	31.95		.14	28.20
	.16	30.95		.16	27.65
	.18	29.90		.18	27.00
	.20	28.80		.20	26.45
	.225	27.70		.225	25.95
	.25	26.85		.275	25.35
	.275	26.25		.325	25.15
	.30	25.85		.425	25.00
	.35	25.25	null =	.048	
	.45	25.00			
null =	.105				

TEST-62: H = 0.647 ft, L = 70.3 ft, Q_a = 0.020 cfs, Q_w = .0077 cfs

x(ft)	H-y(ft)	T(°C)
2.	0.00	31.20
	.04	31.95
	.10	32.45
	.125	32.55
	.20	32.60
	.275	32.60
	.30	32.40
	.325	32.05
	.35	31.45
	.375	30.60
	.40	29.50
	.425	28.75
	.45	27.90
	.475	27.20
	.50	26.80
	.55	26.15
	.65	25.85
null =	.241	

x(ft)	H-y(ft)	T(°C)
16.	0.00	29.70
	.05	31.80
	.10	32.30
	.16	32.45
	.19	32.35
	.21	32.10
	.23	31.75
	.25	31.20
	.27	30.60
	.29	29.80
	.31	29.00
	.33	28.35
	.35	27.75
	.375	27.10
	.40	26.60
	.45	26.05
	.55	25.80
null =	.175	

x(ft)	H-y(ft)	T(°C)
32.	0.00	29.00
	.03	30.60
	.06	31.40
	.10	31.80
	.125	31.90
	.15	31.60
	.17	31.30
	.19	30.80
	.21	30.20
	.23	29.45
	.25	28.75
	.27	28.00
	.29	27.45
	.32	26.85
	.35	26.35
	.40	25.95
	.45	25.80
null =	.129	

TEST-62 (Continued)

x(ft)	H-y(ft)	T(°C)
49.	0.00	30.05
	.04	30.95
	.07	31.25
	.10	31.00
	.12	30.60
	.14	30.15
	.16	29.40
	.18	28.80
	.20	28.15
	.22	27.60
	.24	27.15
	.26	26.75
	.30	26.20
	.35	25.95
	.40	25.80
	.45	25.75
null =	.083	

x(ft)	H-y(ft)	T(°C)
64.	0.00	28.60
	.025	29.05
	.05	29.35
	.07	29.10
	.09	28.40
	.11	27.80
	.13	27.40
	.15	27.15
	.17	26.85
	.20	26.40
	.25	26.00
	.30	25.85
	.35	25.75
null =	.050	

TEST-63: H = 0.650 ft, L = 51.4 ft, Q_a = 0.026 cfs, Q_w = .0075 cfs

x(ft)	H-y(ft)	T(°C)
2.	0.00	31.35
	.04	32.35
	.07	32.65
	.10	33.10
	.18	33.35
	.26	33.35
	.30	32.75
	.32	32.00
	.34	31.20
	.36	30.25
	.38	29.65
	.40	28.70
	.42	27.75
	.45	27.10
	.49	26.25
	.53	25.70
	.64	25.40

x(ft)	H-y(ft)	T(°C)
10.	0.00	29.45
	.04	31.00
	.08	32.25
	.12	32.95
	.16	33.20
	.20	33.05
	.22	32.75
	.24	32.35
	.26	31.55
	.28	30.50
	.30	29.65
	.32	28.50
	.34	27.95
	.37	26.90
	.40	26.25
	.44	25.80
	.56	25.40
null =	.181	

x(ft)	H-y(ft)	T(°C)
20.	0.00	29.65
	.04	31.20
	.07	32.20
	.10	32.75
	.13	32.95
	.16	32.60
	.19	31.75
	.21	30.85
	.23	30.00
	.25	28.95
	.27	28.00
	.29	27.35
	.31	26.65
	.34	26.05
	.38	25.70
	.42	25.50
	.46	25.40
null =	.133	

TEST-63 (Continued)

x(ft)	H-y(ft)	T(°C)
30.5	0.00	30.05
	.04	31.75
	.07	32.35
	.10	32.40
	.13	31.80
	.15	31.10
	.17	30.30
	.19	29.30
	.21	28.40
	.23	27.65
	.25	27.05
	.28	26.40
	.31	26.00
	.35	25.65
	.43	25.40
null =	.097	

x(ft)	H-y(ft)	T(°C)
43.	0.00	27.50
	.03	29.70
	.06	30.80
	.09	30.00
	.11	29.20
	.13	28.40
	.15	27.80
	.17	27.20
	.20	26.55
	.23	26.05
	.26	25.75
	.30	25.55
	.38	25.40
null =	.057	

TEST-64: H = 0.575 ft

x(ft)	H-y(ft)	T(°C)
2.	0.00	31.55
	.03	32.05
	.06	32.45
	.10	32.65
	.26	32.65
	.29	32.15
	.31	31.60
	.33	30.65
	.35	29.80
	.37	28.90
	.39	28.15
	.41	27.65
	.43	27.40
	.45	26.80
	.49	26.10
	.53	25.75
	.57	25.60

TEST-64 (Continued): L = 48.8 ft, Q_a = 0.027 cfs, Q_w = .0081 cfs

x(ft)	H-y(ft)	T(°C)	x(ft)	H-y(ft)	T(°C)	x(ft)	H-y(ft)	T(°C)
10.	0.00	29.25	20.	0.00	30.40	30.5	0.00	30.45
	.03	31.20		.03	31.60		.03	31.50
	.06	32.10		.06	32.20		.06	32.20
	.10	32.65		.10	32.75		.09	32.20
	.13	32.85		.13	32.65		.12	31.65
	.16	32.95		.16	32.05		.14	31.00
	.19	32.75		.18	31.40		.16	30.30
	.22	32.00		.20	30.40		.18	29.35
	.24	31.20		.22	29.65		.20	28.60
	.26	30.35		.24	28.60		.22	27.80
	.28	29.60		.26	27.85		.25	26.95
	.30	28.55		.28	27.25		.28	26.35
	.32	27.85		.31	26.50		.31	25.95
	.34	27.25		.35	25.90		.35	25.65
	.37	26.40		.39	25.60		.39	25.45
	.41	25.95		.43	25.45			
	.49	25.50	null =	.126				
null =	.167							

TEST-65 (Continued)

x(ft)	H-y(ft)	T(°C)	x(ft)	H-y(ft)	T(°C)
36.5	0.00	31.20	55.	0.00	30.55
	.03	32.00		.03	31.35
	.06	32.40		.06	31.40
	.09	32.60		.09	30.95
	.12	32.35		.11	30.40
	.15	31.50		.13	29.60
	.17	30.80		.15	28.85
	.19	30.10		.17	28.20
	.21	29.30		.19	27.55
	.23	28.50		.21	27.00
	.25	27.75		.24	26.40
	.28	26.85		.27	26.00
	.31	26.30		.30	25.70
	.35	25.75		.34	25.50
	.39	25.55		.38	25.40
	.43	25.40	null =	.076	
null =	.112				

TEST-66: H = 0.523 ft

x(ft)	H-y(ft)	T(°C)
2.	0.00	31.35
	.03	32.20
	.06	32.60
	.09	32.75
	.12	33.00
	.24	33.00
	.27	32.80
	.30	31.85
	.32	31.05
	.34	30.20
	.36	29.05
	.38	28.35
	.40	27.45
	.42	26.85
	.44	26.40
	.47	26.05
	.53	25.65

TEST-65: H = 0.571 ft, L = 70.0 ft, Q_a = 0.021 cfs, Q_w = .0072 cfs

x(ft)	H-y(ft)	T(°C)	x(ft)	H-y(ft)	T(°C)	x(ft)	H-y(ft)	T(°C)
2.	0.00	31.70	10.	0.00	29.60	20.	0.00	30.95
	.06	32.55		.03	31.15		.03	32.05
	.09	32.75		.06	32.05		.06	32.45
	.13	33.00		.09	32.60		.09	32.80
	.17	33.15		.12	33.00		.12	32.85
	.25	33.15		.18	33.00		.15	32.95
	.28	33.05		.21	32.85		.18	32.55
	.31	32.40		.24	32.35		.21	31.65
	.33	31.50		.26	31.70		.23	30.90
	.35	30.75		.28	30.85		.25	30.10
	.37	29.85		.30	29.95		.27	29.20
	.39	29.00		.32	28.20		.29	28.35
	.41	28.20		.36	27.45		.31	27.65
	.43	27.40		.39	26.65		.34	26.80
	.45	26.85		.42	26.05		.37	26.20
	.48	26.10		.46	25.65		.41	25.75
	.52	25.60		.54	25.40		.49	25.40
	.56	25.40	null =	.188		null =	.152	

TEST-66 (Continued): L = 45.8 ft, Q_a = 0.021 cfs, Q_w = .0075 cfs

z(ft)	H-y(ft)	T(°C)	x(ft)	H-y(ft)	T(°C)	x(ft)	H-y(ft)	T(°C)
10.	0.00	31.20	20.	0.00	31.20	36.5	0.00	30.35
	.03	32.05		.03	31.95		.03	30.85
	.06	32.60		.06	32.35		.06	31.05
	.09	32.80		.09	32.50		.09	30.35
	.12	32.90		.12	32.35		.11	29.60
	.15	32.80		.15	31.60		.13	28.80
	.18	32.40		.17	30.65		.15	28.05
	.20	31.95		.19	29.85		.17	27.50
	.22	31.00		.21	28.95		.19	27.00
	.24	30.20		.23	28.20		.21	26.60
	.26	29.25		.25	27.55		.24	26.15
	.28	28.35		.28	26.75		.27	25.85
	.30	27.60		.31	26.20		.30	25.65
	.33	26.85		.34	25.90		.36	25.45
	.36	26.25		.38	25.65	null =	.068	
	.42	25.75		.42	25.55			
	.48	25.55	null =	.114				
null =	.151							

TEST-67: H = 0.526 ft, L = 31.5 ft, Q_a = 0.028 cfs, Q_w = .0076 cfs

x(ft)	H-y(ft)	T(°C)	x(ft)	H-y(ft)	T(°C)	x(ft)	H-y(ft)	T(°C)
2.	0.00	31.65	10.	0.00	31.05	18.	0.00	30.05
	.03	32.20		.03	32.00		.03	31.55
	.06	32.45		.06	32.40		.06	31.90
	.09	32.60		.09	32.60		.09	32.05
	.12	32.70		.12	32.60		.12	31.20
	.15	32.75		.15	32.15		.14	30.15
	.21	32.75		.18	31.00		.16	29.20
	.24	32.45		.20	30.00		.18	28.40
	.27	31.55		.22	29.00		.20	27.60
	.30	30.15		.24	28.20		.22	27.05
	.32	29.20		.26	27.40		.24	26.60
	.34	28.35		.28	26.85		.27	26.05
	.36	27.40		.30	26.45		.30	25.80
	.38	26.80		.33	25.95		.34	25.55
	.40	26.40		.36	25.75		.38	25.40
	.43	25.90		.44	25.40	null =	.087	
	.50	25.45	null =	.123				

TEST-68: Q_w = .0072 cfs (Cont'd)

x(ft)	H-y(ft)	T(°C)
16.	0.00	30.25
	.02	30.60
	.04	31.00
	.06	30.80
	.08	30.00
	.10	28.85
	.12	28.15
	.14	27.65
	.16	27.15
	.18	26.75
	.21	26.25
	.24	26.05
	.36	25.70
null =	.054	

TEST-69: H = 0.498 ft, L = 23.8 ft, Q_a = 0.036 cfs

x(ft)	H-y(ft)	T(°C)	x(ft)	H-y(ft)	T(°C)
2.	0.00	33.40	10.	0.00	32.60
	.03	34.15		.03	33.80
	.06	34.60		.06	34.40
	.09	35.00		.09	34.60
	.12	35.15		.12	34.05
	.20	35.15		.14	33.00
	.22	34.70		.16	31.60
	.24	33.65		.18	30.40
	.26	32.20		.20	29.45
	.28	31.00		.22	28.35
	.30	30.10		.24	27.65
	.32	29.25		.27	26.80
	.34	28.25		.30	26.25
	.37	27.35		.34	25.85
	.40	26.65		.38	25.65
	.44	25.95	null =	.099	
	.498	25.70			

TEST-67 (Continued)

x(ft)	H-y(ft)	T(°C)
26.	0.00	28.20
	.03	30.05
	.06	30.45
	.08	29.90
	.10	28.95
	.12	28.10
	.14	27.65
	.16	27.15
	.18	26.75
	.20	26.40
	.23	26.00
	.26	25.75
	.29	25.60
	.35	25.40
null =	.055	

TEST-68: H = 0.527 ft, L = 19.3 ft, Q_a = 0.036 cfs

x(ft)	H-y(ft)	T(°C)	x(ft)	H-y(ft)	T(°C)
2.	0.00	31.20	10.	0.00	31.00
	.03	31.80		.03	31.75
	.06	32.20		.06	32.10
	.09	32.40		.09	32.00
	.18	32.40		.11	31.55
	.21	32.00		.13	30.70
	.23	31.35		.15	29.75
	.25	30.35		.17	28.80
	.27	29.65		.19	28.05
	.29	28.70		.21	27.40
	.31	27.85		.24	26.75
	.33	27.25		.27	26.35
	.35	26.75		.30	26.00
	.38	26.30		.33	25.85
	.41	26.05		.41	25.70
	.44	25.85	null =	.088	
	.50	25.70			

TEST-69: Q_w = .0070 cfs (Cont'd)

x(ft)	H-y(ft)	T(°C)
18.	0.00	30.70
	.03	32.20
	.06	33.05
	.09	32.05
	.11	30.80
	.13	29.75
	.15	28.95
	.17	28.15
	.20	27.45
	.23	26.60
	.26	26.05
	.30	25.75
	.34	25.70
null =	.064	

TEST-70: H = 0.497 ft, L = 32.4 ft, Q_a = 0.028 cfs

x(ft)	H-y(ft)	T(°C)	x(ft)	H-y(ft)	T(°C)
2.	0.00	32.55	10.	0.00	32.40
	.03	33.40		.03	33.25
	.06	33.95		.06	33.80
	.09	34.10		.09	34.05
	.12	34.25		.12	33.95
	.15	34.35		.14	33.55
	.21	34.35		.16	32.80
	.24	33.85		.18	31.60
	.27	32.40		.20	30.35
	.29	31.40		.22	29.30
	.31	30.10		.24	28.35
	.33	29.10		.27	27.20
	.35	28.20		.30	26.50
	.37	27.30		.33	25.95
	.40	26.35		.37	25.65
	.43	25.85		.41	25.50
	.49	25.55	null =	.116	

TEST-70 (Continued): Q_w = .0079 cfs

x(ft)	H-y(ft)	T(°C)	x(ft)	H-y(ft)	T(°C)
20.	0.00	31.50	26.	0.00	29.60
	.03	32.45		.03	31.00
	.06	33.05		.05	31.40
	.09	32.80		.07	31.30
	.11	32.00		.09	30.40
	.13	30.80		.11	29.40
	.15	29.75		.13	28.45
	.17	28.85		.15	27.95
	.19	28.00		.17	27.35
	.22	27.00		.20	26.65
	.25	26.35		.23	26.15
	.29	25.85		.27	25.75
	.33	25.60		.31	25.55
null =	.074		null =	.058	

TEST-71: H = 0.499 ft, L = 16.0 ft, Q_a = 0.043 cfs, Q_w = .0078 cfs

x(ft)	H-y(ft)	T(°C)	x(ft)	H-y(ft)	T(°C)
2.	0.00	32.45	10.	0.00	31.40
	.03	33.25		.03	32.60
	.06	33.65		.06	33.30
	.09	33.85		.09	32.90
	.12	33.95		.11	31.65
	.15	34.00		.13	30.20
	.18	33.75		.15	29.35
	.21	32.40		.17	28.40
	.23	31.20		.19	27.65
	.25	30.15		.21	27.00
	.27	29.35		.24	26.40
	.29	28.50		.27	25.95
	.31	27.65		.30	25.70
	.33	27.20		.34	25.55
	.36	26.65		.38	25.45
	.40	25.75	null =	.069	
	.48	25.45			

TEST-72: H = 0.501 ft

x(ft)	H-y(ft)	T(°C)
2.	0.00	31.40
	.03	32.45
	.06	33.50
	.09	33.65
	.12	33.95
	.15	34.15
	.21	34.15
	.24	33.90
	.26	33.35
	.28	32.40
	.30	31.00
	.32	30.20
	.34	28.95
	.36	27.90
	.38	27.15
	.41	26.40
	.44	25.80
	.49	25.40

TEST-72 (Continued): L = 41.0 ft, Q_a = 0.028 cfs, Q_w = .0074 cfs

x(ft)	H-y(ft)	T(°C)	x(ft)	H-y(ft)	T(°C)	x(ft)	H-y(ft)	T(°C)
10.	0.00	32.40	20.	0.00	32.20	32.	0.00	29.80
	.03	33.20		.03	33.00		.03	30.80
	.06	33.65		.06	33.40		.06	31.60
	.09	33.80		.09	33.45		.09	31.05
	.12	33.95		.12	32.95		.11	30.30
	.15	33.75		.14	32.20		.13	29.40
	.17	33.25		.16	31.00		.15	28.50
	.19	32.50		.18	30.05		.17	27.80
	.21	31.40		.20	29.00		.19	27.15
	.23	30.20		.22	28.00		.22	26.45
	.25	29.15		.24	27.35		.25	25.95
	.27	28.20		.27	26.50		.29	25.60
	.29	27.55		.30	26.00		.33	25.45
	.32	26.60		.32	25.60	null =	.065	
	.35	26.05		.36	25.45			
	.39	25.60	null =	.102				
	.43	25.45						
null =	.134							

TEST-73: H = 0.503 ft, L = 24.0 ft, Q_a = 0.035 cfs, Q_w = .0085 cfs

x(ft)	H-y(ft)	T(°C)	x(ft)	H-y(ft)	T(°C)	x(ft)	H-y(ft)	T(°C)
2.	0.00	32.05	10.	0.00	32.00	20.	0.00	29.00
	.03	32.50		.03	32.60		.03	30.80
	.06	32.95		.06	32.95		.05	31.45
	.09	33.20		.09	33.15		.07	31.25
	.12	33.25		.12	33.00		.09	30.20
	.15	33.35		.14	32.55		.11	29.20
	.18	33.35		.16	31.85		.13	28.55
	.21	33.25		.18	30.40		.15	28.05
	.23	32.55		.20	29.55		.18	27.30
	.25	31.45		.22	28.60		.21	26.80
	.27	30.25		.24	27.90		.24	26.45
	.29	29.65		.26	27.25		.27	26.25
	.31	28.65		.29	26.75		.30	26.20
	.33	28.00		.32	26.40		.34	26.10
	.35	27.50		.35	26.20		.39	26.00
	.38	26.95		.43	26.00	null =	.058	
	.41	26.30	null =	.104				
	.49	26.00						

TEST-74: H = 0.503 ft, L = 17.5 ft, Q_a = 0.045 cfs, Q_w = .0079 cfs

x(ft)	H-y(ft)	T(°C)	x(ft)	H-y(ft)	T(°C)
2.	0.00	32.35	12.	0.00	30.85
	.03	32.85		.02	31.70
	.06	33.40		.04	32.20
	.09	33.80		.06	32.80
	.12	33.85		.08	32.75
	.15	33.85		.10	31.80
	.18	33.55		.12	30.45
	.20	32.60		.14	29.55
	.22	31.80		.16	28.60
	.24	30.65		.18	27.95
	.26	29.75		.20	27.35
	.28	28.70		.23	26.75
	.30	28.15		.26	26.35
	.33	27.10		.30	26.00
	.36	26.75		.34	25.90
	.40	26.20		.38	25.85
	.48	25.85	null =	.069	

TEST-75: H = 0.560 ft, L = 30.9 ft, Q_a = 0.044 cfs, Q_w = .0080 cfs

x(ft)	H-y(ft)	T(°C)	x(ft)	H-y(ft)	T(°C)	x(ft)	H-y(ft)	T(°C)
2.	0.00	30.25	10.	0.00	31.50	20.	0.00	31.25
	.03	32.15		.03	32.25		.03	32.15
	.06	32.65		.06	32.75		.06	32.60
	.09	32.95		.09	33.15		.09	32.45
	.12	33.20		.12	33.35		.11	31.75
	.15	33.45		.15	33.05		.13	30.65
	.23	33.45		.17	32.45		.15	29.60
	.25	33.10		.19	31.55		.17	28.75
	.27	32.05		.21	30.40		.19	27.95
	.29	30.80		.23	29.45		.22	27.10
	.31	30.00		.25	28.50		.25	26.55
	.33	28.95		.27	27.65		.28	26.20
	.35	28.00		.30	26.85		.32	25.85
	.37	27.50		.33	26.40		.40	25.70
	.40	26.65		.37	25.95		.44	25.60
	.43	26.30		.41	25.75	null =	.079	
	.46	25.95		.49	25.60			
	.54	25.60	null =	.126				

TEST-76: H = 0.552 ft, L = 55.8 ft, Q_a = 0.028 cfs, Q_w = .0080 cfs

x(ft)	H-y(ft)	T(°C)	x(ft)	H-y(ft)	T(°C)	x(ft)	H-y(ft)	T(°C)
2.	0.00	31.00	16.	0.00	30.90	32.	0.00	30.30
	.03	32.05		.03	32.05		.03	31.70
	.06	32.85		.06	32.60		.06	32.30
	.09	33.25		.09	33.20		.09	32.45
	.12	33.50		.12	33.40		.12	31.95
	.18	33.75		.15	33.35		.14	31.35
	.24	33.75		.18	32.80		.16	30.40
	.27	33.55		.20	32.15		.18	29.75
	.29	33.20		.22	31.25		.20	28.85
	.31	32.40		.24	30.40		.22	28.10
	.33	31.45		.26	29.35		.25	27.35
	.35	30.55		.28	28.40		.28	26.75
	.37	29.80		.30	27.75		.32	26.25
	.39	28.80		.33	27.00		.36	26.00
	.41	27.85		.36	26.45		.40	25.90
	.44	26.95		.40	26.15	null =	.092	
	.47	26.40		.44	25.95			
	.53	26.00	null =	.141				

TEST-76 (Continued)

x(ft)	H-y(ft)	T(°C)
49.	0.00	27.40
	.03	28.50
	.05	29.35
	.07	29.25
	.09	28.80
	.11	28.00
	.13	27.55
	.15	27.20
	.17	26.90
	.20	26.45
	.23	26.20
	.27	26.00
	.32	25.90
null =	.041	

TEST-77: H = 0.557 ft, L = 36.0 ft, Q_a = 0.038 cfs

x(ft)	H-y(ft)	T(°C)	x(ft)	H-y(ft)	T(°C)
2.	0.00	30.95	10.	0.00	31.45
	.03	32.00		.03	32.35
	.06	32.95		.06	33.00
	.09	33.20		.09	33.25
	.15	33.45		.12	33.35
	.18	33.50		.15	33.25
	.21	33.40		.17	32.85
	.23	33.20		.19	32.00
	.25	32.60		.21	30.80
	.27	32.00		.23	30.10
	.29	31.00		.25	29.15
	.31	30.10		.27	28.40
	.33	29.30		.30	27.35
	.36	28.20		.33	26.70
	.39	27.20		.37	26.15
	.42	26.65		.41	25.85
	.46	26.05		.49	25.65
	.54	25.65	null =	.135	

TEST-77 (Continued): Q_w = .0379 cfs

x(ft)	H-y(ft)	T(°C)
20.	0.00	31.05
	.03	31.95
	.06	32.55
	.09	32.80
	.12	32.35
	.14	31.50
	.16	30.40
	.18	29.55
	.20	28.55
	.23	27.60
	.26	26.80
	.30	26.30
	.34	25.95
	.38	25.80
	.42	25.70
	.46	25.65
null =	.101	

x(ft)	H-y(ft)	T(°C)
30.5	0.00	29.80
	.03	30.80
	.05	31.20
	.07	31.00
	.09	30.30
	.11	29.20
	.13	28.35
	.15	27.80
	.18	27.10
	.21	26.50
	.25	26.10
	.29	25.85
	.37	25.70
	.41	25.65
null =	.056	

TEST-78: H = 0.504 ft, L = 21.0 ft, Q_a = 0.043 cfs, Q_w = .0081 cfs

x(ft)	H-y(ft)	T(°C)
4.	0.00	32.80
	.03	33.45
	.06	33.95
	.09	34.10
	.12	34.25
	.15	34.20
	.18	33.70
	.20	32.80
	.22	31.60
	.24	30.35
	.26	29.40
	.29	28.15
	.32	27.30
	.36	26.55
	.40	26.20
	.44	26.00
null =	.144	

x(ft)	H-y(ft)	T(°C)
14.	0.00	31.20
	.03	32.70
	.06	33.15
	.08	33.00
	.10	32.20
	.12	30.85
	.14	30.00
	.16	29.15
	.19	28.05
	.22	27.15
	.25	26.70
	.28	26.30
	.32	26.05
	.36	26.00
null =	.074	

TEST-79: H = 0.652 ft, L = 95.2 ft, Q_a = 0.037 cfs, Q_w = .0082 cfs

x(ft)	H-y(ft)	T(°C)
2.	0.00	33.90
	.06	34.75
	.10	35.15
	.14	35.60
	.22	35.60
	.27	35.00
	.29	34.50
	.31	33.55
	.33	32.80
	.35	31.40
	.37	30.35
	.40	29.00
	.43	27.85
	.46	26.95
	.50	26.20
	.58	25.75
	.65	25.65
null =	.239	

x(ft)	H-y(ft)	T(°C)
16.	0.00	32.95
	.03	34.05
	.06	34.80
	.10	35.30
	.14	35.55
	.18	35.55
	.22	35.10
	.24	34.60
	.26	33.75
	.28	32.85
	.30	31.85
	.32	30.75
	.34	29.85
	.37	28.55
	.40	27.45
	.44	26.50
	.56	25.75
null =	.194	

x(ft)	H-y(ft)	T(°C)
32.	0.00	32.60
	.03	33.85
	.06	34.35
	.10	34.80
	.14	35.00
	.17	34.75
	.19	34.35
	.21	33.65
	.23	32.80
	.25	31.85
	.27	30.95
	.29	29.95
	.32	28.55
	.35	27.55
	.39	26.65
	.43	26.15
	.47	25.95
	.51	25.75
null =	.161	

TEST-79 (Continued)

x(ft)	H-y(ft)	T(°C)
52.	0.00	32.65
	.03	33.65
	.06	34.20
	.09	34.35
	.12	34.05
	.14	33.60
	.16	32.90
	.18	32.05
	.20	31.15
	.22	30.10
	.25	29.05
	.28	27.85
	.31	27.05
	.35	26.40
	.39	26.05
	.43	25.90
	.52	25.75
null =	.124	

x(ft)	H-y(ft)	T(°C)
72.	0.00	31.40
	.03	32.45
	.06	32.80
	.09	32.55
	.11	32.05
	.13	31.30
	.15	30.45
	.17	29.70
	.20	28.55
	.23	27.55
	.27	26.80
	.31	26.30
	.35	26.05
	.39	25.90
	.43	25.75
null =	.089	

APPENDIX II

Translation of

FRICTION COEFFICIENTS ON THE INTERFACE OF A TWO-LAYER SYSTEM

Literature Survey by C. B. Vreugdenhil

Delft Hydraulics Laboratory

Internal Information Report No. V204

November 1971

1. Statement of Problem

In order to make calculations for a two-layer system as discussed in reference 17, it is necessary to have information on the bottom shear stress, the interfacial shear stress, and in case one considers mixing between the layers, it is also necessary to have information on the turbulent interchange and entrainment across the interface. No clear conclusion concerning entrainment can be made from the literature known to this writer. There is essentially no data concerning turbulent mixing. In the first approximation it can be assumed that the bottom shear is known. The most important remaining point is then the interfacial shear, about which there are a number of publications. This information report attempts to draw a workable conclusion concerning interfacial shear from these publications.

2. Data

A review of the available literature is given by Lepetit and Rogan (9) and Sjöberg (14). The latter reference (14) also attempts to find correlations between the interfacial friction and the parameters

that influence it, namely the Reynolds number and the Froude number. In order to accomplish this, data were used from Macagno and Rouse (11), Lofquist (10), and Michon, Goddet and Bonnefille (12). Lepetit and Rogan (9) mention that according to Averkiev and Kind (2) the dependence of the interfacial friction coefficient on the Reynolds number disappears when the Reynolds number is greater than 12,000. In addition, some data were published in Iwasaki (6).

There is also data available for some special cases, namely for a lock exchange flow (summarized by Abraham and Eysink (1)) and for an arrested salt wedge (Boulot and Daubert (3), Ippen and Harleman (5), Keulegan (7), Lanzoni (8), Riddell (13), Zanotti (18), Hendrikse (14)).

3. Interfacial Friction and Friction Coefficient

The parameter τ_i represents the shear stress associated with the movement of the two overlying layers. The relative velocity of the two layers is U. For laminar flow

$$\tau_i = \rho\nu \left.\frac{\partial u}{\partial z}\right|_i \tag{1}$$

where u is the velocity at elevation z, ν is the kinematic viscosity and ρ is the density. Thus, it is convenient to investigate the proportionality

$$\beta = \frac{\tau_i}{\rho\nu \left.\frac{\partial u}{\partial z}\right|_i} \tag{2}$$

(See Sjöberg (14), among others.) It may be anticipated that this ratio in Equation 2 will be unity for laminar flow and greater than unity otherwise. Sjöberg has found a correlation for β.

Unfortunately, a coefficient such as β is not directly usable in calculations for two-layer systems because the velocity gradient

cannot be determined. A useful definition for a friction coefficient k_i for turbulent flow is (17)

$$|\tau_i| = \rho\, k_i\, U^2 \tag{3}$$

A direct relationship between k_i and β cannot be given. If the velocity gradient is approximated by

$$\frac{\partial u}{\partial z} = \frac{U}{h} \tag{4}$$

where h is a characteristic distance over which the velocity difference U exists, then

$$\beta = \frac{\rho\, k_i\, U^2\, h}{\rho \nu\, U} = k_i\, \frac{Uh}{\nu} \tag{5}$$

With the definition of the Reynolds number as

$$Re = \frac{Uh}{\nu} \tag{6}$$

then

$$k_i = \beta\, Re^{-1} \tag{7}$$

Furthermore, according to the data, there is an influence of the Froude number, which is defined as

$$F = \frac{U}{\sqrt{\frac{\Delta\rho}{\rho}\, gh}} \tag{8}$$

where $\Delta\rho$ is a characteristic density difference.

It may be anticipated for laminar flow that (4)

$$k_i \sim Re^{-1} \qquad \text{(small Re)} \tag{9}$$

while for turbulent flow the influence of the Reynolds number will disappear so that

$$k_i = f(F) \qquad \text{(large Re)} \qquad (10)$$

The purpose of this information report is to find these relationships from literature data. For practical application in the field, Equation 10 will be the most important relationship; for model measurements the transition between Equations 9 and 10 will be important.

The definitions used by the various authors are given in the figures. The numerical values from the measurements are not comparable because of the use of different definitions and because of measurements in dissimilar situations. Even so, it may be anticipated that there is a definite similarity between the various measurements.

Discussion

Figures 1 through 4 show the results of Iwasaki (6), Lofquist (10), Macagno and Rouse (11), and Michon, Goddett and Bonnefille (12) plotted with ReF^2 as the independent variable. This combination $ReF^2 = U^3/g\nu$ is appropriately called the Keulegan number. Iwasaki's results are available only in this form. According to Equation 9, the following relationship is anticipated for small constant F

$$k_i \sim (ReF^2)^{-1}$$

A few similar lines have been sketched for orientation purposes; these lines do not follow directly from the measurements. The line given by Iwasaki has a slightly different slope. The relationship given by him, however, probably is not valid for large values of ReF^2, considering Equation 10. Moreover, it is noteworthy that the Froude

number appears to have no influence. This cannot be explained without knowledge of the measurements; it is possible that there was little variation in F or that there was a correlation between Re and F. For large values of ReF^2, horizontal lines for constant F are anticipated (Fig. 4). However, it becomes evident that from these data a relationship with the parameters F and ReF^2 can hardly be established.

Valembois (16) gives an analysis of the data of Lofquist, on the basis of which a relationship of k_i with Re and F follows. One means of obtaining this result is by representing as turbulent diffusion the entrainment velocity (advective transport through the interface) which has been measured by Lofquist. This is definitely a questionable approach since entrainment and diffusion are two distinct phenomena. Squarer (15) found for small values of Re that Valembois' relationship gave values for k_i which were much too large in comparison with the theoretical relationship of Ippen and Harleman (5) (see figure 8); he found the same to be true when the hydraulic radius was used instead of the water depth in the definition of the parameters.

On the basis of Equation 10, an attempt is made in figures 5 through 7 to find a relationship between k_i and the Froude number. In these figures Re appears as a parameter. Especially for the larger values of Re, an unambiguous relationship could be expected, according to Equation 10. This appears to be true only for the tests in the flume at Ventavon (figure 7). This actually has another cause, as indicated also in reference 12: In the case of essentially uniform flow (thickness of the lower layer approximately constant) the equation of motion becomes (see (17), Equation 6.3.20)

$$\frac{k_i h}{a_1 a_2} U^2 = \frac{\Delta\rho}{\rho} gI \qquad (11)$$

where a_1 and a_2 are the thicknesses of the upper and lower layers. With $\varepsilon = \Delta\rho/\rho$, Equation 11 can be rewritten as

$$\frac{k_i}{I} \sim \frac{\varepsilon\, g\, h}{U^2} = \frac{1}{F^2} \tag{12}$$

This relationship is also seen in figure 7. This is apparently a result of the special circumstances of the experiments and is of no value for other cases.

Figure 8 gives a final summary of the theoretical and experimental results for the arrested salt wedge according to Riddell (13), Ippen and Harleman (5), Hendrikse (4), Lanzoni (8), Zanotti (18), Boulot and Daubert (3) and Keulegan (7). The k_i values for the experiments of Riddell were determined through a comparison with the theoretical form of the arrested salt wedge (17). The value of F is not indicated. It appears that the theoretical relationship of Ippen and Harleman

$$k_i = \frac{2.8}{Re}$$

for Re less than 10^4 agrees reasonably well with the various measurements. The experiments of Lanzoni agree well in the indicated domain with the relationship which he defined (see figure 8); actually it is probable that this cannot be extrapolated. For large values of Re, it appears that a more nearly constant value of k_i will arise. The number of measurements is insufficient in order to be able to clearly define a possible relationship with F.

Figure 8 also present the results of flume experiments for lock exchange flow at the Delft Hydraulics Laboratory (1). Although these data, strictly speaking, apply to a different situation and thus

are not comparable, they are in good agreement with the general representation in figure 8.

5. Conclusions

1. From the available data in the literature it is not possible to define a definite relationship between the friction coefficient k_i and the Reynolds number Re and Froude number F.
2. Only vague indications can be found for the theoretical predictions expressed in Equations 9 and 10.
3. For the case of an arrested salt wedge, it appears that a relationship exists between k_i and Re. For large values of Re there is probably also a dependence on F, but this cannot be demonstrated because of limited measurements.

References

1. Abraham, G. and W. D. Eysink - Magnitude of interfacial shear in exchange flow, J. Hydr. Res. 9, 2 (1971) 125-151.

2. Averkiev and Kind - Etude expérimentale de certaines charactéristiques des courants de densité, IAHR Congress 1965 (Leningrad), 2-23.

3. Boulot, F. and A. Daubert - Modèle mathématique de la salinité sous une forme stratifiée en regime non-permanent, 13th Congress IAHR, Kyoto 1969, paper C 38.

4. Hendrikse, M. - The effect of resistance bars upon an arrested salt wedge, Master of Science Thesis M.I.T. 1965, Speurwerkverslag S57 W.L.

5. Ippen, A. T. and D.R.F. Harleman - Steady state characteristics of subsurface flow, Symposium "Gravity Waves", Nat. Bur. Standards Circ. 521, 1952, 79-94.

6. Iwasaki, T. - On the shear stress at the interface and its effect on the stratified flow, 9th Conf. Coastal Eng. 1964.

7. Keulegan, G. H. - The mechanism of an arrested saline wedge, in Ippen (ed). Estuary and coastline hydrodynamics, McGraw-Hill, New York, 1966.

8. Lanzoni, G. - Correnti di densitá; contributo allo studio sperimentale del cuneo d' intrusione di acqua salata, Energia Elettrica 1959 no. 10, 877-882.

9. Lepetit, J. P. and A. Rogan - Etude bibliographique du coin salé. E.D.F. Bull., Dir. Etudes et Recherches, Serie A, 4 (1970) 73-104.

10. Lofquist, K. - Flow and stress near an interface between stratified liquids, Phys. Fluids 3, 2 (1960) 158-175.

11. Macagno, E. O. and H. Rouse - Interfacial mixing in stratified flow, J. ASCE 87 EM 6 (1961) 55-81.

12. Michon, X., J. Goddett and R. Bonnefille - Etude théorique et experimentale des courants de densité I, II Lab. Nat. d' Hydraulique, Chatou, 1955.

13. Riddell, J. F. - Densimetric exchange flow in rectangular channels, IV. The arrested saline wedge, La Houille Blanche 25, 4 (1970) 317-329.

14. Sjöberg, A. - Diffusive properties of interfacial layers, IAHR Congress Fort Collins 1967, paper D8.

15. Squarer, D. - Interfacial resistance of laminar and turbulent stratified flow, Informatieblad W.L. no. V 149, 1964.

16. Valembois, J. - Courants de densité: tension tangentielle à l'interface. Essai d'interprétation des résultats de Lofquist, E.D.F. Bull. Centre de Recherches et d'Essais Chatou no. 5 (1963) 37-40.

17. Vreugdenhil, C. B. - Computation of gravity currents in estuaries, Delft Hyd. Lab. Publ. no. 86, 1970.

18. Zanotti, A. - II cuneo salino nei canali con sfocio in mare, Energia Elettrica 1965 no. 7, 462-473.

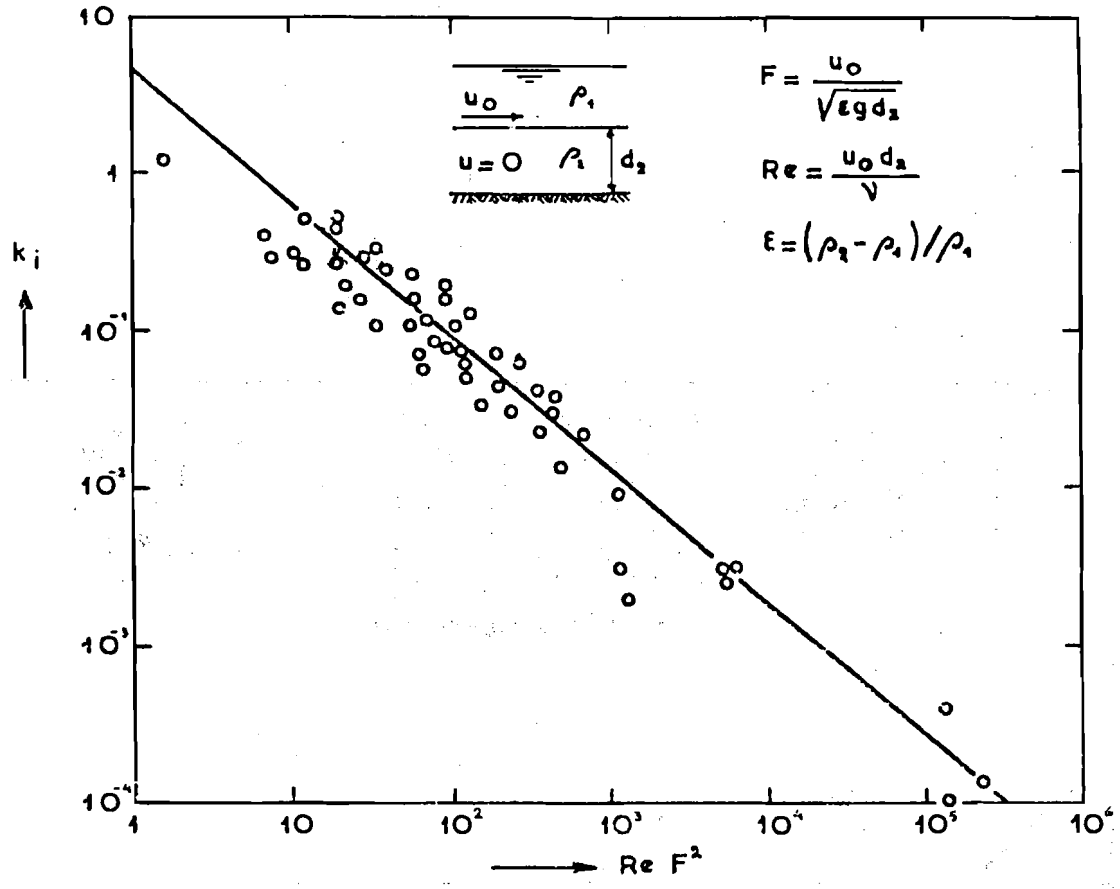

FIG. 1 RESULTS OF IWASAKI [6]

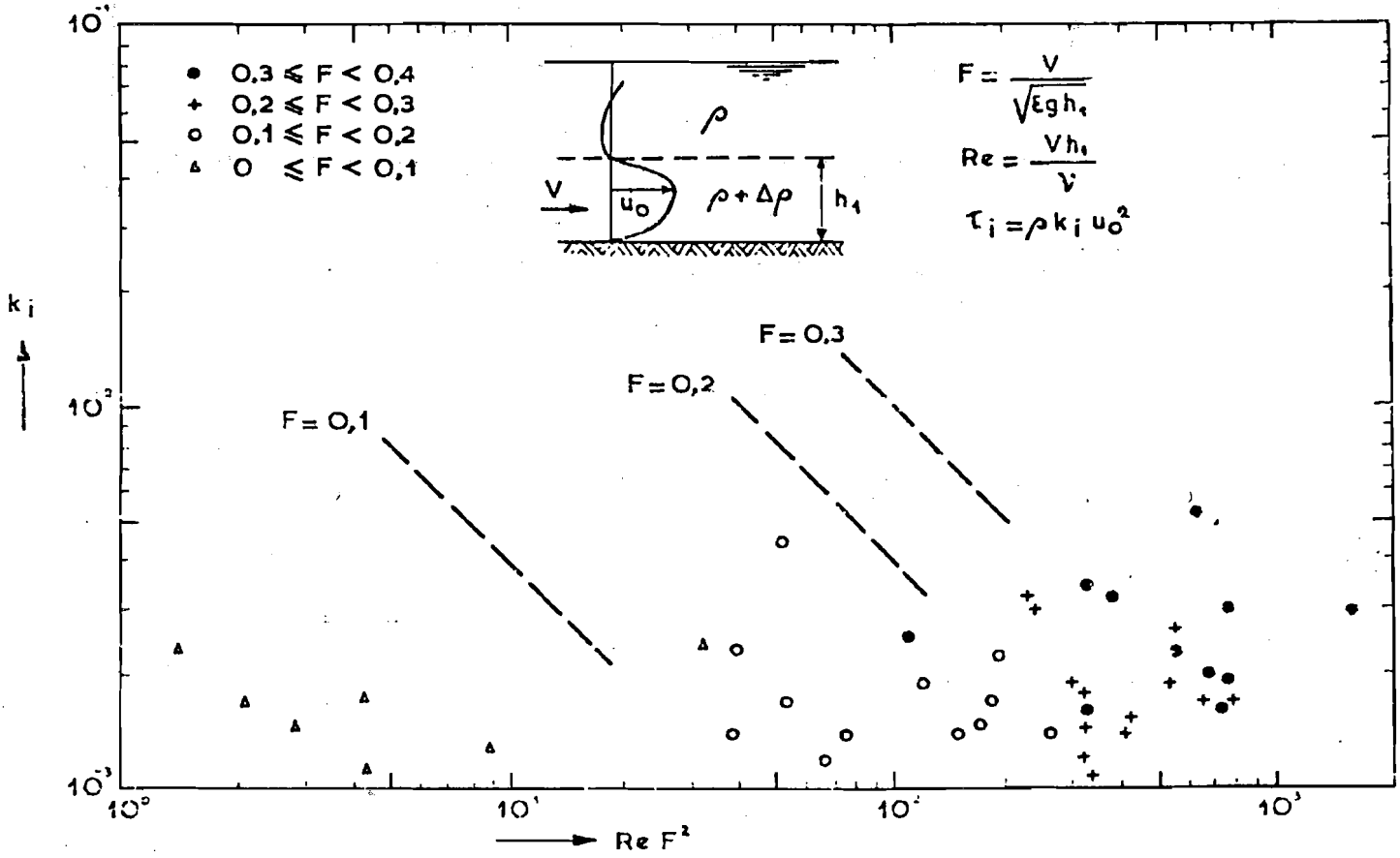

FIG. 2 RESULTS OF LOFQUIST [10]

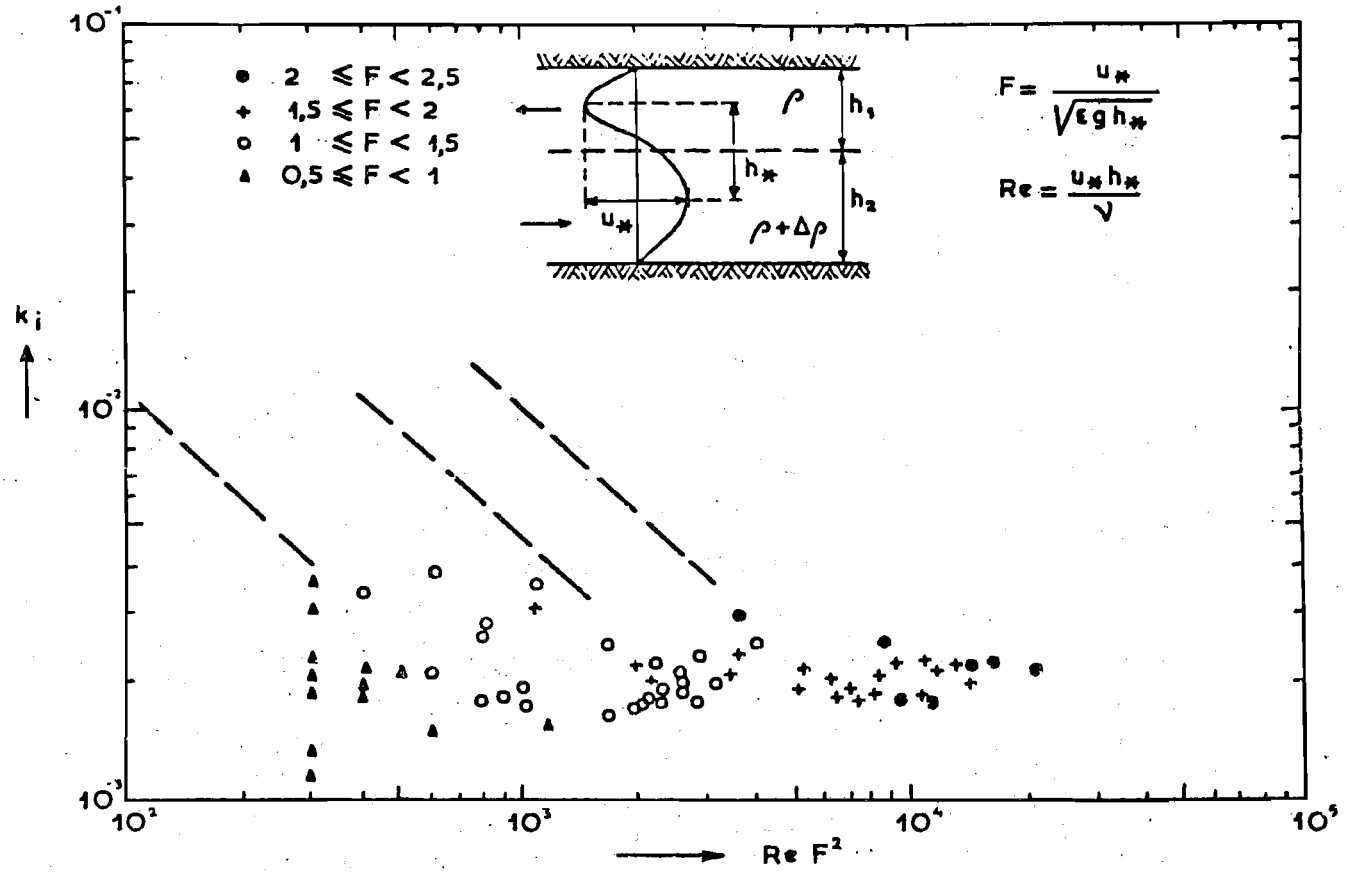

FIG. 3 RESULTS OF MACAGNO AND ROUSE [11]

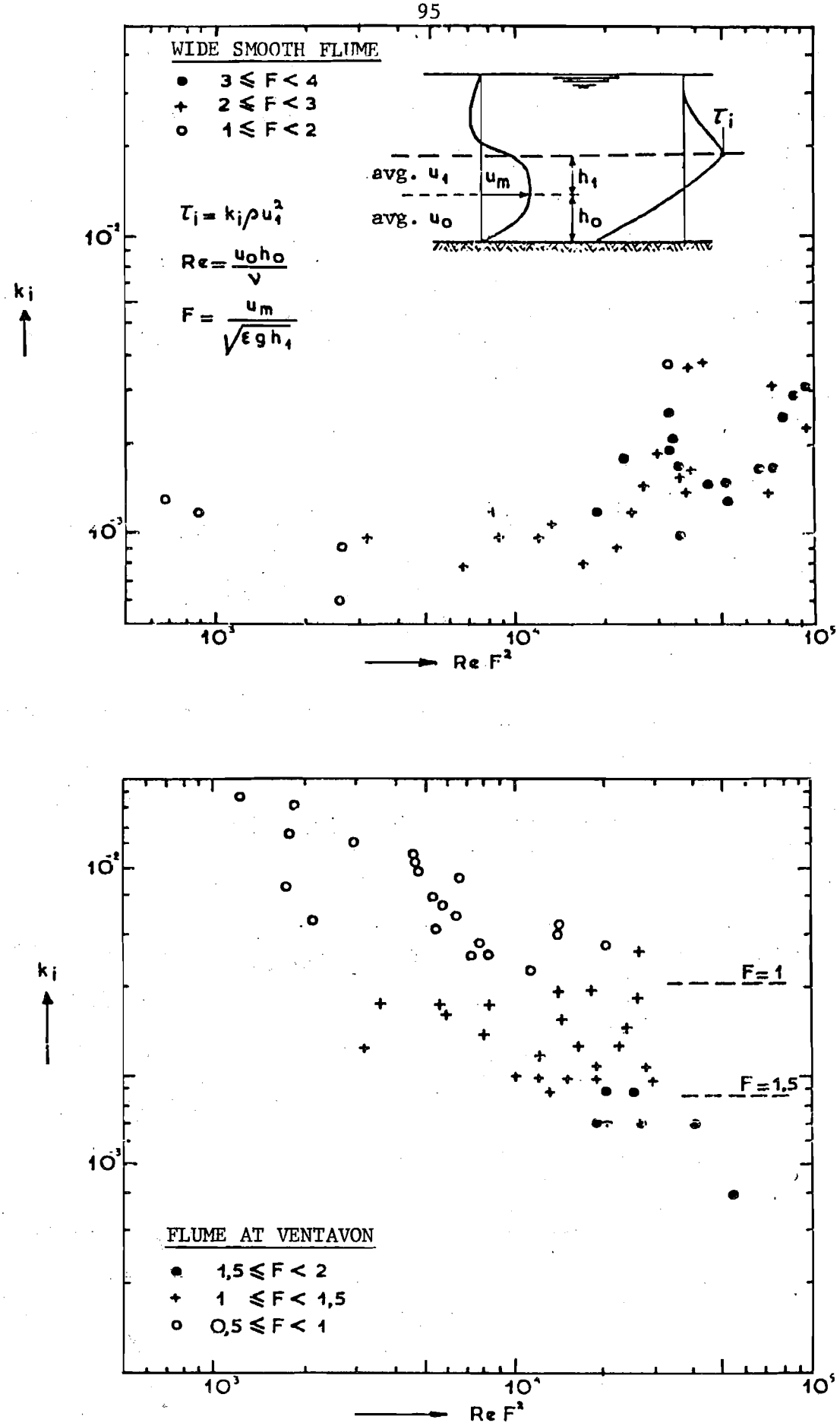

FIG. 4 RESULTS OF MICHON, GODDET AND BONNEFILLE [12]

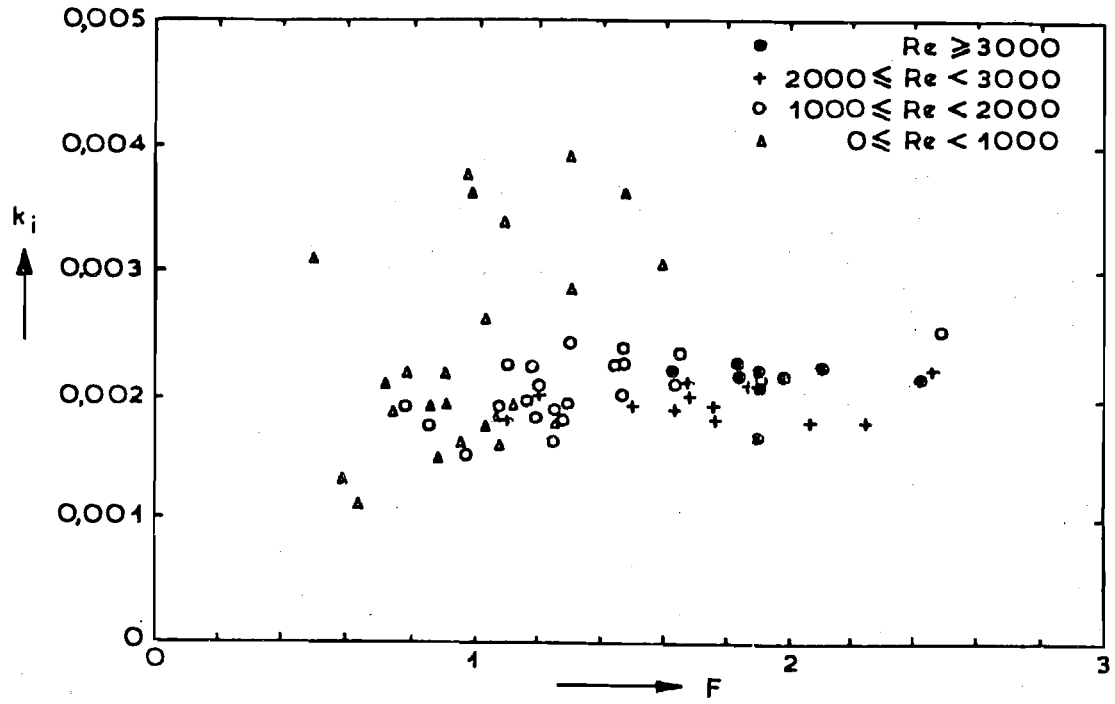

FIG. 5 RESULTS OF MACAGNO AND ROUSE [11]

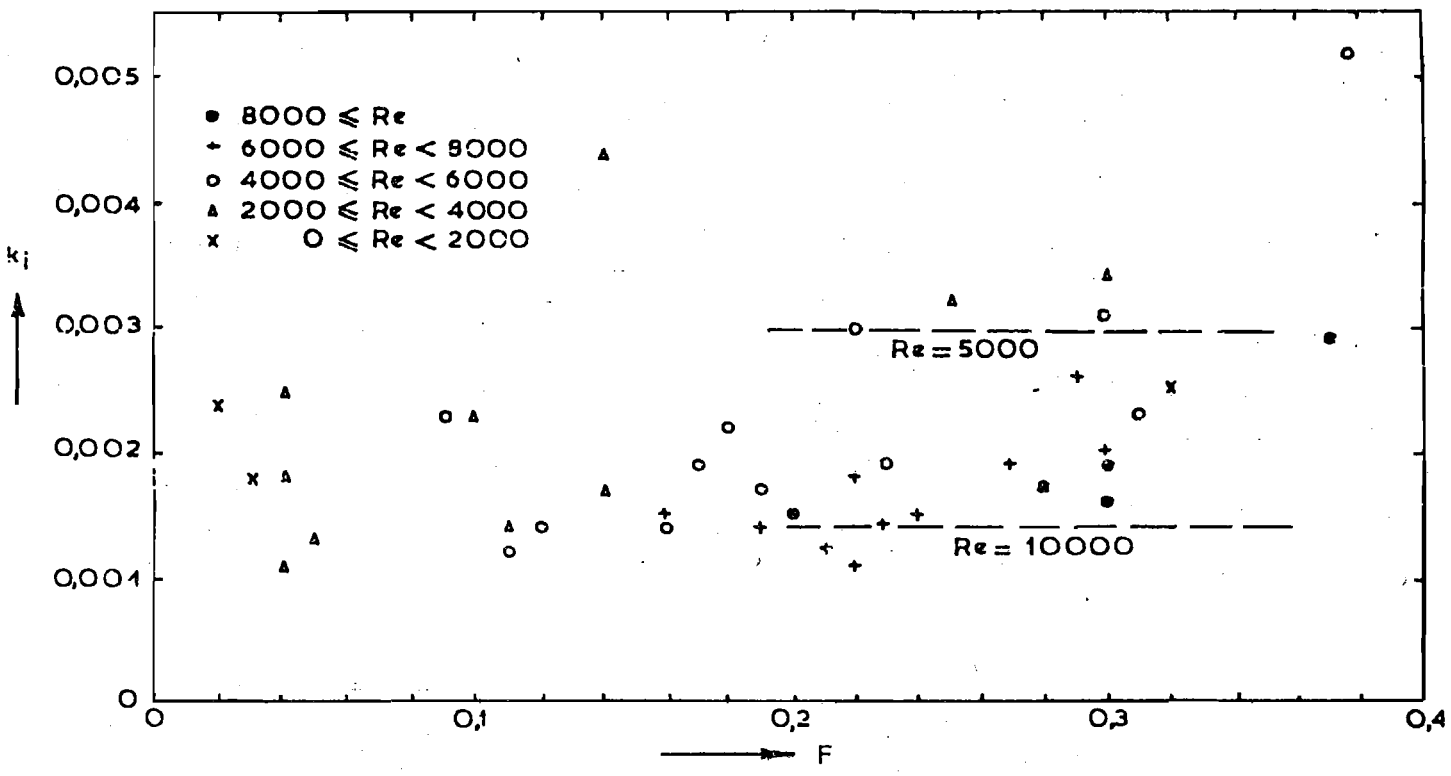

FIG. 6 RESULTS OF LOFQUIST [10]

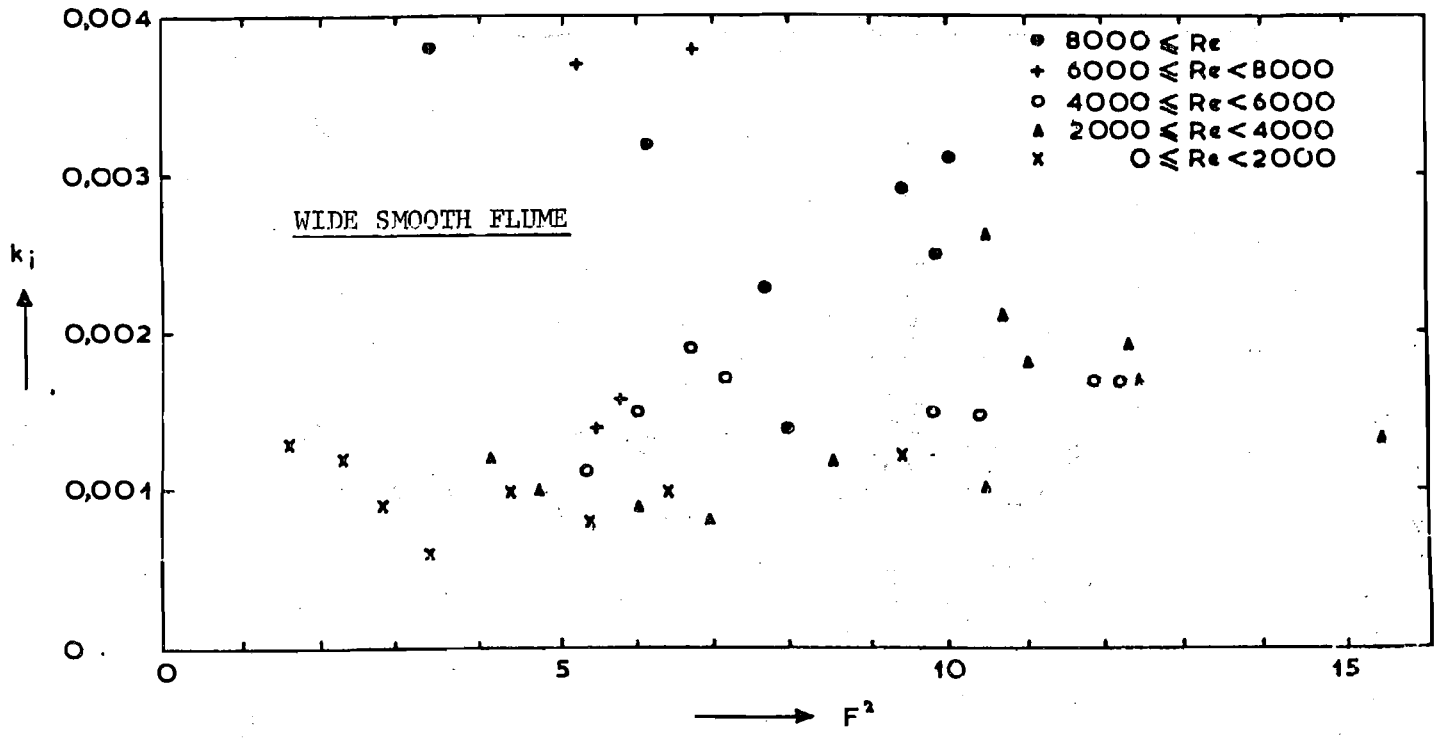

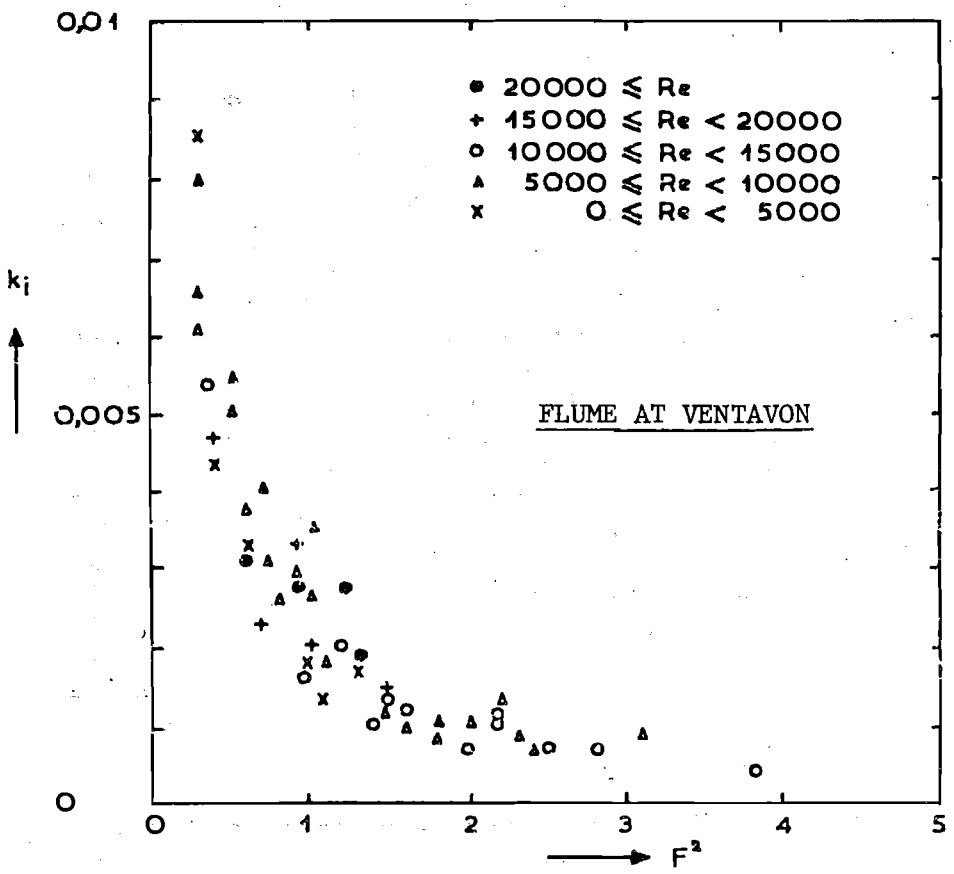

FIG. 7 RESULTS OF MICHON, GODDET AND BONNEFILLE [12]

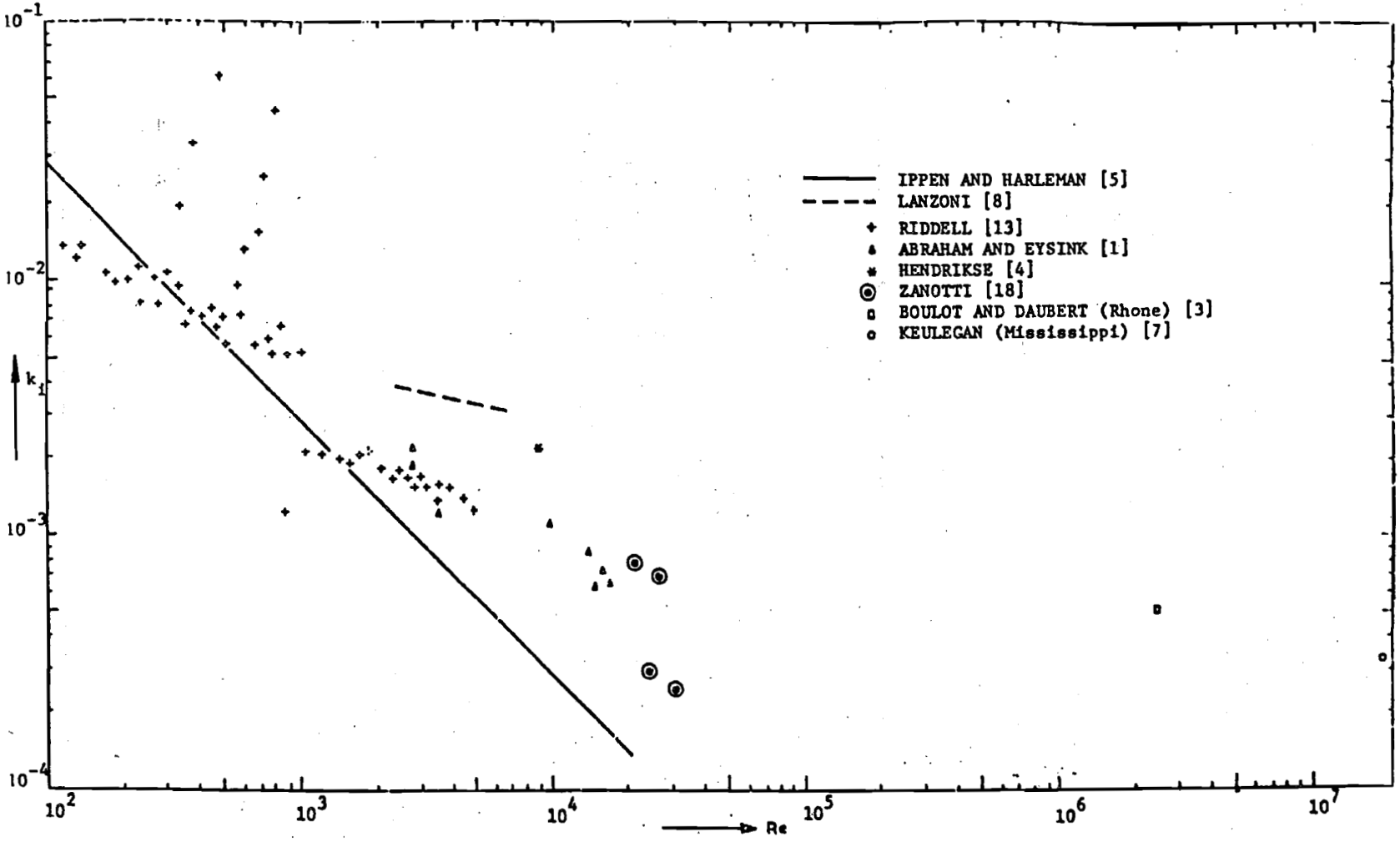

FIG. 8 RESULTS FOR ARRESTED SALT WEDGE